

Nozzle flow dynamics during control system response of pulse width modulated (PWM)
technology-equipped agricultural sprayer

by

Jonathan Viernes Fabula

B.S., Central Luzon State University, 2006
M.S., Central Luzon State University, 2011

AN ABSTRACT OF A DISSERTATION

submitted in partial fulfillment of the requirements for the degree

DOCTOR OF PHILOSOPHY

Carl and Melinda Helwig Department of Biological and Agricultural Engineering
Carl R. Ice College of Engineering

KANSAS STATE UNIVERSITY
Manhattan, Kansas

2021

Abstract

Crop producers utilize agricultural sprayers equipped with modern technologies such as pulse width modulation (PWM) system that can manage flow at nozzle-by-nozzle, thus have the potential to provide greater resolution for section control and reducing the environmental contamination. The introduction of precision technologies such as the PWM system has obvious benefits to the producers; however, a greater understanding of system functionality and operational accuracy is required for adoption and implementation. One of the greatest challenges is to manage nozzle level target application rate for large self-propelled systems during active section control and ground speed transitions. Therefore, this study was conducted to quantify the PWM system's performance under real-world operating conditions, with a goal to develop knowledge for producers to accurately implement this technology and suggest technology improvements for manufacturer's. A methodology was established to conduct system-level evaluation of the PWM system both in laboratory and field settings. In the laboratory setting, the pressure and flow dynamics of three commercially available PWM systems (Capstan PinPoint, John Deere ExactApply, and Raven Hawkeye) were evaluated. On the other hand, field tests were conducted using a New Holland SPF370F and Case Patriot 4440 agricultural sprayer to evaluate the PWM system's performance in varying field conditions. Both sprayers were equipped with a Raven Hawkeye PWM system and had a 36.6 m boom width. Novel analytical techniques were developed to generate a high spatial control-section level mapping of system performance parameters to quantify advantages and instances of application rate errors.

Laboratory test results show that different PWM systems provided different pressure drops when applying different application rates and pressures. The pressure drop was unique for different PWM systems, and it significantly increased with the increase in the application rate for three

systems. The pressure drop could vary the nozzle flow rate, which may significantly impact the application rate, thereby reducing the product efficacy. A pressure drop greater than 70.0 kPa from the target application pressure could cause the flow rate to vary beyond $\pm 10.0\%$ error. The three PWM systems also had an ON/OFF latency before attaining the target application pressure and inherent fall time before the system stops spraying after the solenoid valves close. These latencies could increase the error, particularly when using a system that operates at a higher frequency. Moreover, the PWM systems operated at stable pressures for less than the specified duty cycle time may have resulted in the inaccurate nozzle flow rate observed during the study. The tests were conducted with a specific nozzle, however, it is very much possible that different nozzles might also exhibit different magnitudes of pressure drop.

In the field tests, the PWM system maintained the target application pressure within the acceptable range for 77.0% to 89.0% of the time, indicating its ability to provide the application rate within the $\pm 10.0\%$ error. The pressure CV was below 5.0% for most of the time, signifying a consistent pressure between boom sections during operation. These results were significantly improved from using a flow-based system when applying the product at similar settings wherein it only operates for 32.0% of the time within the $\pm 10.0\%$ error. The droplet size spectra deviation when using a PWM system could occur mainly due to the improper nozzle selection. The system may deliver consistent droplet size spectra if the selected nozzle provides the desired droplet size within the wide range of application pressure thus, providing uniform product application. The systems' ability to manage pressure and thus provide uniform droplet spectra is particularly important for nozzle flow rate management and managing drift potential.

Moreover, the duty cycle accuracy within $\pm 5.0\%$ was lower in fields with irregular shapes and varying terrain (12.0%) than in a rectangular field with relatively flat terrain (54.0%). Accurate

duty cycle implementation is the key to achieving an accurate application rate; therefore newer approach as implemented during these tests might be executed to quantify control system response enhancements. The application rate accuracy within $\pm 5.0\%$ error was also lower in irregular-shaped fields (10.0% of the time) than the rectangular fields (46.0% of the time). Furthermore, the PWM system varied the duty cycles on the inner and outer boom section based on each control section's ground speed at various turning radii. The turn compensation functionality significantly reduced the application errors on curvilinear passes, thus effectively controlling pests and minimizing pesticide resistance and environmental damage.

In conclusion, crop producers will continue to adopt new liquid application technologies such as the PWM system to improve product application efficiency. However, operators should understand the system component and control system responses to achieve desired performance in the varying field and operating conditions to reduce the application errors. Future research and development on nozzle pressure monitoring, flow dynamic optimization during the application cycle, and new sensor integration for accurate duty cycle implementation might be considered to refine real-time nozzle flow management to truly realize the concept of precision agriculture to reduce application error, pesticide resistance, and environmental pollution.

Nozzle flow dynamics during control system response of Pulse Width Modulated technology-
equipped agricultural sprayer

by

Jonathan Viernes Fabula

B.S., Central Luzon State University, 2006

M.S., Central Luzon State University, 2011

A DISSERTATION

submitted in partial fulfillment of the requirements for the degree

DOCTOR OF PHILOSOPHY

Carl and Melinda Helwig Department of Biological and Agricultural Engineering
Carl R. Ice College of Engineering

KANSAS STATE UNIVERSITY

Manhattan, Kansas

2021

Approved by:

Major Professor
Dr. Ajay Sharda

Copyright

© Jonathan Viernes Fabula 2021.

Abstract

Crop producers utilize agricultural sprayers equipped with modern technologies such as pulse width modulation (PWM) system that can manage flow at nozzle-by-nozzle, thus have the potential to provide greater resolution for section control and reducing the environmental contamination. The introduction of precision technologies such as the PWM system has obvious benefits to the producers; however, a greater understanding of system functionality and operational accuracy is required for adoption and implementation. One of the greatest challenges is to manage nozzle level target application rate for large self-propelled systems during active section control and ground speed transitions. Therefore, this study was conducted to quantify the PWM system's performance under real-world operating conditions, with a goal to develop knowledge for producers to accurately implement this technology and suggest technology improvements for manufacturer's. A methodology was established to conduct system-level evaluation of the PWM system both in laboratory and field settings. In the laboratory setting, the pressure and flow dynamics of three commercially available PWM systems (Capstan PinPoint, John Deere ExactApply, and Raven Hawkeye) were evaluated. On the other hand, field tests were conducted using a New Holland SPF370F and Case Patriot 4440 agricultural sprayer to evaluate the PWM system's performance in varying field conditions. Both sprayers were equipped with a Raven Hawkeye PWM system and had a 36.6 m boom width. Novel analytical techniques were developed to generate a high spatial control-section level mapping of system performance parameters to quantify advantages and instances of application rate errors.

Laboratory test results show that different PWM systems provided different pressure drops when applying different application rates and pressures. The pressure drop was unique for different PWM systems, and it significantly increased with the increase in the application rate for three

systems. The pressure drop could vary the nozzle flow rate, which may significantly impact the application rate, thereby reducing the product efficacy. A pressure drop greater than 70.0 kPa from the target application pressure could cause the flow rate to vary beyond $\pm 10.0\%$ error. The three PWM systems also had an ON/OFF latency before attaining the target application pressure and inherent fall time before the system stops spraying after the solenoid valves close. These latencies could increase the error, particularly when using a system that operates at a higher frequency. Moreover, the PWM systems operated at stable pressures for less than the specified duty cycle time may have resulted in the inaccurate nozzle flow rate observed during the study. The tests were conducted with a specific nozzle, however, it is very much possible that different nozzles might also exhibit different magnitudes of pressure drop.

In the field tests, the PWM system maintained the target application pressure within the acceptable range for 77.0% to 89.0% of the time, indicating its ability to provide the application rate within the $\pm 10.0\%$ error. The pressure CV was below 5.0% for most of the time, signifying a consistent pressure between boom sections during operation. These results were significantly improved from using a flow-based system when applying the product at similar settings wherein it only operates for 32.0% of the time within the $\pm 10.0\%$ error. The droplet size spectra deviation when using a PWM system could occur mainly due to the improper nozzle selection. The system may deliver consistent droplet size spectra if the selected nozzle provides the desired droplet size within the wide range of application pressure thus, providing uniform product application. The systems' ability to manage pressure and thus provide uniform droplet spectra is particularly important for nozzle flow rate management and managing drift potential.

Moreover, the duty cycle accuracy within $\pm 5.0\%$ was lower in fields with irregular shapes and varying terrain (12.0%) than in a rectangular field with relatively flat terrain (54.0%). Accurate

duty cycle implementation is the key to achieving an accurate application rate; therefore newer approach as implemented during these tests might be executed to quantify control system response enhancements. The application rate accuracy within $\pm 5.0\%$ error was also lower in irregular-shaped fields (10.0% of the time) than the rectangular fields (46.0% of the time). Furthermore, the PWM system varied the duty cycles on the inner and outer boom section based on each control section's ground speed at various turning radii. The turn compensation functionality significantly reduced the application errors on curvilinear passes, thus effectively controlling pests and minimizing pesticide resistance and environmental damage.

In conclusion, crop producers will continue to adopt new liquid application technologies such as the PWM system to improve product application efficiency. However, operators should understand the system component and control system responses to achieve desired performance in the varying field and operating conditions to reduce the application errors. Future research and development on nozzle pressure monitoring, flow dynamic optimization during the application cycle, and new sensor integration for accurate duty cycle implementation might be considered to refine real-time nozzle flow management to truly realize the concept of precision agriculture to reduce application error, pesticide resistance, and environmental pollution.

Table of Contents

List of Figures	xiv
List of Tables	xvii
Acknowledgments.....	xviii
Dedication.....	xx
Chapter 1 - Introduction.....	1
1.1 Background.....	1
1.2 Agricultural Sprayer	2
1.2.1 Flow-based system.....	4
1.2.2 Pulse width modulation system	6
1.3 Problem Statement.....	9
1.4 Research Objectives.....	13
Chapter 2 - Nozzle Pressure and Flow Dynamics of Pulse Width Modulation (PWM) Nozzle	
Control Systems.....	15
2.1 Abstract.....	15
2.2 Introduction.....	17
2.3 Materials and Methods.....	20
2.3.1 PWM nozzle control systems.....	20
2.3.2 System set-up and instrumentation	21
2.3.3 Data collection	23
2.3.4 Data analysis	28
2.4. Results and Discussions.....	28
2.4.1 Pressure drop.....	28
2.4.2 Response time	35
2.4.2.1 Peak time and fall time	35
2.4.2.2 Stabilized pressure application time	38
2.4.3 Flowrate	41
2.5 Conclusion	44
Chapter 3 - Nozzle Pressure Uniformity and Expected Droplet Size Spectra of Pulse Width	
Modulation (PWM) Spray Technology	46

3.1 Abstract.....	46
3.2 Introduction.....	47
3.3 Materials and Methods.....	49
3.3.1 Machine set-up.....	49
3.3.2 Instrumentation	51
3.3.3 Data collection	53
3.4 Results and Discussions.....	56
3.4.1 Speed range.....	56
3.4.2 Pressure uniformity	58
3.4.2.1 Pulse width modulation system	58
3.4.2.2 Flow-based system.....	62
3.4.3 Coefficient of variation (CV).....	63
3.4.4 Expected droplet size spectra.....	66
3.4.4.1 Pulse width modulation system	66
3.4.4.2 Flow-based system.....	68
3.5 Conclusion	70
Chapter 4 - Duty Cycle Implementation of Pulse Width Modulated (PWM) – Equipped Agricultural Sprayer	72
4.1 Abstract.....	72
4.2 Introduction.....	74
4.3 Materials and Methods.....	77
4.3.1 Machine set-up.....	77
4.3.2 Instrumentation	79
4.3.3 Data collection	81
4.4 Results and Discussions.....	83
4.4.1 Speed data	83
4.4.2 Duty cycle accuracy.....	86
4.4.3 Application rate accuracy.....	88
4.5 Conclusion	91
Chapter 5 - Field Evaluation of Turn Compensation Feature of Pulse Width Modulation (PWM) – Equipped Agricultural Sprayer	92

5.1 Abstract.....	92
5.2 Introduction.....	94
5.3 Materials and Methods.....	96
5.3.1 Sprayer set-up	96
5.3.2 Data collection and analysis.....	98
5.4 Results and Discussions.....	99
5.5 Conclusion	106
Chapter 6 - Conclusion, Recommendation, and Practical Implication.....	107
6.1 General Conclusions	107
6.2 Recommendations for Future Work and Product Improvement.....	109
6.3 Practical Implications	111
References.....	114
Appendix A - Equipment Specifications	121
A.1 New Holland SP370F Sprayer.....	121
A.2 Case Patriot 4440 Sprayer.....	122
A.3 PCB Piezotronics Thin Film Membrane Pressure Transducer	123
A.4 Flow Technology Inc. Flow Meter	124
A.5 High Sensitivity DC Accelerometer	125
A.6 Baumer Ultrasonic Sensor	126
A.7 Topcon GR5 Receiver.....	127
A.8 Raven Viper 4+ Monitor.....	129
A.9 Capstan Solenoid Valve.....	130
A.10 Raven Hawkeye Nozzle Control Valve	131
A.11 John Deere ExactApply Solenoid Valve.....	132
A.12 FT205EV Digital Wind Sensor.....	133
A.13 WatchDog Sprayer Station 3349SSH	135
A.14 Topcon B110 GNSS Receiver	136
Appendix B - Data Acquisition System Specifications	138
B.1 CompactRIO (cRIO) Controller.....	138
B.2 National Instruments 9221 C Series Voltage Input Module	144
B.3 National Instruments 9870 C Series Serial Interface Module.....	146

B.4 National Instruments 9853 2-Port, High Speed Serial Interface Module	148
B.5 National Instruments 9205 C Series Voltage Input Module	150
B.6 Dell Latitude 14 3470.....	154
B.7 Keysight U8030 Triple-Output DC Power Supply	155
Appendix C - LabVIEW Program	157
C.1 The LabVIEW Program User Interface	157
C.2 The LabVIEW Program, Block Diagram.....	158
Appendix D - SAS Code Used in Data Analysis	162
D.1 Pressure Drop.....	162
D.2 Stabilized Pressure Application Time Change	170
D.3 Flow Rate Change.....	178

List of Figures

Figure 1.1. World and U.S Pesticide Applied in 2012 by Type (Atwood et al., 2017).	1
Figure 1.2. Pulled-Type (a) and Self-Propelled (b) Agricultural Sprayer.	3
Figure 1.3. Basic Components of Agricultural Sprayer.....	4
Figure 1.4. Solenoid ON State Time Variation during 40% and 80% Duty Cycle in 10 Hz Frequency. (Sharda et al., 2016)	7
Figure 1.5. Turn Compensation of PWM System Modulating the Individual Nozzles to Provide Uniform Application Regardless of Varying Speed Between the Inner and Outer Boom Sections (a) and a Spray System without Turn Compensation where Application Rate Error is Inevitable due to Inconsistent Product Application (b).....	8
Figure 2.1. Different Commercially Available Solenoid Valves and Nozzle Bodies Used in the Study.	21
Figure 2.2. System Set-Up and Instrumentation of S1 PWM System.....	24
Figure 2.3. Turret Position of S2 Nozzle Body when Operating at 15 Hz (a) and 30 Hz (b) System Frequency.	25
Figure 2.4. System Set-Up and Instrumentation of S2 PWM System.....	25
Figure 2.5. System Set-Up and Instrumentation of S3 PWM System.	26
Figure 2.6. Evaluation of PWM Nozzle Control System Response Time.....	27
Figure 2.7. Pressure Drop of the Different PWM Nozzle Control Systems (a) 10 Hz, (b) 15 Hz, and (c) 30 Hz when Applying at a Rate of 112.2 L ha ⁻¹ and 275.8 kPa Application Pressure at 50% Duty Cycle.	33
Figure 2.8. Pressure Response of the Different PWM Nozzle Control Systems (a) 10 Hz, (b) 15 Hz, and (c) 30 Hz when Applying at a Rate of 112.2 L ha ⁻¹ and 275.8 kPa Application Pressure at 50% Duty Cycle.	38
Figure 3.1. The New Holland SP370F Agricultural Sprayer Used in the Study.	49
Figure 3.2. Layout of the Sprayer Boom with 73 Nozzle Sections with a Group of either 1, 2, or 3 Nozzles. The Nozzles are Numbered from Left to Right Across the Boom.....	50
Figure 3.3. Capped Nozzle Body with the Solenoid Valve Removed to Measure Real-Time Boom Pressure.	51
Figure 3.4. The flowmeter Used to Measure the System Flow Rate.	52

Figure 3.5. Data Acquisition System Set-Up.....	53
Figure 3.6. Speed Distribution Plot (a) and Speed Range Distribution Map (b) for Field 1.	57
Figure 3.7. Speed Distribution Plot (a) and Speed Range Distribution Map (b) for Field 2.	58
Figure 3.8. Pressure Uniformity Plot (a) and Pressure Uniformity Map (b) for Field 1 when Using a PWM System.....	60
Figure 3.9. Pressure Uniformity Plot (a) and Pressure Uniformity Map (b) for Field 2 when Using a PWM System.....	60
Figure 3.10. Pressure Uniformity Plot (a) and Pressure Uniformity Map (b) for Field 1 in a Flow-Based System.	63
Figure 3.11. Pressure Uniformity Plot (a) and Pressure Uniformity Map (b) for Field 2 in a Flow-Based System.	63
Figure 3.12. Pressure CV Plot (a) and CV Distribution Map (b) for Field 1 when Using a PWM System.....	65
Figure 3.13. Pressure CV Plot (a) and CV Distribution Map (b) for Field 2 when Using a PWM System.....	65
Figure 3.14. Droplet Size Spectra Uniformity Plot (a) and Map (b) for Field 1 when Using a PWM System.	66
Figure 3.15. Droplet Size Spectra Uniformity Plot (a) and Map (b) for Field 2 when Using a PWM System.	67
Figure 3.16. Droplet Size Spectra Uniformity Map when Using a Nozzle Tip with a Wide Range of Application Pressure to Provide the Target Droplet Size.....	68
Figure 3.17. Droplet Size Spectra Uniformity Plot (a) and Map (b) for Field 1 in a Flow-Based System.....	69
Figure 3.18. Droplet Size Spectra Uniformity Plot (a) and Map (b) for Field 2 in a Flow-Based System.....	70
Figure 4.1. The Case Patriot 4440 Agricultural Sprayer Used in the Study.....	78
Figure 4.2. Layout of the Sprayer Boom with 72 Nozzle Sections with Groups of Either 1, 2, or 3 Nozzles. The nozzles are Numbered from Left to Right Across the Boom.	78
Figure 4.3. Capped Nozzle Body with the Solenoid Valve Removed to Measure Real-Time Boom Pressure.	80
Figure 4.4. GNSS Receiver and Base Station.....	80

Figure 4.5. Auxiliary GNSS Receiver (B110) Located Right Next to Nozzle 16.	81
Figure 4.6. Data Acquisition system Set-Up (a) and LabVIEW Program Used to Record the Data.	83
Figure 4.7. Speed Accuracy map in Field 1 Considering the Difference in Speed During Straight Passes Between the GPS 1 and GPS 2.	84
Figure 4.8. Speed Accuracy Map in Field 2 Considering the Difference in Speed During Straight Passes Between the GPS 1 and GPS 2.	85
Figure 4.9. Duty Cycle Accuracy Distribution Plot (a) and Map (b) when Using a PWM System in Field 1.	86
Figure 4.10. Duty Cycle Accuracy Distribution Plot (a) and Map (b) when Using a PWM System in Field 2.	88
Figure 4.11. Application Rate Accuracy Distribution Plot (a) and Map (b) when Using a PWM System Field 1.	89
Figure 4.12. Application Rate Accuracy Distribution Plot (a) and Map (b) when Using a PWM System in Field 2.	90
Figure 5.1. The Self-Propelled Agricultural Sprayer Used in the Study.	97
Figure 5.2. Layout of the Sprayer's Auto-Nozzle Control Function with Nozzle Valves Controlled Individually, in Tandem, or in a Group of Three.	98
Figure 5.3. Maps Showing the Different Types of Turns in Field 1 (a), Field 2 (b), and Field 3 (c).	101
Figure 5.4. Speed of Each Nozzle During Right Turn at Different Turning Radii.	103
Figure 5.5. Application Rate of Each Nozzle when Turning Right at Different Turning Radii.	105
Figure 5.6. A Sprayer with Turn Compensation Feature Applying the Product Uniformly Across the Field.	106

List of Tables

Table 2.1. Different Nozzle Tips Used in the Study.....	23
Table 2.2. Pressure Drop at the Nozzle when Applying at Different Application Rates and Pressures at 10 Hz.	29
Table 2.3. Pressure Drop at the Nozzle when Applying at Different Application Rates and Pressures at 15 Hz.	30
Table 2.4. Pressure Drop at the Nozzle when Applying at Different Application Rates and Pressures at 30 Hz.	31
Table 2.5. Average Peak and Fall Time of Each PWM System at 10 Hz Frequency.....	35
Table 2.6. Average Peak and Fall Time of Each PWM System at 15 Hz Frequency.....	36
Table 2.7. Average Peak and Fall Time of Each PWM System at 30 Hz Frequency.....	36
Table 2.8. Stabilized Pressure Application Time Change when Using the Different PWM Systems at 10 Hz.....	40
Table 2.9. Stabilized Pressure Application Time Change when Using the Different PWM Systems at 15 Hz.....	40
Table 2.10. Stabilized Pressure Application Time Change when Using the Different PWM Systems at 30 Hz.....	41
Table 2.11. Flow Rate Change when Using the Different PWM Systems at 10 Hz.	42
Table 2.12. Flow Rate Change when Using the Different PWM Systems at 15 Hz.	43
Table 2.13. Flow Rate Change when Using the Different PWM Systems at 30 Hz.	43
Table 3.1. Expected Droplet Size Spectra at Different Application Pressures of the Nozzles Used in the Study. (www.teejet.com)	55
Table 4.1. Speed Difference Between the GPS 1 and GPS 2 During Straight Passes in Field 1.	84
Table 4.2. Speed Difference Between the GPS 1 and GPS 2 During Straight Passes in Field 2.	85
Table 5.1. Turn Classification for Different Ranges of Turning Radii.....	99
Table 5.2. Field Area Applied with Product at Different Turning Radii.	102
Table 5.3. Speed Difference Between the Boom Sections at Each Turning Radius.	103
Table 5.4. Application Rate Error on the Left and Right Boom at Each Turning Radius.	104

Acknowledgments

First and foremost, I would like to thank our Lord for all the blessings that He bestowed upon me and all the guidance that He provided throughout my life. I would like to express my profound gratitude to Dr. Ajay Sharda, my major professor, for the opportunity that he had given me to be part of his research team. Thank you very much for the support, guidance, and words of encouragement that motivated me to complete my degree. Likewise, sincere appreciation is also extended to my supervisory committee, Dr. Daniel Flipppo, Dr. Ignacio Ciampitti, and Dr. Qing Kang, for their invaluable support, insightful, and technical feedback to accomplish this undertaking. Special thanks also to Dr. Scott Thompson for serving as the chairperson of my examining committee.

I would also like to give my grateful appreciation to William “Billy” Crable for his support and assistance during our field tests. Without his help, this work will not be possible. Thank you also to the FARMS (Fusing Automation and Robotics in Ag Machine Systems) Lab research team – Sylvester, Manoj, Braden, Eli, Prashanta, Ketan, and Amar, for the assistance in conducting my research; to the Biological and Agricultural Engineering – Graduate Student Organization (BAE-GSO); to the Philippine Student Association (PhilSA); to the Filipino Community in Kansas, and all my fellow graduate students at the Biological and Agricultural Engineering Department. I would also like to express my sincerest appreciation to my fellow ERDT scholars – Elmar, Wendy, Claire, Pau, and Melba, for the camaraderie and moral support.

Special thanks to Dr. Joseph Harner, Department Head of the Biological and Agricultural Engineering, staff members – Arlene Jacobson, Jamie Boeckman, Lisa Wuggazer, and the faculty members for their unwavering support throughout my journey as a graduate student. I would also like to extend my sincerest appreciation to the industry partners (CNH Industrial, Raven Industries,

John Deere, Capstan Ag Systems, Inc., and Teejet Technologies) that provided all the necessary equipment and technical support to finish my research.

My deepest gratitude to the Department of Science and Technology – Engineering Research and Development for Technology (DOST-ERDT) of the Republic of the Philippines and the Central Luzon State University (CLSU) for the financial support and the opportunity that they had given me to pursue higher education. Sincerest thanks also to Ms. Precious Joan Sibulboro for her untiring effort to provide all the support needed to finish my degree.

My heartfelt appreciation also to my parents, Lolito (+) and Filipina, my brothers, John David, and Janssen Van, for all the love and support they have given me throughout my career.

Most importantly, I deeply appreciate all the love, support, and understanding from my wife, Jeannie-Rose, and my kids, Shawn Lawrence and Mishka Attiya, who have been the source of my strength and inspiration through these years. Your love and encouragement pushed me to strive harder. Without you, none of this would have been possible. I love you 3000!

Lastly, to everyone who, in one way or the other, contributed and helped to make this work a reality, thank you very much!

Go Cats!

Dedication

This work is dedicated to;
my kids Shawn Lawrence and Mishka Attiya,
my wife, Jeannie-Rose,
my brothers, John David and Janssen Van,
my parents, Lolito (+) and Filipina.
I hope I've made you all proud.

Chapter 1 - Introduction

1.1 Background

The global population is projected to increase to 10.9 billion by 2100 (United Nations, 2019). This projection is going to raise the demand for food, fiber, feed, and energy. The agricultural sector needs to boost its production to ensure enough food supply to the growing population. It has been a common practice among crop producers in the U.S. to apply an extensive amount of pesticides to protect crops from pests and diseases and increase crop yields. In the 2017 U.S Environmental Protection Agency report, about 6 billion pounds of pesticides were applied globally while crop producers in the U.S utilized over 1.1 billion pounds annually in 2011 and 2012 (Figure 1.1), with herbicides accounting for the biggest portion of the usage (Atwood et al., 2017).

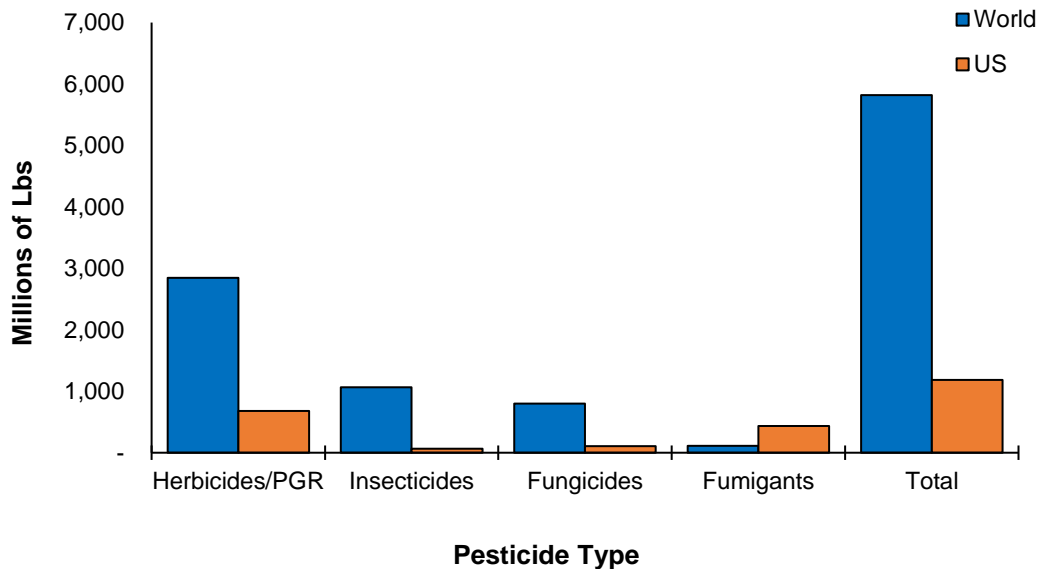


Figure 1.1. World and U.S Pesticide Applied in 2012 by Type (Atwood et al., 2017).

This volume accounted for \$56 billion and \$ 9 billion of pesticide expenditures worldwide and in the U.S in 2012, respectively

The pesticide application increases in areas wherein crop producers practice no-till farming (Luck et al., 2011) since it's common to spray more than twice to minimize weed growth. The advantages of pesticide application have been undeniable. However, the inappropriate application of these chemicals may present a threat to human health and the environment (Sharda et al., 2016; Nicolopoulou-Stamati et al., 2016; WHO-UN, 1990). Agricultural chemicals are resistant to degradation and may easily volatilize and may remain on the soil surface for a longer period and therefore susceptible to surface run-off (Larson et al., 1995) and leaching (Van Der Werf., 1996). Balsari et al. (2009) and Panneton et al. (2001) estimated that more than 45% of applied agricultural chemicals missed the target and end-up polluting the surface and groundwater. In a survey conducted by Pimentel et al. (2014), the excessive application of pesticides contaminated 10% of the community wells and 14% of the rural domestic wells. Therefore, it is important to evaluate the efficiency at which these chemicals were applied, considering the enormous amount of product applied and the investments involved.

1.2 Agricultural Sprayer

The continuous development of agricultural production techniques helps improve the soil, water, nutrient, and pests management to increase the crop yield potential. Agricultural sprayers have become more efficient in applying pesticides due to technological advancements in computers, sensors, and actuators. It had changed how the farmers and applicators apply pesticides on the field. Employing sprayers equipped with these sensor technologies in the chemical

application may potentially improve crop quality and yield (Sharda et al., 2013; Popp et al., 2013; Chen et al., 2012).

A sprayer is an equipment that is utilized to apply pesticides on crops. Agricultural sprayer varies in types and sizes, from pulled-type sprayers (Figure 1.2.a) and self-propelled units (Figure 1.2.b) with boom widths ranging from 4 to 120-feet depending on its design. It's a fully integrated system composed of several parts and components that work together to apply the correct product rate on the crops based on the product label specifications.



Figure 1.2. Pulled-Type (a) and Self-Propelled (b) Agricultural Sprayer.

A typical agricultural sprayer comprises of different major components, including the tank, pump, plumbing system, control valve, pressure relief valve, boom shut-off valve, and nozzle to deliver the product to the target (Figure 1.3). The spray system is expected to apply the agricultural chemicals to the field uniformly. This can be achieved by selecting a nozzle based on the target application rate and desired operating speed. The application pressure can be set using the control valve to deliver the target nozzle flow rate. The sprayer is calibrated to apply the product uniformly across the field by ensuring that the target application pressure is maintained to deliver the right

flow rate and droplet size. The nozzles are replaced once the flow rate exceeded the 10% threshold of the expected flow rate.

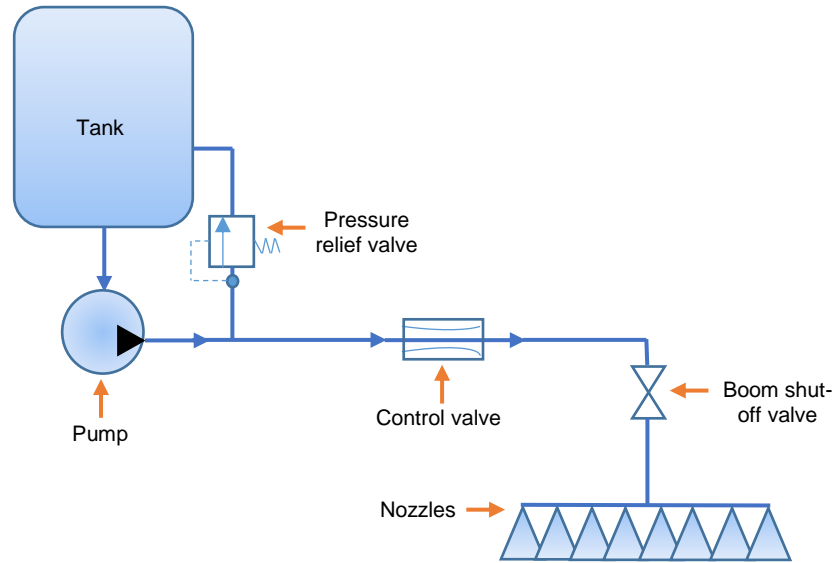


Figure 1.3. Basic Components of Agricultural Sprayer.

The application accuracy depends on the proper system calibration and the operator's driving skills during operation. Electronic spray control systems were developed to minimize the operator errors and errors caused by varying operating speeds. These type of systems is now commonly used to manage the application rate during speed transitions.

1.2.1 Flow-based system

A flow-based control system regulates the flow to vary the rate. It is commonly employed in agricultural spray application because it is easier to manage than pressure-based systems. The flow-based system is calibrated by programming the flow meter and regulating valve calibration number (VCN) recommended by the manufacturer. Once it is set-up, the operator mostly does not need to change the recommended VCNs. The flow meter controls the system flow rate depending

on the calibration number, while the VCN manages the expected response of the flow control valve motor. The VCN should be properly selected to implement optimal system response (Sharda et al., 2016). The system uses the speed information provided by the global positioning system (GPS). The system flow rate is measured through an inline flow meter that provides feedback to the rate controller, which adjusted the regulating valve to maintain the target system flow based on the operating speed, sprayer swath, and application rate commonly programmed in the controller by the operator. The control system also utilizes the feedback from the flow meter and sends commands to the regulating valve that adjusted the system flow with the calculated value.

The boom shut-off valve controls the product flow to the boom. The operator can shut the sprayer ON and OFF when turning on headlands or in the no-spray zone using the boom -shut-off valves. The majority of agricultural sprayers have boom sections that allow independent control of each section across the boom. This setting permits the operator to manually turn-off a portion of the boom rather than the whole boom itself using the switch box. Therefore, over-application may be reduced by partially turning the sections OFF, especially on areas where partial boom widths are required.

Two types of valves can supply the fluid to the boom; a two-way and a three-way boom valve. A 2-way boom valve means that there is a product flow during ON-state or no flow during OFF-state. During OFF-state, the product volume remains in the system while the control system manages the flow to the new target value. The system flow is adjusted using the flow feedback and regulating valve to represent the number of boom valves on the ON state. The target application rate is maintained through flow compensation, wherein the flow is regulated during boom valves ON and OFF state. In a 3-way boom valve, the flow from the boom sections that are

off is redirected to the tank through one outlet. Therefore, system pressure or the corresponding flow are maintained regardless of section actuation.

1.2.2 Pulse width modulation system

To compensate for the challenges caused by application errors as a result of using larger and faster machines, technologies such as pulse width modulation (PWM) systems are implemented to apply chemicals at finer spatial resolution (Needham et al., 2012). PWM system is one of the technologies that are currently being implemented in large self-propelled sprayers. PWM spray control technology operates on two major components: duty cycle, which is the percentage of the total time the signal is in the HIGH or ON state to complete one cycle, and frequency, which is the number of cycles completed a second. A digital signal regulates the nozzle period in the ON-state (high with 12 V direct current) and OFF state (low with 0 V direct current). Majority of PWM system from manufacturers including Capstan, Raven, and Teejet operates at 10 Hz frequency while John Deere had a system that operates at a higher frequency (15 Hz and 30 Hz). A 10 Hz frequency system means that they operate at ten cycles per second or a 100 millisecond (ms) cycle to actuate the solenoids. For example, when operating at 40% duty cycle, it indicates that the solenoids are in the ON state for 40 ms and in the Off state for 60 ms during a 100 ms cycle. On the other hand, a system operating at 80% duty cycle means that the nozzle will be in the ON state for 80 ms and in the OFF state for 20 ms. Therefore, an 80% duty cycle will provide twice the product volume than the 40% duty cycle during a 100 ms cycle (Figure 1.4)

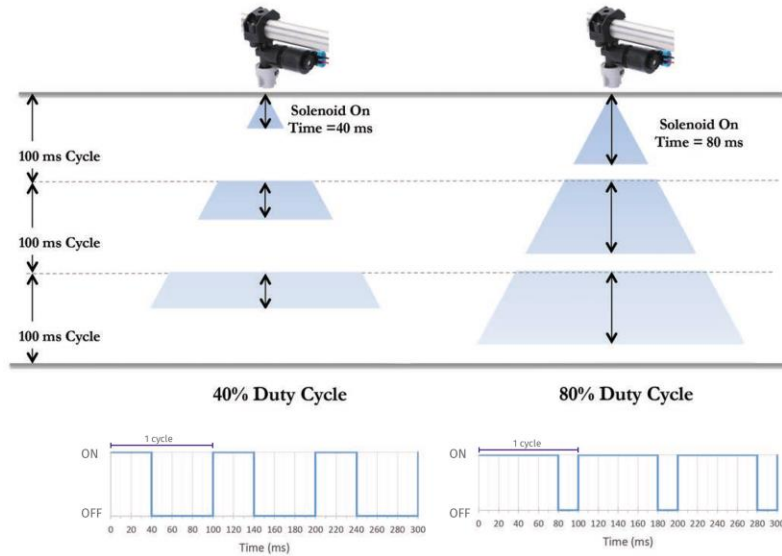


Figure 1.4. Solenoid ON State Time Variation during 40% and 80% Duty Cycle in 10 Hz Frequency. (Sharda et al., 2016)

In a PWM system, the target pressure is set within the electronic control unit, and the liquid control system provides the application fluid to pressurized the boom. Nozzle flow rate is varied by pulsing an electronically-actuated solenoid valve fitted in the nozzle by changing the duty cycle. The solenoid is an electromagnet that opens and closes the nozzle flow using the plunger and a spring. The initial solenoid position is closed held shut by the spring to retain the drip check's original purpose. Therefore, flow can be controlled on a nozzle by nozzle basis by employing the right duty cycle according to each nozzle's speed and target application rate during parallel and curvilinear passes (i.e turning). PWM technology uses the as-applied map coverage information to control individual nozzles' actuation.

The PWM system intends to deliver real-time flow rate changes without impacting the application pressure, improving the application accuracy by providing a uniform droplet size distribution during product application. The PWM system is also capable of instantly turning the solenoid ON and OFF, which is possible because of the actuation response of the solenoid valve.

The product is applied at the desired pressure while immediately closing, thus eliminating product drain when the solenoids are de-energized. The even and odd nozzles are also programmed to turn On and Off alternately, preventing skips during operation. The PWM system is also capable of compensating the flow from the inner and outer boom sections by regulating the product flow to the individual nozzles when applying in curvilinear paths based on each nozzle's speed during operation. For example, if the sprayer is turning left, the PWM system compensates the flow rate at each nozzle by increasing the nozzles' duty cycle on the outer boom sections, thereby increasing the flow rate. On the other hand, the system reduces the nozzles' flow rate on the inner boom sections by decreasing the duty cycle resulting in uniform coverage (Figure 1.5.a). Application errors could occur if the system does not compensate for each nozzle's flow rate when applying in curvilinear paths (Figure 1.5.b).

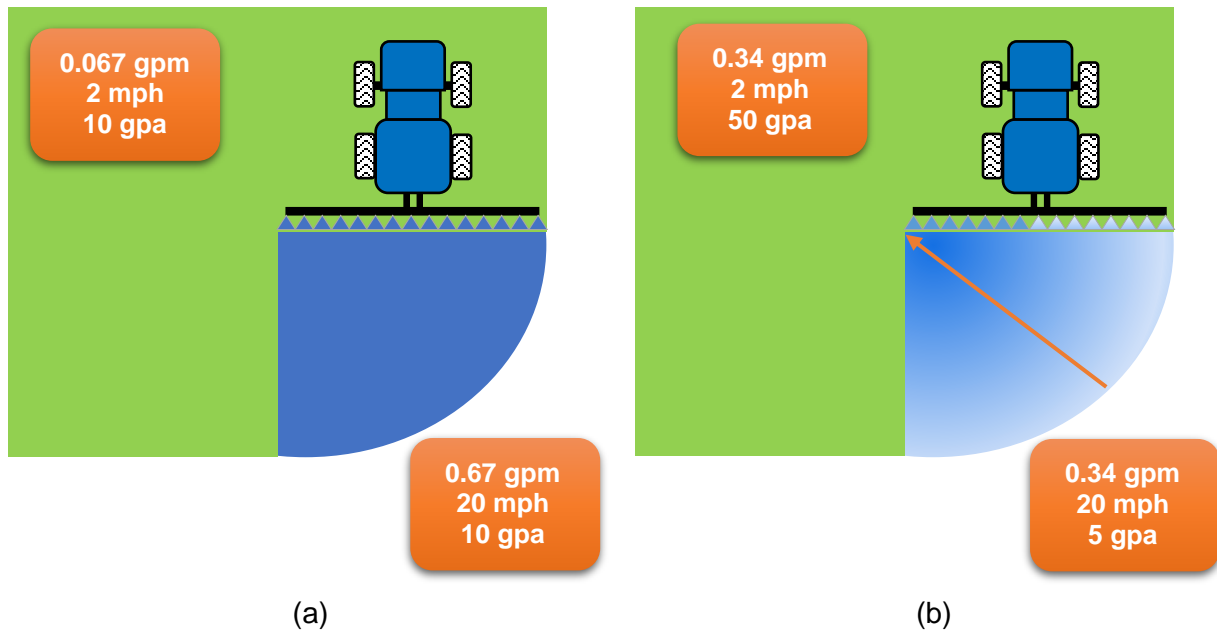


Figure 1.5. Turn Compensation of PWM System Modulating the Individual Nozzles to Provide Uniform Application Regardless of Varying Speed Between the Inner and Outer Boom Sections (a) and a Spray System without Turn Compensation where Application Rate Error is Inevitable due to Inconsistent Product Application (b).

Several manufacturers of agricultural sprayers are providing options for a PWM liquid application technology, which includes Raven Industries, Capstan Ag Systems, Teejet Technologies, and John Deere. These PWM systems can be retrofitted to the sprayer using the existing feedback mechanism and flow control systems to increase and decrease the system's flow rate. Changing the flow rate is necessary to maintain the target application rate and provide a sufficient product in the system while changing the duty cycle.

1.3 Problem Statement

Agriculture is highly dependent on the application of agricultural chemicals. Hence, chemical application became one of the most significant aspects of the crop production system as it may potentially increase the yield and provide a better crop quality. The application of chemicals reduces crop damage, which ensures that the agricultural sector can supply enough foods and fibers to the increasing global population. However, the chemical application has been highly scrutinized because it produces volatile organic compounds that may pose a threat to humans and the environment. Agricultural chemicals may also impact waterways through surface run-off and contaminate groundwater through deep percolation because they are resistant to degradation (Brady et al., 2006; Kuivila & Foe, 1995; Werner et al., 2004).

Agricultural sprayers became an important part of agricultural production due to their capability to cover large areas. Spray application technologies have been continuously developed to improve product application (Giles et al., 2008; Han et al., 2001; Lebeau et al., 2004; Miller et al., 1992; Zhang et al., 1995). These technologies have become important components of agricultural sprayers. Crop producers utilize current spray application technologies to ensure that the product is applied to effectively control pests (Luck et al., 2011; Rockwell et al., 1996). These

technologies should be able to maintain the target rate all the time. This can be achieved by ensuring that the product flow management in the plumbing system is accurate regardless of speed, nozzle or boom section actuation, or operating in straight or contour passes. Most importantly, the flow should match the nozzle ground speed. The system should also maintain the coverage by maintaining a uniform droplet size irrespective of travel speed. It should maintain the target pressure to provide the desired droplet size and a uniform overlap between nozzles to minimize drift potential and reduce environmental contamination.

The flow-based system has been implemented in agricultural sprayers about 10 to 15 years ago. Flow-based system regulates the flow to vary the rate. It utilizes the feedback from the flow meter and sends a command to the regulating valve based on the target rate, speed, and boom width to adjust the system flow. However, there have been continuous concerns regarding the flow-based system in the past decade. The system cannot maintain the application pressure during operation, which could impact the droplet size. Sharda et al. (2013) reported a pressure variation of 7.0% to 20.0% during operation. There is also an issue regarding controller response error due to the system's latency to immediately adjust the flow based on the field conditions aside from the pressure taking too much time to stabilize. Previous study shows that pressure stabilization times in the flow-based system were 25.2 s during section control actuation (Sharda et al., 2011). There is also a concern about the off-rate error. The flow-based system does not take into consideration the speed of each nozzle when delivering the flow. The system provides a single flow value across all the nozzles in the boom regardless of the nozzle or boom section speed. Sharda et al. (2011) reported a nozzle off-rate between -36.0% to +28.7% during point row operation due to the system's latency. Due to the flow-based system's inability to maintain the application pressure,

there is also a concern regarding off-target application due to drift, particularly when applying at a higher pressure.

Concerns regarding application rate error still exist when operating large agricultural sprayers as it may increase the cost of production due to product loss (Luck et al., 2010a). The application error can be due to under-and over-application. One of the most critical problems that have been sustaining and expanding over the year is pesticide resistance. Due to the inaccurate, inappropriate, and incomplete application, some of the pests do not receive a complete dosage or are not covered and eventually become resistant to pesticides. Heap (2020) reported that there are 547 instances of herbicide resistance in the US, and 47 resistant weeds are found in Kansas and Nebraska. Therefore, producers need to be cautious when applying chemicals to manage pests and diseases in field crops.

PWM system is one of the current spray technologies implemented in agricultural sprayers. In a PWM system, the application pressure should be rapidly achieved and maintained for the right duration depending on the duty cycle. Then, it should immediately shut off the flow when the solenoids are turned off. In addition, any variation in the application pressure caused by the PWM valves and the system's inability to immediately attain the target pressure and maintain that pressure during each cycle to deliver the target flow rate may influence the chemical application accuracy (Shahemabadi et al., 2008). The nozzle flow rate is managed by changing the duty cycle based on the speed of each nozzle. Each nozzle must deliver a uniform flow rate and maintain a uniform product application during operation (Needham et al., 2012). Any fluctuation in the flow rate could result in the inaccuracy of spray outputs (Silva et al., 2018). The system should deliver the product at the target application pressure to attain the desired nozzle flow rate. Operating at the target application pressure is also critical in maintaining a correct spray angle and droplet size.

The recommended droplet size based on product label specification must be followed when applying chemicals to efficiently control pests and achieve the right spray coverage and minimize spray drift (Needham et al., 2012). Applying pressure lower than 207.0 kPa may reduce the spray fan angle (Daggupati, 2007) and produce courser droplets. Operating at 276.0 kPa or above is recommended to minimize the pulsing effect on droplet size due to pressure drop across the nozzle valves (Butts et al., 2019). But, there are still issues concerning the PWM system's operation at lower duty cycle and capability to maintain a uniform pressure during operation at varying field conditions. Lang (2013) reported inconsistency in the volume median diameter when using a pre-orifice nozzle and increased driftable fines when operating at lower duty cycles.

Also, Shahemabadi et al., (2008) reported the control system's inability to maintain the target application pressure across the sprayers boom due to fluctuations caused by PWM valves. Latencies in the response of the control system are also reported in several studies. Mangus et al. (2017) reported a 20.0 millisecond (ms) latency before the system attains the target pressure. Bennur et al. (2010) reported a 0.5 to 2.1 s response time of the PWM system when using variable rate nozzles, while Yang (2001) concluded that a 1.0 to 2.0 s is required for the VRA system to provide the target application rate with application errors ranging from 5.2% to 5.8%. Application errors can be magnified by the latency on the control system's response to the GPS signal and attaining the target pressure.

The increase in the cost of agricultural inputs demands an efficient and timely application of chemicals. The producers aim to minimize losses caused by under- and over-application since profits are declining. Producers utilize new spray application technologies to efficiently and effectively manage agricultural inputs. The industry has responded to the rising demand for self-

propelled sprayers with a larger swath by developing new control technologies and real-time data management.

With the information available in the flow-based system and the knowledge on how the PWM system is set-up, there is a need to systematically study each of the components that will impact flow delivery, flow rate management, and flow rate implementation.

These spray control technologies need to be evaluated and properly understood to ensure their proper operation and performance. Understanding the impact of the pressure, flow dynamics, and the control system response of the PWM technology to the application accuracy is necessary when utilizing this new spray application technology. This study will provide the producers with information regarding the actual benefits of utilizing new technologies such as the PWM system and provide the operators with a better understanding of machine factors that may impact the sprayer's performance when applying the product in field conditions. The knowledge that will be gained in this study will not only provide helpful information to the sprayer manufacturer to further improve the existing technology but will also give confidence to the producers in implementing the PWM technology for better management of crop inputs, increase profits, and minimize the environmental impacts of agricultural chemicals.

1.4 Research Objectives

Inconsistencies in pressure and flow rate may occur during field operation due to the ON/OFF actuation of the solenoid valves. The variation in duty cycle is dictated by the speed of operation, which could frequently change due to terrain and the field's shape. Sprayer operators do not have the means of recognizing if the system is properly applying the correct amount of product and the potential application error during operation. Operators will be unable to make the necessary

adjustment to the sprayer to minimize such errors. Therefore, producers, operators, and even the sprayer manufacturers must understand the PWM technology's performance to utilize its full potential and improve the system further. The overall objective of this study is to evaluate the control system response of the PWM control system. This research specifically aims to;

1. Understand the pressure drop, flow dynamics, and control system response of solenoid and nozzle body,
2. Quantify application pressure and droplet size spectra uniformity during field operation,
3. Assess the application rate accuracy through correct duty cycle implementation, and
4. Evaluate the importance of turn compensation technology in product application.

Chapter 2 - Nozzle Pressure and Flow Dynamics of Pulse Width Modulation (PWM) Nozzle Control Systems

2.1 Abstract

Crop producers in the United States apply 1.1 billion pounds of various types of agricultural chemicals that cost \$10.6 billion per year. These chemicals are resistant to degradation and volatilization. Most of them end up contaminating surface waters and groundwaters through surface run-off and leaching. PWM is an emerging application technology that applies the product at a constant pressure by varying the solenoid duty cycle to maintain the application rate. Limited knowledge and studies are available that show how commercial PWM systems perform during operation. This study evaluates the pressure drop, flow rate variations, and response time of the different PWM systems during application. Three PWM nozzle control systems, Capstan PinPoint II, John Deere ExactApply, and Raven Hawkeye, referred to as S1, S2, and S3, were used in this study. Data on nozzle pressure, boom pressure, flow rate, and response time were recorded under different duty cycles (25%, 50%, 75%, and 100%) and operating frequencies (10 Hz, 15 Hz, and 30 Hz) for different application rates (112.2 L ha⁻¹ and (187.1 L ha⁻¹) and application pressures (275.8 kPa and 448.2 kPa) at 1kHz using a LabVIEW program and a cRIO data acquisition system. Results indicated that the PWM systems perform differently when operating at various application rates, pressures, duty cycles, and system frequencies. Each PWM system provided a different pressure drop at the nozzle during operation. The increase in application rate and target pressure increased pressure drop. The percent change in flow rate with respect to the expected flow was also significantly different between the PWM systems, which could be due to the differences in pressure provided at the nozzle during operation. The PWM systems also showed latency before

reaching the target application pressure during operation. The systems also operated at less time than the specified duty cycle at stable target pressure while also continued to spray even after the solenoid valves were closed. The application pressure during peak and fall time, and time of stable application pressure within a cycle should be given careful consideration when selecting a PWM system, as they can contribute to product application errors. Operators should also consider the pressure drop both with the selected PWM system and target application rates to set-up the system to apply at the desired pressure. The manufacturers mostly recommend operating the PWM system at 10 Hz system frequency. But for the purpose of this study, the system frequency of each PWM system was varied to 10 Hz and 15 Hz for S1, 15 Hz and 30 Hz for S2, and 10 Hz, 15 Hz , and 30 Hz for S3. Producers should expect a difference in pressure drop, stabilized pressure application time, and flow rate if they opted to operate at a higher frequency. The results of this study were only applicable to the type of nozzle bodies and nozzle tips used. The data will differ based on the dual orifice valve coefficient equation. The larger the second orifice, the more the pressure drop. This will affect the final orifice pressure, as well as the flow rate. This study did not address the impact of flow resistance caused by the differences in the design of nozzle bodies and nozzle types.

2.2 Introduction

The agricultural chemical application remains one of the most important elements of crop production systems, with U.S. farmers using 1.1 billion pounds of 600 different pesticides amounting to \$ 9.0 billion in 2012 (Atwood et al., 2017). The application of agricultural chemicals has increased, especially in no-till farming (Luck et al., 2011; Lebeau et al., 2004). Producers practicing no till-farming usually spray more than twice to minimize the impact of pests and diseases on their crops. The increase in agricultural chemical use potentially poses a threat to human health and the environment (Nicolopoulou-Stamati et al., 2016; Townson, 1992). It is estimated that more than 45% of applied agricultural chemicals are not deposited on the target and end up contaminating the surface waters and groundwater. (Balsari et al., 2009; Panneton et al., 2001). The main reason behind this is that most of the agricultural chemicals are resistant to degradation and volatilization and will remain on the soil surface for a longer period and, therefore, susceptible to run-off (Larson et al., 1995) and leaching (Van Der Werf., 1996)

To minimize the impact of agricultural chemicals and also to be more efficient with chemicals to save inputs costs, producers are now adopting newer application technologies with wider booms to make sure the target sites receive right rate of pesticides and to reduce application inaccuracies. (Luck et al., 2011; Rockwell et al., 1996). Precision application technologies, including variable rate and section control technologies, can potentially reduce off-rate application errors that might occur due to skipped-application, multiple-application, or unintentional-application to environmentally sensitive crops or areas. However, application errors (over- and under-application) still exist especially when operating large self-propelled sprayers during section control and ground speed transitions. Application errors also potentially increase the production cost (Luck et al., 2010a) due to the system's inability to provide the correct amount of pesticides

resulting in over-and under-application (Lebeau et al., 2004). One of the most critical impacts of application errors has been the growing resistance to pesticides making many formulations no longer effective for required pest control. Currently, there are 547 cases of herbicide-resistant weeds globally wherein 23 weed species have developed resistance to 167 different herbicides. Forty-seven resistant weeds are found in Kansas and Nebraska (Heap, 2020)

Currently, most spray application systems utilize flow-based systems. However, past studies have exhibited that application errors could occur in a flow-based system due to pressure deviations (Sharda et al., 2010; Sharda et al., 2013). System latencies primarily caused the pressure variation to maintain accurate pressure for the desired application rate during speed transitions and section control. Similar results were observed during field application using large self-propelled sprayers where application errors beyond $\pm 10\%$ of target application rate were observed in 64% of the field (Luck et al., 2011, Sharda et al., 2012).

Pulse width modulation (PWM) technology is currently being utilized more commonly on large self-propelled agricultural sprayers. PWM spray control systems operate on two key components: duty cycle and frequency. The duty cycle is the amount of time that the signal is in a HIGH or ON state as a percentage of the total time to complete a cycle. The frequency, indicated in Hertz (Hz), is the number of cycles completed in a second. The PWM technology allows the flow rate of spray through a nozzle to be controlled independent of pressure and droplet size (Giles, 2009) This allows the PWM system to control the product flow without significant variation on droplet size spectra, distribution, and velocity (Giles et al., 1996; Giles et al., 2003). Target liquid pressure is programmed within the electronic control unit, and the system maintains the boom pressurized by supplying it with the right amount of application fluid. Nozzle flow rate is accomplished by pulsing an electronically actuated solenoid valve located directly upstream of the

nozzle by changing the duty cycle. Since flow rate can be controlled on a nozzle by nozzle basis by implementing the correct duty cycle based on the speed of each nozzle, PWM rate control system has the potential to implement rate control for applications both during straight and curvilinear maneuvers (i.e turning). Commercial PWM controllers are developed for boom sprayers with all the nozzles having a synchronized control while the accuracy of the controllers still needs further improvement (Giles et al., 2008). Past research in a laboratory set-up has shown that PWM system could maintain the boom pressure irrespective of the number of active nozzles during nozzle section actuation (Mangus et al., 2017), but simulated application rate maps showed application errors especially at a lower duty cycle.

Once the solenoid is actuated during each cycle, desired application pressure should be attained rapidly and should remain stable for correct duration representative of duty cycle; and then quickly drop to shut-off flow when the solenoid is switched off. Additionally, any potential fluctuation in the pressure caused by PWM valves and the PWM system's inability to quickly achieve the desired pressure and maintain that pressure during the cycle time to deliver the desired flow rate may impact the accuracy of chemical application (Shahemabadi et al., 2008). Therefore, it is imperative to understand the pressure and flow dynamics during solenoid On and Off actuation during a cycle at different duty cycles, since these parameters manage product flow rate at each nozzle.

Understanding pressure dynamics is particularly critical as the PWM system intends to provide real-time flow changes based on selected target application pressure. Sufficient knowledge is not available on the extent of pressure drop across different solenoid-operated nozzle bodies. The pressure drop across solenoids and pressure dynamics during a PWM cycle could impact the flow consistencies, resulting in application rate errors. This study was conducted to understand the

pressure and flow dynamics across different solenoid-actuated nozzle bodies for PWM control systems. The specific objective of this research was to quantify the pressure drop, flow rate, and response time across different solenoid-actuated nozzle bodies operated by PWM control systems at different application rates and pressures as influenced by duty cycles and operating frequencies.

2.3 Materials and Methods

2.3.1 PWM nozzle control systems

Three commercially available solenoid-actuated nozzle bodies, including PWM nozzle control systems, were used in this study. These PWM systems were the Capstan Pinpoint II (Capstan Ag Systems, Inc., Topeka, KS), John Deere ExactApply (Deere and Company, Moline Il), and Raven Hawkeye (Raven Industries, Inc., Sioux Falls, SD), hereafter referred as S1, S2, and S3 respectively. Wilger nozzle bodies (Wilger Inc., Lexington, TN) and Capstan solenoid valves (Capstan Ag Systems, Inc., Topeka, KS) were used to evaluate the S1 PWM system (Figure 2.1.a). In contrast, a John Deere ExactApply nozzle bodies (Deere and Company, Moline, Il) were employed to assess the S2 PWM system (Figure 2.1.b). On the other hand, Teejet nozzle bodies (Teejet Technologies, Springfield, Il) and Raven nozzle control valves (Raven Industries, Inc., Sioux Falls, SD) were used to evaluate the S3 PWM system (Figure 2.1.c). A set of five nozzle bodies were utilized to operate each PWM system. The performance of each PWM system was evaluated in terms of pressure drop, response time, and flow rate.

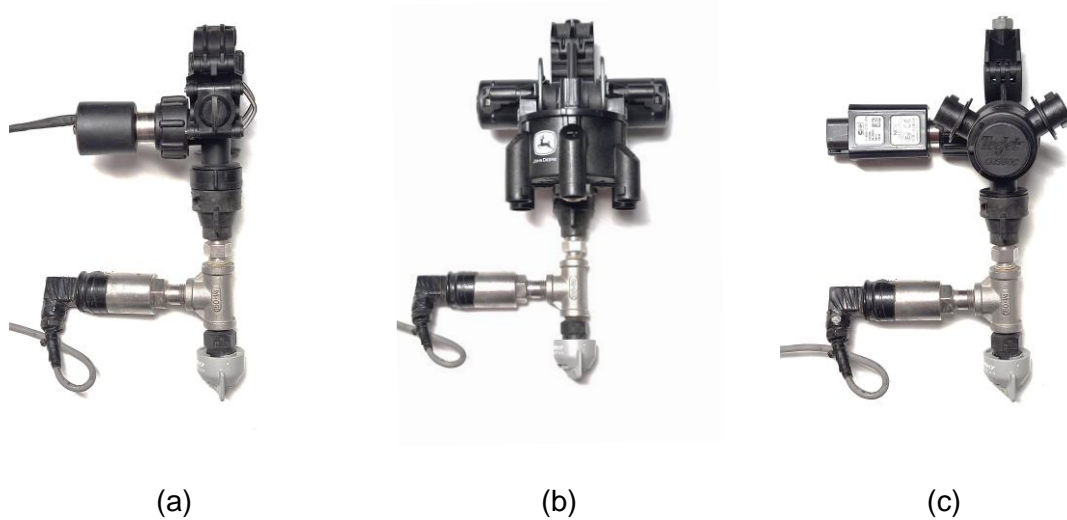


Figure 2.1. Different Commercially Available Solenoid Valves and Nozzle Bodies Used in the Study.

2.3.2 System set-up and instrumentation

A Kawasaki mule (Kawasaki Motors Corp., USA) equipped with a commercial liquid control system was used to evaluate the solenoid-actuated nozzle bodies operated by PWM nozzle control systems. The mule has a 2.54 centimeters (cm) diameter boom with a length of 6.5 meters (m) having three sections. The boom has 13 nozzles spaced at 0.508 m.

In this study, one boom section with five nozzles was utilized. A centrifugal pump was used to pressurize the system. The pump was powered by a 3.6 kilowatts (kW) gasoline engine (Honda GX 160, Honda Engines Group, Alpharetta, GA). A control system (Raven Viper 4, Raven Industries, Inc., Sioux Falls, SD) was used to regulate the system flow using the valve located at the backend of the sprayer system.

A thin-film membrane pressure transducers (Model 1502B81EZ100PSIG, PCB Piezotronics, Farmington, MI) were used to measure the real-time nozzle and boom pressure. Nozzle pressure was measured by installing a pressure transducer between the nozzle body and nozzle cap with a tip. For boom pressure, the pressure transducer was mounted on the boom using

a nozzle body with a cap. In both cases, the pressure transducers were mounted in a fitting between the nozzle body and nozzle tips. A similar set-up was used by Mangus et al. (2017) in their study. A preliminary test was conducted to evaluate the nozzles' response with and without the pressure transducer fittings using a high-speed camera. The result indicated that the pressure transducer and fitting assembly did not affect the nozzle pressure actuation response and spray fan pattern. The pressure transducer has a measuring range of 0 to 689.5 kilopascal (kPa) and a linear analog output of 0 to 10 Volts. Five pressure transducers, one for each nozzle body, provided the real-time nozzle pressure, and one pressure transducer measured the real-time boom pressure. The regression equation from the sensor calibration curve provided by the manufacturer was used to convert the pressure transducers voltage reading into pressure.

A turbine type flowmeter (Model FT-16, Flow Technology Inc., Tempe, AZ) was used to measure the system flow rate. The flowmeter was installed at the upstream portion of the active boom section and is capable of measuring flow up to 227.1 liters per minute (L min^{-1}) with a linear analog output of 0 to 10 V. The calibration data sheet provided by the manufacturer was used to establish the correlation between the flow meters' analog output in V to its flow measurement range in L min^{-1}

A Compact Rio (cRIO-9042, National Instruments, Austin, TX) data acquisition system and a customized LabVIEW program (National Instruments, Austin, TX) were used to record the real-time nozzle pressure, boom pressure, and flow rate using a sampling frequency of 1 kHz.

Different flat-fan nozzles (Pentair Hypro, Minneapolis, MN) recommended for use in a PWM system, were selected to deliver the required application rates of 112.2 liters per hectare (L h^{-1}) and 187.1 L h^{-1} based on the application pressure of 275.8 kPa and 448.1 kPa (Table 2.1). The

focus was to compare and contrast pressure dynamics across PWM systems at different application rates and pressures.

Table 2.1. Different Nozzle Tips Used in the Study.

Application Rate, L ha ⁻¹	Application Pressure, kPa	Nozzle Tip
112.2	275.8	120-06
	448.1	120-05
187.1	275.8	120-08
	448.1	120-08

2.3.3 Data collection

The target application rate was programmed to the Raven Viper 4 rate controller. The pressure in the boom was adjusted using a switch to control the butterfly valve located at the backend of the spray system. The boom pressure was adjusted to the target pressure of 275.8 kPa and 448.1 kPa during each test before data were collected. Different procedures were performed to vary the duty cycle and system frequency for each PWM nozzle control system. In S1, the duty cycle defined by the user was implemented by the Capstan controller (Capstan Ag Systems, Inc., Topeka KS). The S1 PWM system was operated at 10 Hz and 15 Hz system frequency. Figure 2.2 shows the set-up and instrumentation used in evaluating the S1 PWM system.

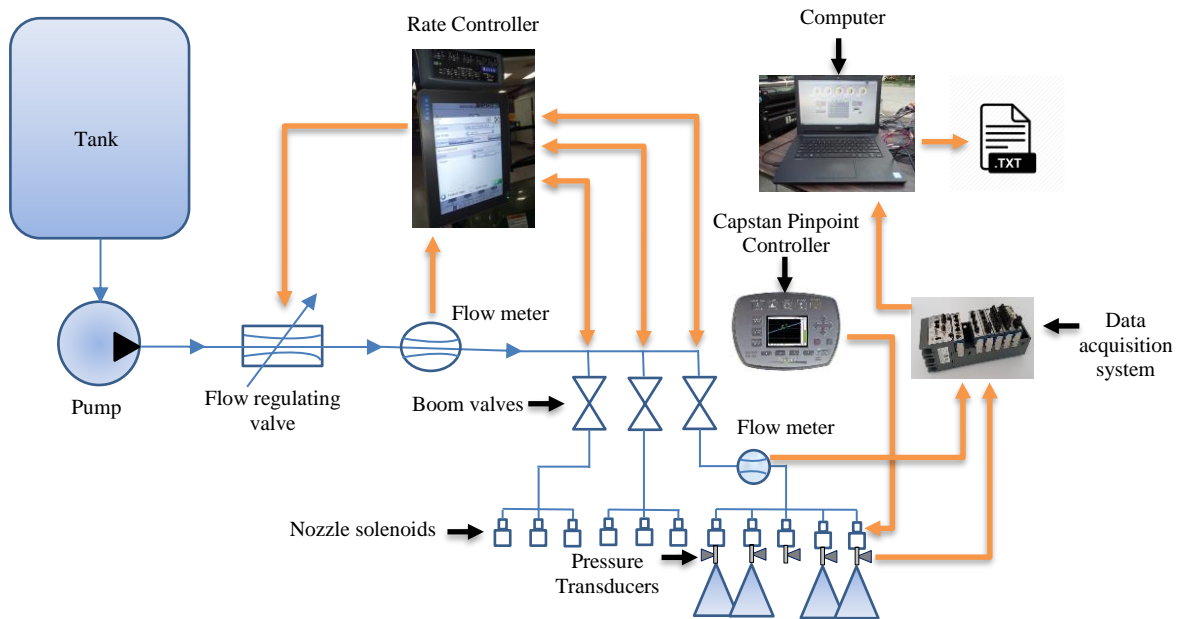


Figure 2.2. System Set-Up and Instrumentation of S1 PWM System

For S2, the duty cycle and system frequency were varied using the GreenStar 2630 display monitor (Deere and Company, Moline, IL). The turrets of the nozzle body were oriented based on the system frequency that it was operating and manually changed to match the orientation on the monitor. When operating at 15 Hz system frequency, the turret routes the flow from A and B solenoids to the individual outlets. The outlets can be a combination of 1 and 4, 2, and 5, or 3 and 6 with the outlets 1, 2, or 3 in the front position (Figure 2.3.a). For a 30 Hz system frequency, the turrets combine the flow from A and B solenoids to a single outlet, either to outlets 4, 5, or 6, whichever is in the front position (Figure 2.3.b). The set-up and instrumentation used for the S2 PWM system was shown in Figure 2.4.

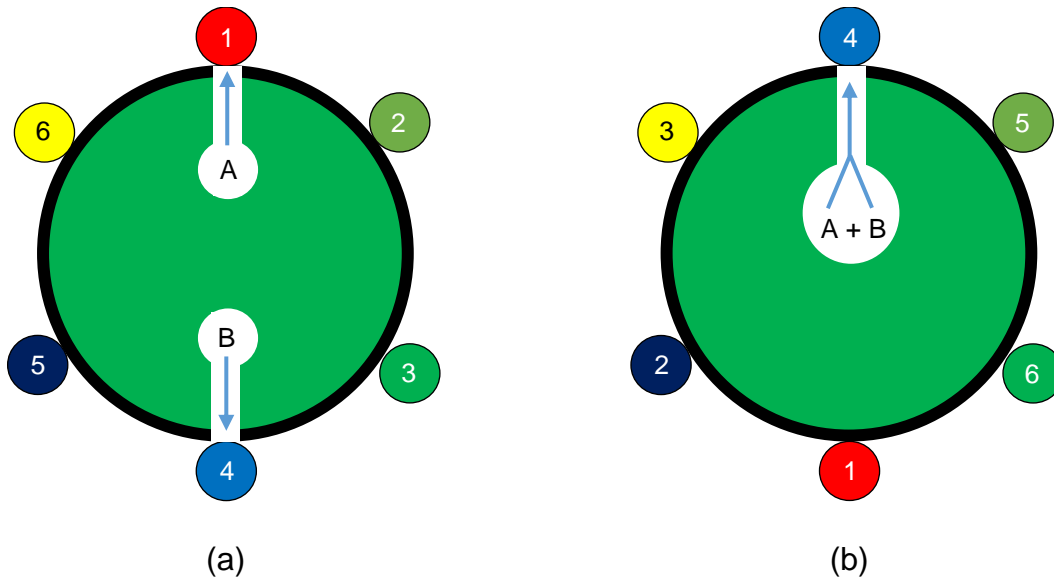


Figure 2.3. Turret Position of S2 Nozzle Body when Operating at 15 Hz (a) and 30 Hz (b) System Frequency.

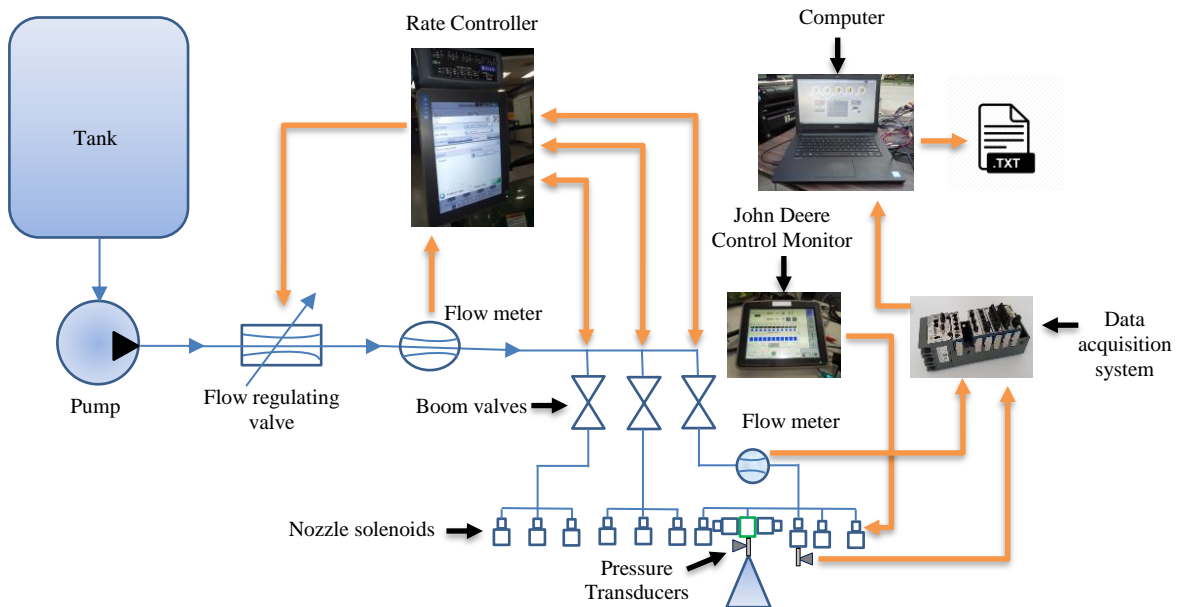


Figure 2.4. System Set-Up and Instrumentation of S2 PWM System.

The duty cycle and system frequency in S3 were varied by using the Raven Viper 4 display monitor. Figure 2.5 shows the set-up and instrumentation when the test was conducted using the S3 PWM system.

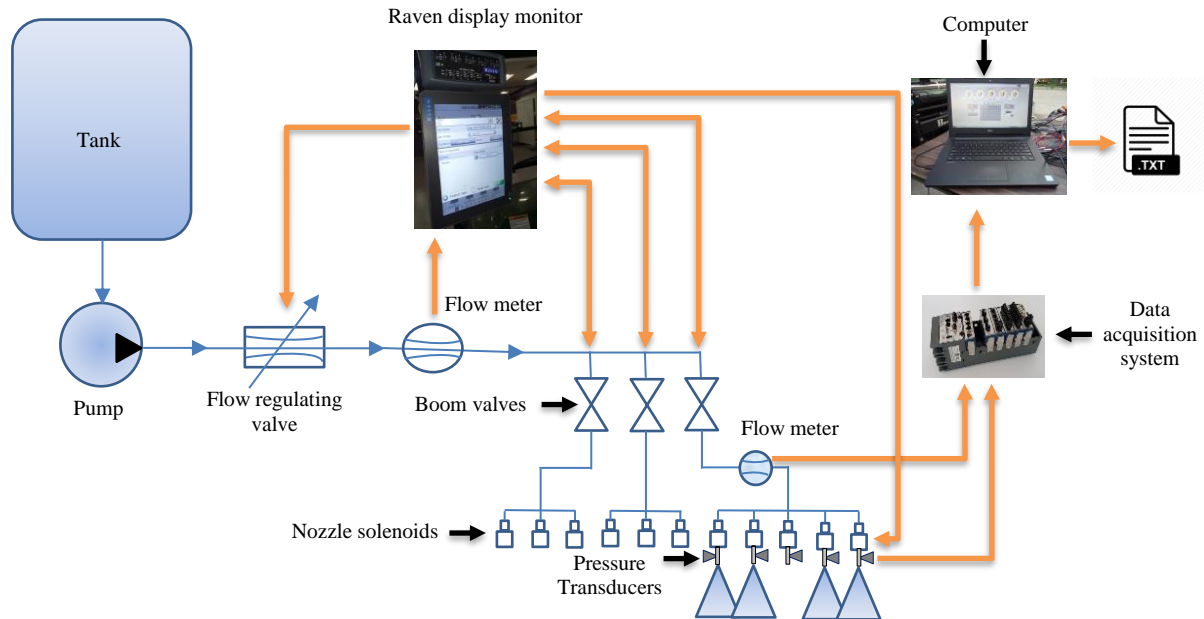


Figure 2.5. System Set-Up and Instrumentation of S3 PWM System.

Although the manufacturer commercially provides and recommends operating the PWM system at 10 Hz system frequency, the S1 PWM system has the option to vary the frequency to 10 Hz, 15 Hz, and 30 Hz system frequency. However, the data collected using the 30 Hz frequency in S1 PWM system was not included in the analysis, since it provided a 10 Hz data points when tested. The S2 PWM system can be programmed to operate at 15 Hz and 30 Hz system frequency as well. On the other hand, the S3 PWM system also had the functionality to change the system frequency to 10 Hz, 15 Hz, and 30 Hz. The pressure and flow rate data using each PWM nozzle control system were recorded for 30 seconds, which provided 30,000 data points for data analysis.

The impact of the different treatment combinations on the pressure drop, flow rate, and response time of the system was evaluated. The pressure drop from each nozzle body was

calculated by obtaining the difference between the boom pressure and the actual nozzle pressure. The actual nozzle pressure considered in this study was when the solenoid valves were on the ON state and spraying at steady condition between the peak and fall times. The response time of the system to achieve the target application pressure was evaluated by determining the peak time, the percent change in stabilized pressure application time, and the fall time (Figure 2.6). The total system flow rate measured by the flowmeter was divided into the number of active nozzles across the boom to determine the flow rate per nozzle. The percent change in flow rate was the percent difference between the actual flow rate and the expected flow rate based on the nozzle size, application pressure, and duty cycle.

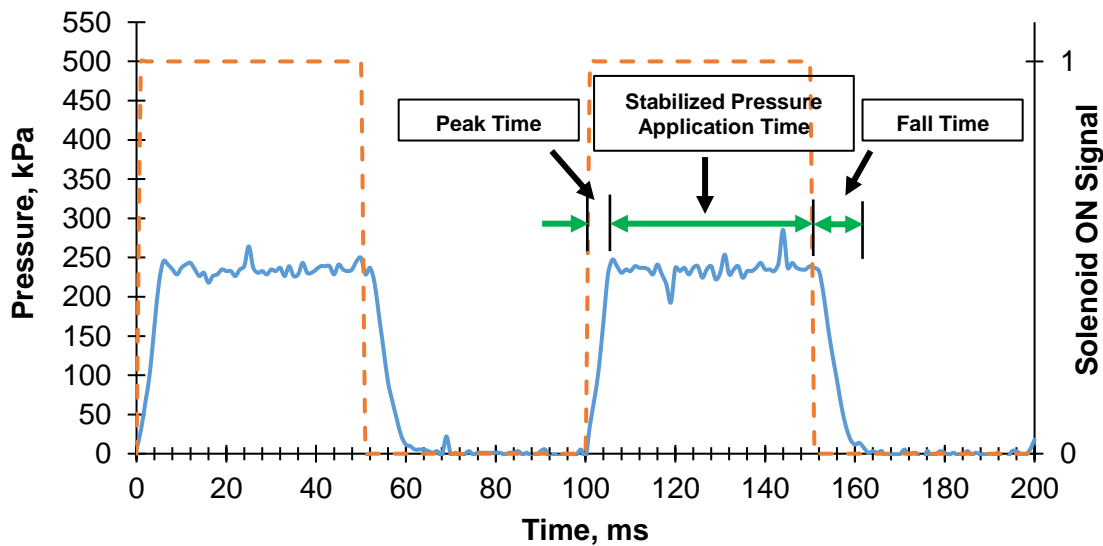


Figure 2.6. Evaluation of PWM Nozzle Control System Response Time.

The peak time was evaluated by determining the time it takes for the nozzle pressure to reach the initial peak pressure from the system's OFF state. The fall time was determined when the pressure begins to drop by 68.9 kPa from the average nozzle pressure during the stabilized pressure application time. The actual stabilized pressure application time was the time of application

between the peak time and fall time. The percent change in stabilized pressure application time was the percent difference between the actual stabilized pressure application time and the expected application time based on the specified duty cycle. Although the measurements were done at the millisecond level but to present averages, one decimal place results were utilized.

2.3.4 Data analysis

This study implemented a split-plot design. The PWM nozzle control system with three (3) levels (S1, S2, and S3) were randomly assigned to the whole plot while the duty cycle with four (4) levels (25%, 50%, 75%, and 100%) was randomly assigned to the sub-plot. Analysis of Variance (ANOVA) was implemented using the mixed procedure in SAS University Edition software (SAS Institute Inc., Cary, NC). The comparison between treatment means was conducted using Tukey's Least Significant Difference (LSD) test. The effects of the treatments were considered statistically significant at the 0.05 probability level.

2.4. Results and Discussions

2.4.1 Pressure drop

The pressure drop at the nozzle between the different PWM nozzle control systems differs significantly when applying at a rate of 112.2 L ha⁻¹ and 187.1 L ha⁻¹ at an application pressure of 275.8 kPa and 448.1 kPa at different duty cycles and 10 Hz system frequency (Table 2.2). The S3 system provided a pressure drop ranging from 45.17 kPa to 52.58 kPa, while S1 delivered a pressure drop ranging from 23.36 kPa to 29.27 kPa when applying at a rate of 112.2 L ha⁻¹ at an application pressure of 275.8 kPa and 448.1 kPa at 10 Hz system frequency. The pressure drop in both systems increased with the increase in the application rate. The S3 system provided a pressure

drop ranging from 70.21 kPa to 108.92 kPa, while the S1 system had a pressure drop ranging from 40.00 kPa to 70.90 kPa when applying at a rate of 187.1 L ha⁻¹ at application pressures of 275.8 kPa and 448.1 kPa

Table 2.2. Pressure Drop at the Nozzle when Applying at Different Application Rates and Pressures at 10 Hz.

Application Rate, L ha ⁻¹	Application Pressure, kPa	Duty Cycle, % ^[2]	PWM System ^[1]					
			S1		S2 ^[3]		S3	
			Pressure Drop, kPa	Std. Dev.	Pressure Drop, kPa	Std. Dev.	Pressure Drop, kPa	Std. Dev.
112.2	275.8	25	29.16 ^{Aa}	0.67	-	-	46.63 ^{Bab}	0.41
		50	24.67 ^{Ab}	0.51	-	-	47.33 ^{Ba}	0.28
		75	24.77 ^{Ab}	0.33	-	-	45.83 ^{Bbc}	0.17
		100	23.36 ^{Ac}	0.28	-	-	45.17 ^{Bc}	0.32
	448.1	25	28.24 ^{Aa}	1.06	-	-	49.15 ^{Ba}	0.40
		50	29.27 ^{Ab}	0.70	-	-	52.56 ^{Bb}	0.25
		75	26.82 ^{Ac}	0.34	-	-	50.61 ^{Bc}	0.18
		100	28.16 ^{Aa}	0.53	-	-	52.58 ^{Bb}	0.36
187.1	275.8	25	40.00 ^{Aa}	0.89	-	-	72.47 ^{Ba}	0.31
		50	40.85 ^{Abc}	0.42	-	-	70.23 ^{Bb}	0.21
		75	41.44 ^{Ab}	0.42	-	-	70.87 ^{Bb}	0.21
		100	40.21 ^{Aac}	0.53	-	-	70.21 ^{Bb}	0.35
	448.1	25	65.19 ^{Aa}	1.02	-	-	103.26 ^{Ba}	0.50
		50	66.57 ^{Ab}	0.46	-	-	108.92 ^{Bb}	0.36
		75	69.38 ^{Ac}	0.53	-	-	105.96 ^{Bc}	0.27
		100	70.90 ^{Ad}	0.77	-	-	104.84 ^{Bc}	0.56

Note:

[1] – Means with the same uppercase letters within the same row for each application pressure are not significantly different at $\alpha=0.05$.

[2] – Means with the same lowercase letters within the same column for each application pressure are not significantly different at $\alpha=0.05$.

[3] – The S2 PWM system cannot be operated at 10 Hz frequency.

Table 2.3 shows the pressure drop of the different PWM system when operating at different application rates and pressures at 15 Hz system frequency. The pressure drop between the S1, S2, and S3 PWM systems was significantly different when applying at different rates and application pressures. The S1 PWM system had a pressure drop ranging from 23.46 kPa to 31.50 kPa. The S2 PWM system provided a pressure drop ranging from 12.81 kPa to 17.22 kPa, while the S3 PWM system had a pressure drop ranging from 42.16 kPa to 51.87 kPa when applying at 112.2 L ha⁻¹ at 275.8 kPa and 448.1 kPa. The increase in application rate to 187.1 L ha⁻¹ also increases the PWM

systems' pressure drop when operating at 15 Hz system frequency. The S1 PWM system delivered a pressure drop of 39.51 kPa to 72.29 kPa. The S2 PWM system provided a pressure drop ranging from 24.13 kPa to 41.12 kPa, while the S3 PWM system had a pressure drop ranging from 67.45 kPa to 113.94 kPa when operating at 275.8 kPa and 448.1 kPa.

Table 2.3. Pressure Drop at the Nozzle when Applying at Different Application Rates and Pressures at 15 Hz.

Application Rate, L ha ⁻¹	Application Pressure, kPa	Duty Cycle, % ^[2]	PWM System ^[1]					
			S1		S2		S3	
			Pressure Drop, kPa	Std. Dev.	Pressure Drop, kPa	Std. Dev.	Pressure Drop, kPa	Std. Dev.
112.2	275.8	25	31.23 ^{Aa}	1.37	13.19 ^{Ba}	0.38	49.93 ^{Ca}	0.42
		50	28.00 ^{Ab}	1.14	13.96 ^{Bab}	0.32	46.46 ^{Cb}	0.27
		75	24.04 ^{Ac}	0.46	13.46 ^{Bab}	0.24	45.25 ^{Cc}	0.30
		100	23.46 ^{Ac}	0.39	14.48 ^{Bb}	0.28	44.69 ^{Cc}	0.33
	448.1	25	31.50 ^{Aa}	1.46	12.81 ^{Ba}	0.56	42.16 ^{Ca}	0.76
		50	29.49 ^{Ab}	0.92	16.61 ^{Bb}	0.44	48.35 ^{Cb}	0.29
		75	27.89 ^{Ab}	0.45	16.03 ^{Bb}	0.19	51.87 ^{Cc}	0.33
		100	26.22 ^{Ac}	0.41	17.22 ^{Bb}	0.36	51.81 ^{Cc}	0.33
187.1	275.8	25	40.97 ^{Aa}	0.68	24.13 ^{Ba}	0.68	67.81 ^{Ca}	0.45
		50	39.51 ^{Ab}	0.73	24.29 ^{Ba}	0.42	67.45 ^{Ca}	0.27
		75	40.66 ^{Aab}	0.44	24.42 ^{Ba}	0.31	72.23 ^{Cb}	0.27
		100	40.29 ^{Aab}	0.45	24.25 ^{Ba}	0.48	69.97 ^{Cc}	0.30
	448.1	25	72.29 ^{Aa}	1.20	35.73 ^{Ba}	0.61	113.94 ^{Ca}	1.96
		50	69.65 ^{Aab}	0.87	37.73 ^{Bab}	0.25	105.07 ^{Cb}	0.45
		75	68.19 ^{Abc}	0.60	38.75 ^{Bbc}	0.21	107.87 ^{Cc}	0.38
		100	66.69 ^{Ac}	0.77	41.12 ^{Bc}	0.29	106.30 ^{Cbc}	0.61

Note:

[1] – Means with the same uppercase letters within the same row for each application pressure are not significantly different at $\alpha=0.05$.

[2] – Means with the same lowercase letters within the same column for each application pressure are not significantly different at $\alpha=0.05$.

Similar results were observed for 30 Hz system frequency, which exhibited significantly different pressure drop between S2 and S3 PWM systems (Table 2.4). The S2 PWM system provided a pressure drop ranging from 0.23 kPa to 12.49 kPa at an application rate of 112.2 L ha⁻¹ at an application pressure of 275.8 kPa to 448.1 kPa. On the other hand, the S3 PWM system has a pressure drop ranging from 44.46 kPa to 53.03 kPa when operating at the same settings. Increasing the application rate to 187.1 L ha⁻¹ increases the pressure drop of the two systems, with

the S2 providing a pressure drop ranging from 4.88 kPa to 41.38 kPa while the pressure drop when using the S3 PWM system ranges from 68.44 kPa to 108.87 kPa.

Table 2.4. Pressure Drop at the Nozzle when Applying at Different Application Rates and Pressures at 30 Hz.

Application Rate, L ha ⁻¹	Application Pressure, kPa	Duty Cycle, % ^[2]	PWM System ^[1]					
			S1 ^[3]		S2		S3	
			Pressure Drop, kPa	Std. Dev.	Pressure Drop, kPa	Std. Dev.	Pressure Drop, kPa	Std. Dev.
112.2	275.8	25	-	-	11.38 ^{Aa}	0.46	52.91 ^{Ba}	0.79
		50	-	-	11.76 ^{Aa}	0.36	46.55 ^{Bb}	0.40
		75	-	-	11.50 ^{Aa}	0.25	44.46 ^{Bc}	0.29
		100	-	-	0.23 ^{Ab}	0.26	44.75 ^{Bc}	0.29
	448.1	25	-	-	10.58 ^{Aa}	0.55	47.72 ^{Ba}	0.69
		50	-	-	11.63 ^{Aab}	0.40	47.78 ^{Ba}	0.54
		75	-	-	12.49 ^{Ab}	0.40	52.32 ^{Bb}	0.44
		100	-	-	1.14 ^{Ac}	0.22	53.03 ^{Bb}	0.32
187.1	275.8	25	-	-	23.37 ^{Aa}	0.71	68.44 ^{Ba}	0.76
		50	-	-	23.28 ^{Aa}	0.49	74.62 ^{Bb}	0.50
		75	-	-	22.74 ^{Aa}	0.44	72.96 ^{Bbc}	0.45
		100	-	-	4.88 ^{Ab}	0.37	71.41 ^{Bc}	0.34
	448.1	25	-	-	41.38 ^{Aa}	0.72	87.72 ^{Ba}	1.44
		50	-	-	39.67 ^{Aa}	0.58	99.67 ^{Ba}	0.74
		75	-	-	39.51 ^{Aa}	0.56	108.87 ^{Bb}	0.59
		100	-	-	10.50 ^{Ab}	0.41	105.97 ^{Bb}	0.74

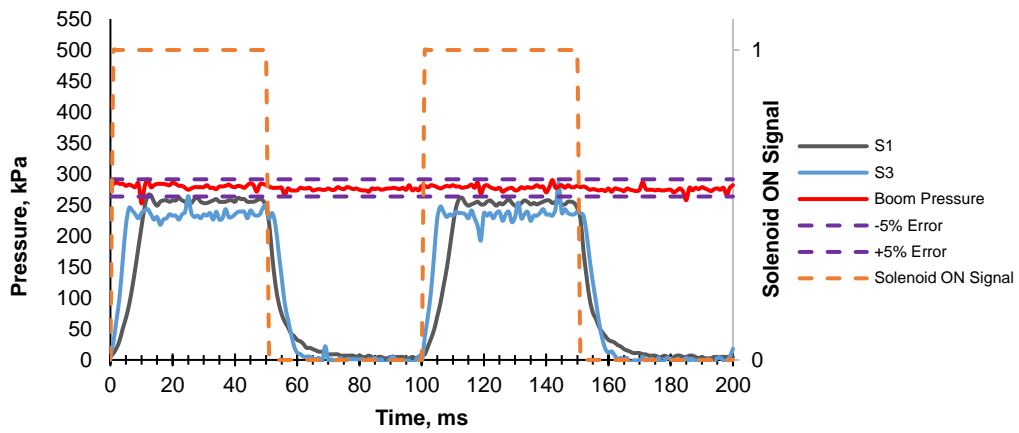
Note:

[1] – Means with the same uppercase letters within the same row for each application pressure are not significantly different at $\alpha=0.05$.

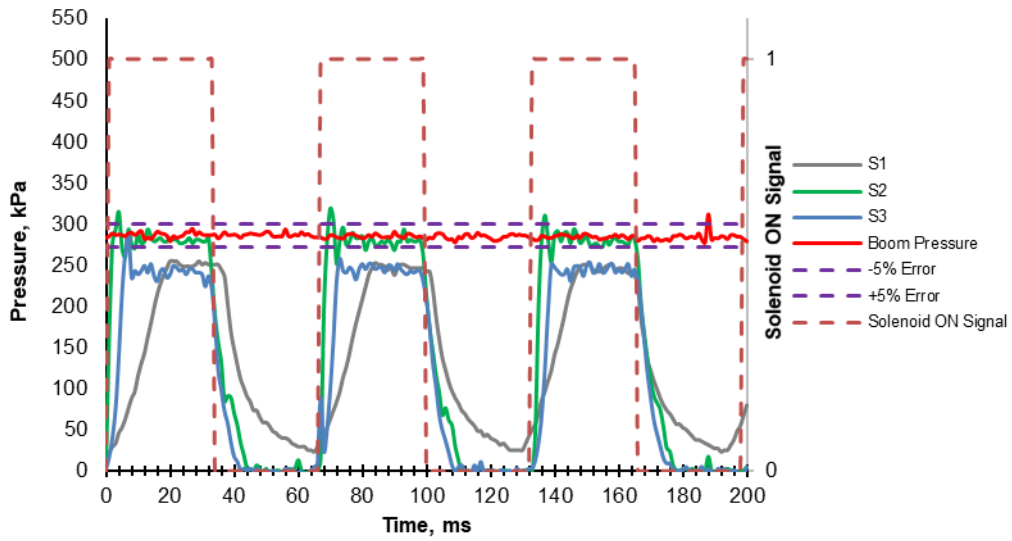
[2] – Means with the same lowercase letters within the same column for each application pressure are not significantly different at $\alpha=0.05$.

[3] – The S1 PWM system cannot be operated at 30 Hz frequency.

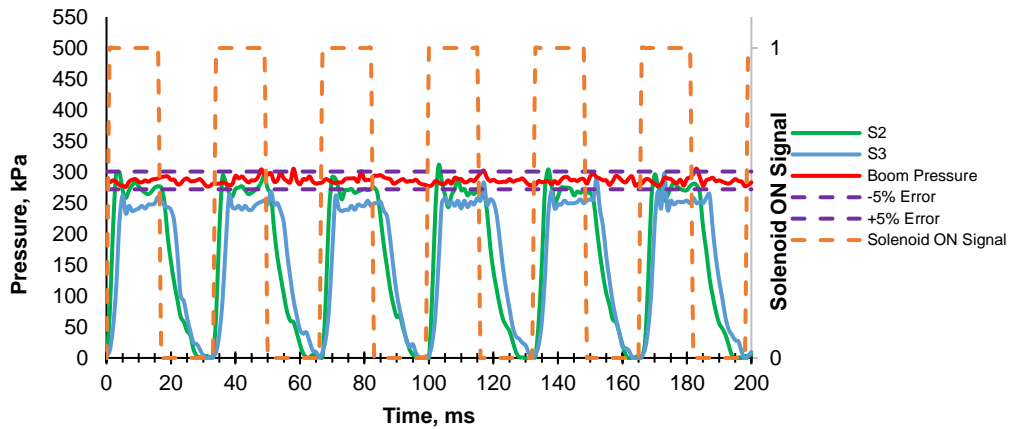
Figure 2.7 shows an example of each PWM system's performance when applying at 112.2 L ha⁻¹ and 275.8 kPa application pressure at 50% duty cycle operating at 10 Hz (Figure 2.7.a), 15 Hz, (Figure 2.7.b), and 30 Hz (Figure 2.7.c). For the purpose of presentation, the 50% duty cycle was selected to show the pressure dynamics of each PWM system when operating at different system frequencies since a similar trend was observed when the system operates at different application rates and duty cycles.



(a) 10 Hz



(b) 15 Hz



(c) 30 Hz

Figure 2.7. Pressure Drop of the Different PWM Nozzle Control Systems (a) 10 Hz, (b) 15 Hz, and (c) 30 Hz when Applying at a Rate of 112.2 L ha^{-1} and 275.8 kPa Application Pressure at 50% Duty Cycle.

In the three PWM systems, the pressure drop increase was expected since a nozzle with a bigger orifice was selected to apply the product at 187.1 L ha^{-1} application rate. The results were similar to the previous study, wherein a significant decrease in the nozzle pressure was observed when using a nozzle with a bigger orifice in a PWM system (Butts et al., 2019). However, the pressure drop between each PWM system was significantly different when applying at a rate of 112.2 L ha^{-1} and 187.1 L ha^{-1} at 275.8 kPa and 448.1 kPa application pressure.

Overall, the results showed that each PWM system exhibited significantly different pressure drop. Within each PWM system, pressure drops were significantly different and increased with an increase in application rates. These pressure drops were enough to cause significant changes in flow rate. Pressure also drop with duty cycles, frequencies, and application pressures when using each PWM system, however not to significantly impact the flow rate. The inconsistency in pressure could change the intended flow rate delivery during each cycle, thus impacting spray output (Silva et al., 2018). Additionally, the inconsistencies in the pressure drop

at different duty cycles during operation could cause an under-application, potentially resulting in inefficient control of pests and diseases (Mangus et al., 2017). Likewise, based on the nozzle selected for field operation, operating at a pressure lower than the recommended may lead to a reduction in spray overlap between nozzles and may also impact the spray droplet size (especially at lower duty cycles), which could contribute to off-rate errors (Butts et al., 2019; Daggupati, 2007).

Producers usually select a particular nozzle to use during operation, which depends on the recommended droplet size of the chemical that will be applied. From the manufacturer's catalog, producers may choose a nozzle that will provide the target droplet size at the desired application pressure, application rate, and operation speed. These nozzle tips were rated to apply a specific flow rate and droplet size at a certain pressure, and therefore, should be operated within that pressure as much as possible. Since the current system does not measure the pressure at the nozzle, sprayer operators should be aware of the pressure drop at the nozzle when setting the target application pressure in a controller when using a particular PWM system. Setting the target application pressure by considering the pressure drop would compensate for pressure drops at the nozzle, thus maintaining target application pressure across the nozzle, whereas setting without considering pressure drop would have the spray system operating at reduced pressure and potentially implementing under-application. Operating spray application systems at recommended application pressure would also maintain the desired droplet size characteristics, which is critical from both product label standpoint and achieving desired coverage for efficient control of pests in the field. Operating at lower pressure, especially when using a nozzle with a bigger orifice, may also affect the spray characteristics such as the spray fan angle and droplet size distribution during pulsing, which may reduce the efficacy of product application (Butts et al., 2019). Newer PWM

systems might consider installing pressure sensors on the nozzles bodies located at different boom sections to provide the average pressure as feedback to the controller to accurately manage nozzle application pressure and automatically compensate pressure drop.

2.4.2 Response time

2.4.2.1 Peak time and fall time

The average peak time when applying at 112.2 L ha⁻¹ and 187.1 L ha⁻¹ and application pressures of 275.8 kPa and 448.1 kPa at different system frequencies shows that each system has time latency before reaching the target application pressure (Tables 2.5, 2.6, and 2.7). This finding was similar to the study of Mangus et al. (2017) and Holtz et al., (2000), wherein the PWM system has an ON/OFF time latency before achieving the target application pressure per cycle. This latency is primarily due to the response time of the system to actuate when a command is sent to turn On solenoids from Off state.

Table 2.5. Average Peak and Fall Time of Each PWM System at 10 Hz Frequency.

Application Rate, L ha ⁻¹	Application Pressure, kPa	Duty Cycle, %	PWM System					
			S1		S2 [1]		S3	
			Peak Time, ms	Fall Time, ms	Peak Time, ms	Fall Time, ms	Peak Time, ms	Fall Time, ms
112.2	275.8	25	10.4	24.4	-	-	5.0	9.2
		50	9.6	21.4	-	-	4.8	10.2
		75	10.2	20.6	-	-	5.4	10.2
	448.1	25	5.6	16.6	-	-	2.2	12.0
		50	6.2	18.0	-	-	2.0	14.2
		75	6.0	16.2	-	-	2.0	12.0
187.1	275.8	25	3.8	6.4	-	-	2.6	7.0
		50	4.0	7.0	-	-	2.4	7.6
		75	4.0	6.4	-	-	2.8	7.2
	448.1	25	3.0	9.6	-	-	2.8	9.2
		50	3.8	11.4	-	-	2.6	12.8
		75	3.6	10.0	-	-	2.4	10.6

Note: [1] – The S2 PWM system cannot be operated at 10 Hz frequency

Table 2.6. Average Peak and Fall Time of Each PWM System at 15 Hz Frequency.

Application Rate, L ha ⁻¹	Application Pressure, kPa	Duty Cycle, %	PWM System					
			S1		S2		S3	
			Peak Time, ms	Fall Time, ms	Peak Time, ms	Fall Time, ms	Peak Time, ms	Fall Time, ms
112.2	275.8	25	11.4	26.6	2.4	10.0	4.6	8.2
		50	16.0	22.8	1.6	12.0	4.8	10.0
		75	7.4	10.8	2.6	10.2	4.4	8.4
	448.1	25	5.8	13.4	1.8	13.8	2.4	10.6
		50	5.8	14.0	1.6	16.6	2.0	10.6
		75	5.4	11.4	2.0	14.0	1.8	11.4
187.1	275.8	25	4.4	0.5	2.2	9.8	2.4	6.2
		50	4.8	0.8	2.4	11.0	2.4	7.2
		75	4.8	0.8	2.4	9.6	2.0	8.0
	448.1	25	3.6	0.9	2.6	14.6	2.6	9.2
		50	3.8	0.4	2.2	16.6	3.0	12.6
		75	3.8	0.4	2.2	14.6	2.8	10.2

Table 2.7. Average Peak and Fall Time of Each PWM System at 30 Hz Frequency.

Application Rate, L ha ⁻¹	Application Pressure, kPa	Duty Cycle, %	PWM System					
			S1 ^[1]		S2		S3	
			Peak Time, ms	Fall Time, ms	Peak Time, ms	Fall Time, ms	Peak Time, ms	Fall Time, ms
112.2	275.8	25	-	-	2.4	7.0	3.0	7.4
		50	-	-	2.0	10.6	3.4	9.8
		75	-	-	1.8	7.4	2.4	5.0
	448.1	25	-	-	2.2	10.2	2.6	9.8
		50	-	-	2.2	9.4	2.0	11.4
		75	-	-	1.8	8.4	0.8	6.2
187.1	275.8	25	-	-	2.4	10.4	2.6	7.6
		50	-	-	2.6	7.4	2.6	6.4
		75	-	-	2.2	7.2	1.0	5.4
	448.1	25	-	-	2.4	10.8	3.4	9.4
		50	-	-	3.0	8.8	3.0	8.6
		75	-	-	1.6	8.6	1.2	5.8

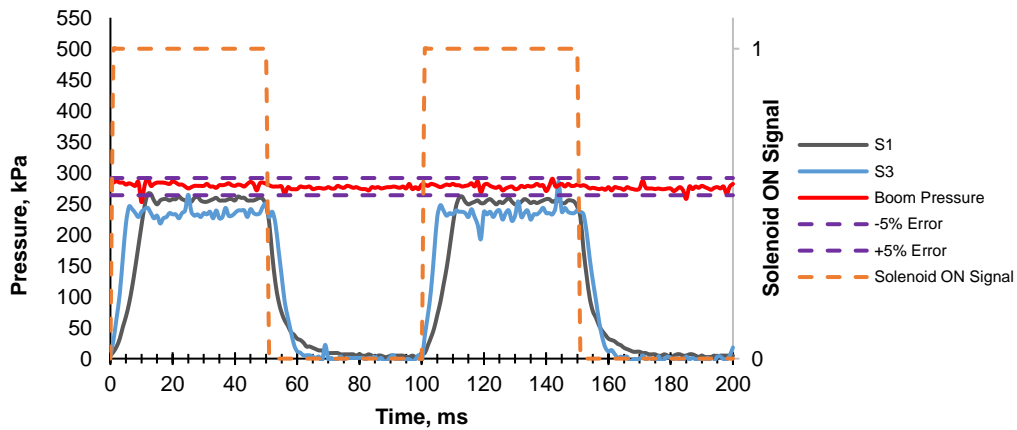
Note: [1] – The S1 PWM system cannot be operated at 30 Hz frequency

The PWM systems also have an inherent fall time before the system stops spraying after the solenoid valves close (Figure 2.8). Mangus et al. (2017) also reported that a PWM system continues to spray for 10 ms after the solenoid valves were fully de-energized. Although the peak time and fall times varied per PWM system, but when adding these times for the number of cycles in one second and time of application for a typical field, the total impact of these times could significantly affect product delivery accuracy. During the peak and fall times, PWM system applies

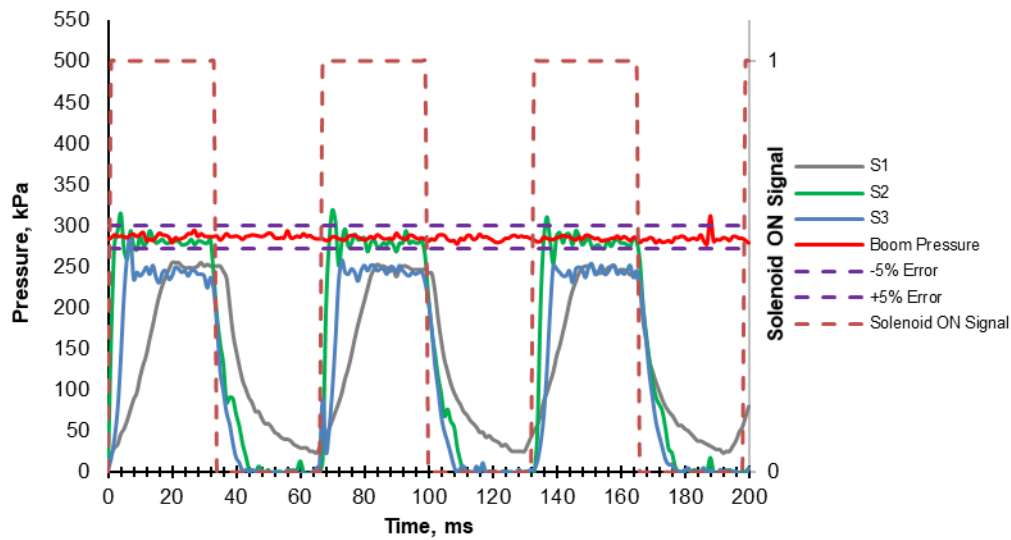
products below the recommended pressure, which could change the spray droplet size and may impact the product volume and deposition (Lang, 2013). In addition, the spray angle may also be significantly affected during peak and fall times, potentially impacting the spray overlap (Luck et al., 2015).

The fall time could potentially lead to off-rate errors due to additional time that the system continues to apply the product at variable pressure beyond the actuation signal to turn Off. In addition, the rise in the number of cycles per second, like for higher frequency systems, lag, and peak times, could potentially increase the cumulative time at which nozzles operate at variable pressure, droplet size, and spray overlap.

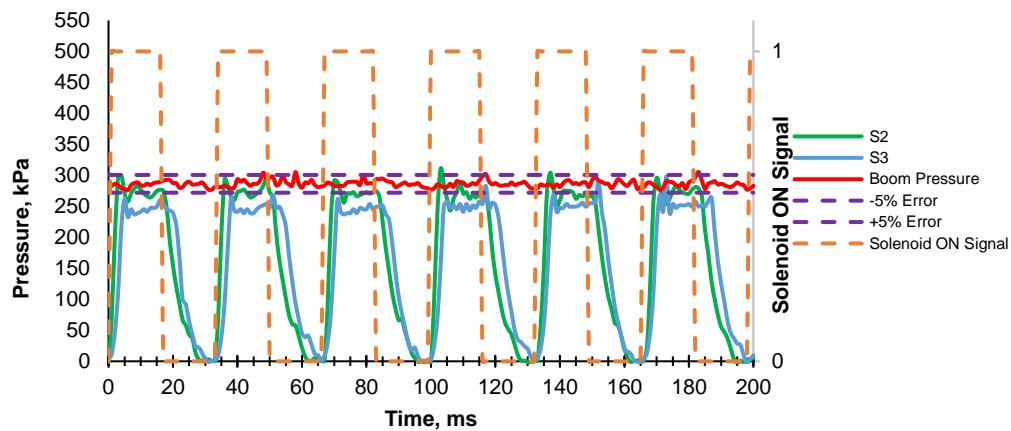
The difference in the control algorithm and solenoid valve response characteristics of each rate controller might have affected the average peak time when operating at different application rates and frequencies (Sharda et al., 2013). Though there are no published studies on the standard acceptable response of the PWM nozzle control system to achieve the target application pressure quickly, this factor may still affect the accuracy of pesticide application in the field and should be given attention when selecting a PWM system.



(a) 10 Hz



(b) 15 Hz



(c) 30 Hz

Figure 2.8. Pressure Response of the Different PWM Nozzle Control Systems (a) 10 Hz, (b) 15 Hz, and (c) 30 Hz when Applying at a Rate of 112.2 L ha^{-1} and 275.8 kPa Application Pressure at 50% Duty Cycle.

2.4.2.2 Stabilized pressure application time

The percent change in stabilized pressure application time shows significant differences between PWM systems when applying at a rate of 112.2 L ha^{-1} and 187.1 L ha^{-1} and application pressures of 275.8 kPa and 448.1 kPa at different system frequencies (Tables 2.8, 2.9, and 2.10). The negative value indicates that the actual time that the system operates at stabilized pressure was

lower than the specified duty cycle. In both application rates, the stabilized pressure application time with respect to the expected time within each system was significantly different when operating at different duty cycles. The results show that the stabilized pressure application percent time change was higher at a 25% duty cycle, while the lowest percent time change was observed when the PWM systems operated at a 75% duty cycle. It is important to note that correct stabilized pressure time is critical to achieving target flow rate each nozzle. The variation in stabilized pressure application times, indicated that the PWM systems could deliver incorrect flow rate during each cycle, especially at lower duty cycles which could also impact the product application uniformity (Mangus et al., 2017).

A lower percent change in stabilized pressure application time indicated that the control system was programmed to apply products for approximately the designated amount of time in each cycle, thus maintaining greater flow rate delivery accuracy. However, for a system with the lowest percent change in stabilized pressure application time, the peak time and fall time could potentially add volume to overall flowrate, potentially resulting in over-application of product. Further research efforts should be considered to optimize the peak time, percent change in stabilized pressure application time, and fall time to 1) minimize the impact of peak and fall times on droplet size and fan angle; and 2) optimize peak, fall, and stabilized pressure application time to achieve accurate volume delivery in each cycle

Table 2.8. Stabilized Pressure Application Time Change when Using the Different PWM Systems at 10 Hz.

Application Rate, L ha ⁻¹	Application Pressure, kPa	Duty Cycle, % ^[2]	PWM System ^[1]					
			S1		S2 ^[3]		S3	
			Stabilized Application Time, % Change	Std. Dev.	Stabilized Application Time, % Change	Std. Dev.	Stabilized Application Time, % Change	Std. Dev.
112.2	275.8	25	-35.20 ^{Aa}	1.79	-	-	-7.20 ^{Ba}	1.79
		50	-16.00 ^{Ab}	0.00	-	-	-2.80 ^{Bb}	1.10
		75	-10.67 ^{Ac}	0.00	-	-	-3.20 ^{Bb}	0.73
	448.1	25	-24.80 ^{Aa}	1.79	-	-	2.40 ^{Ba}	2.19
		50	-14.80 ^{Ab}	1.10	-	-	2.40 ^{Ba}	0.89
		75	-7.73 ^{Ac}	1.12	-	-	1.33 ^{Ba}	0.00
187.1	275.8	25	-17.60 ^{Aa}	2.19	-	-	8.00 ^{Ba}	0.00
		50	-6.40 ^{Ab}	0.89	-	-	0.40 ^{Bb}	0.89
		75	-6.67 ^{Ab}	0.00	-	-	0.80 ^{Bb}	0.73
	448.1	25	-16.00 ^{Aa}	0.00	-	-	0.80 ^{Ba}	1.79
		50	-8.40 ^{Ab}	1.67	-	-	2.00 ^{Ba}	1.41
		75	-5.33 ^{Ac}	0.00	-	-	0.00 ^{Ba}	0.94

Note:

[1] – Means with the same uppercase letters within the same row for each application pressure are not significantly different at $\alpha=0.05$.

[2] – Means with the same lowercase letters within the same column for each application pressure are not significantly different at $\alpha=0.05$.

[3] – The S2 PWM system cannot be operated at 10 Hz frequency.

Table 2.9. Stabilized Pressure Application Time Change when Using the Different PWM Systems at 15 Hz.

Application Rate, L ha ⁻¹	Application Pressure, kPa	Duty Cycle, % ^[2]	PWM System ^[1]					
			S1		S2		S3	
			Stabilized Application Time, % Change	Std. Dev.	Stabilized Application Time, % Change	Std. Dev.	Stabilized Application Time, % Change	Std. Dev.
112.2	275.8	25	-41.20 ^{Ca}	0.00	-18.82 ^{Da}	2.63	-3.53 ^{Ba}	3.22
		50	-32.70 ^{Cb}	1.40	-6.06 ^{ABb}	0.00	-12.73 ^{Eb}	1.36
		75	-8.00 ^{Ac}	0.00	-8.80 ^{Ab}	2.28	0.00 ^{Ea}	0.00
	448.1	25	-14.10 ^{ACa}	3.20	-15.29 ^{Aa}	3.22	3.53 ^{Dab}	3.22
		50	-4.24 ^{Eb}	3.50	-9.70 ^{BCb}	1.36	6.06 ^{Da}	0.00
		75	-7.20 ^{Bb}	1.10	-9.20 ^{Bb}	1.10	1.20 ^{Db}	1.10
187.1	275.8	25	-7.06 ^{Aa}	2.60	-16.47 ^{Ca}	2.63	2.35 ^{Ba}	3.22
		50	-4.85 ^{Bb}	1.70	-10.30 ^{Ab}	1.66	3.03 ^{Ba}	0.00
		75	-1.60 ^{Bb}	1.70	-10.00 ^{Ab}	0.00	1.20 ^{Ba}	1.10
	448.1	25	-8.24 ^{Aa}	3.20	-27.06 ^{Da}	3.22	0.00 ^{BCa}	4.16
		50	-2.42 ^{BCb}	5.40	-15.15 ^{Db}	5.25	3.03 ^{Ca}	0.00
		75	-5.60 ^{Bb}	0.90	-12.80 ^{Ab}	1.10	1.20 ^{BCa}	1.10

Note:

[1] – Means with the same uppercase letters within the same row for each application pressure are not significantly different at $\alpha=0.05$.

[2] – Means with the same lowercase letters within the same column for each application pressure are not significantly different at $\alpha=0.05$.

Table 2.10. Stabilized Pressure Application Time Change when Using the Different PWM Systems at 30 Hz.

Application Rate, L ha ⁻¹	Application Pressure, kPa	Duty Cycle, % ^[2]	PWM System ^[1]					
			S1 ^[3]		S2		S3	
			Stabilized Application Time, % Change	Std. Dev.	Stabilized Application Time, % Change	Std. Dev.	Stabilized Application Time, % Change	Std. Dev.
112.2	275.8	25	-	-	-15.56 ^{Aa}	6.09	-35.56 ^{Ca}	4.97
		50	-	-	-8.24 ^{Aab}	3.22	4.71 ^{Cb}	2.63
		75	-	-	-7.20 ^{Bb}	1.79	-0.80 ^{Bb}	1.79
	448.1	25	-	-	-20.00 ^{Aa}	4.97	-20.00 ^{Aa}	4.97
		50	-	-	-12.94 ^{Bb}	2.63	1.18 ^{Cb}	2.63
		75	-	-	-12.00 ^{Bb}	2.83	0.80 ^{Cb}	1.79
187.1	275.8	25	-	-	-20.00 ^{Aa}	9.30	-11.11 ^{ABCa}	0.00
		50	-	-	-16.47 ^{ABab}	4.92	-5.88 ^{Cab}	0.00
		75	-	-	-10.40 ^{BCb}	5.37	3.20 ^{Db}	1.79
	448.1	25	-	-	-24.44 ^{Aa}	4.97	-55.56 ^{Ca}	11.11
		50	-	-	-18.82 ^{Aab}	2.63	-3.53 ^{Bb}	3.22
		75	-	-	-11.20 ^{Bb}	3.35	0.80 ^{Cb}	1.79

Note:

[1] – Means with the same uppercase letters within the same row for each application pressure are not significantly different at $\alpha=0.05$.

[2] – Means with the same lowercase letters within the same column for each application pressure are not significantly different at $\alpha=0.05$.

[3] – The S1 PWM system cannot be operated at 30 Hz frequency.

2.4.3 Flowrate

The percent change on flow rate with respect to the expected flow per nozzle when applying at a rate of 112.2 L ha⁻¹ and 187.1 L ha⁻¹ and application pressures of 275.8 kPa and 448.1 kPa at 10 Hz, 15 Hz, and 30 Hz system frequencies were shown in Tables 2.11, 2.12, and 2.13. A negative value indicates that the measured flow rate was smaller than the expected flow rate that the nozzle should be provided at a specific application pressure. Applying at a rate of 112.2 L ha⁻¹ and 187.1 L ha⁻¹ and application pressures of 275.8 kPa and 448.1 kPa at 10 Hz system frequency shows significant differences in the flow rate change between the S1 and S3 PWM systems (Table 2.11). The flow rate change at different duty cycles when using the S1 PWM system shows no significant differences except when applying at a higher application rate (187.1 L ha⁻¹) and pressure (448.1 kPa). The S3 system, on the other hand, shows significant differences in the flow rate change at different duty cycles. Significant differences in the flow rate change were observed

between S1, S2, and S3 PWM systems when operating at 15 Hz system frequency (Table 2.12). The increase in application rate and pressure also increases the flow rate change when using the three PWM systems. At 30 Hz system frequency, significant differences in the flow rate change were observed between the S2 and S3 PWM systems (Table 2.13). In both PWM systems, the flow rate change increases with the duty cycle increase when operating at 30 Hz frequency. The percent change in flow rate with respect to the expected flow rate shows significant differences within the PWM system at different duty cycles. The change in flow rate with respect to the expected flow rate may be caused by the varying peak time, stabilized pressure application time, and fall times. In addition, applying at lower application pressure may also influence the percent change in flow rate because the amount of product that a particular nozzle will provide also depends on the correct pressure settings during operation.

Table 2.11. Flow Rate Change when Using the Different PWM Systems at 10 Hz.

Application Rate, L ha ⁻¹	Application Pressure, kPa	Duty Cycle, % [2]	PWM System [1]		
			S1	S2 [3]	S3
			Flow rate, % Change	Flow rate, % Change	Flow rate, % Change
112.2	275.8	25	6.67 ^{Aa}	-	5.33 ^{Aa}
		50	0.00 ^{Bb}	-	0.00 ^{Bb}
		75	-1.78 ^{BDb}	-	-4.00 ^{CDc}
		100	-6.00 ^{Cc}	-	-6.33 ^{Cc}
	448.1	25	-5.66 ^{Ca}	-	-5.66 ^{Ca}
		50	-2.52 ^{ACa}	-	2.52 ^{Bc}
		75	-2.94 ^{ACa}	-	-5.04 ^{ACab}
		100	-4.57 ^{ACa}	-	-1.42 ^{ABbc}
187.1	275.8	25	-5.00 ^{Ba}	-	-12.00 ^{Aa}
		50	-8.50 ^{ABa}	-	-8.00 ^{ABa}
		75	-7.67 ^{ABa}	-	-12.00 ^{Aa}
		100	-6.00 ^{Ba}	-	-11.00 ^{Aa}
	448.1	25	-13.73 ^{ABa}	-	-15.29 ^{Aa}
		50	-12.16 ^{ABa}	-	-5.88 ^{Cc}
		75	-11.37 ^{Ba}	-	-11.37 ^{Bb}
		100	-7.84 ^{Cb}	-	-13.73 ^{ABab}

Note:

[1] – Means with the same uppercase letters within the same row for each application pressure are not significantly different at $\alpha=0.05$.

[2] – Means with the same lowercase letters within the same column for each application pressure are not significantly different at $\alpha=0.05$.

[3] – The S2 PWM system cannot be operated at 10 Hz frequency.

Table 2.12. Flow Rate Change when Using the Different PWM Systems at 15 Hz.

Application Rate, L ha ⁻¹	Application Pressure, kPa	Duty Cycle, % [2]	PWM System [1]		
			S1	S2	S3
			Flow rate, % Change	Flow rate, % Change	Flow rate, % Change
112.2	275.8	25	1.33 ^{Aa}	5.33 ^{Da}	0.00 ^{Aa}
		50	1.33 ^{Aa}	0.00 ^{Ab}	0.00 ^{Aa}
		75	0.00 ^{Aa}	-0.89 ^{ABb}	-4.00 ^{BCb}
		100	-4.33 ^{BCb}	0.00 ^{Ab}	-6.00 ^{Cb}
	448.1	25	-18.20 ^{Aa}	-5.66 ^{BCGa}	-8.18 ^{BCa}
		50	-6.29 ^{BCGbc}	-3.77 ^{DFGab}	2.52 ^{Eb}
		75	-8.40 ^{Bb}	-4.62 ^{CFGa}	-5.88 ^{BCGa}
		100	-2.99 ^{DFGc}	-0.79 ^{DEb}	-1.42 ^{DFc}
187.1	275.8	25	-15.00 ^{Aa}	-6.00 ^{DEAc}	-8.00 ^{BCDEa}
		50	-11.00 ^{ABCa}	-9.50 ^{BCDab}	-5.50 ^{DEa}
		75	-11.70 ^{ABa}	-11.67 ^{ABb}	-7.00 ^{CDEa}
		100	-11.50 ^{ABa}	-4.50 ^{Ec}	-9.25 ^{BCDa}
	448.1	25	-38.00 ^{Aa}	-12.94 ^{Fa}	-21.57 ^{Ba}
		50	-19.20 ^{BDb}	-12.94 ^{Fa}	-15.69 ^{CEfb}
		75	-17.10 ^{CDEc}	-12.68 ^{Fa}	-17.65 ^{BCDEab}
		100	-19.20 ^{BDEbc}	-5.69 ^{Gb}	-13.92 ^{CFb}

Note:

[1] – Means with the same uppercase letters within the same row for each application pressure are not significantly different at $\alpha=0.05$.

[2] – Means with the same lowercase letters within the same column for each application pressure are not significantly different at $\alpha=0.05$.

Table 2.13. Flow Rate Change when Using the Different PWM Systems at 30 Hz.

Application Rate, L ha ⁻¹	Application Pressure, kPa	Duty Cycle, % [2]	PWM System [1]		
			S1 [3]	S2	S3
			Flow rate, % Change	Flow rate, % Change	Flow rate, % Change
112.2	275.8	25	-	24.00 ^{Aa}	-12.00 ^{Ea}
		50	-	10.00 ^{Bb}	8.67 ^{BDc}
		75	-	4.89 ^{BDbc}	-1.78 ^{Cb}
		100	-	3.67 ^{CDc}	-7.33 ^{Eab}
	448.1	25	-	29.56 ^{Aa}	-16.98 ^{Ea}
		50	-	9.43 ^{Bb}	9.43 ^{Bb}
		75	-	2.94 ^{Cc}	2.10 ^{Cc}
		100	-	2.68 ^{Cc}	-3.62 ^{Dd}
187.1	275.8	25	-	15.00 ^{Aa}	-6.00 ^{Ea}
		50	-	0.00 ^{BDb}	1.50 ^{Bb}
		75	-	-3.00 ^{Cc}	0.00 ^{BDb}
		100	-	-1.25 ^{CDbc}	-3.75 ^{Ca}
	448.1	25	-	9.80 ^{Aa}	-54.51 ^{Ba}
		50	-	-2.75 ^{Ab}	-20.78 ^{Bb}
		75	-	-7.45 ^{Ac}	-21.05 ^{Bb}
		100	-	-3.73 ^{Ab}	-15.29 ^{Bc}

Note:

[1] – Means with the same uppercase letters within the same row for each application pressure are not significantly different at $\alpha=0.05$.

[2] – Means with the same lowercase letters within the same column for each application pressure are not significantly different at $\alpha=0.05$.

[3] – The S1 PWM system cannot be operated at 30 Hz frequency.

Producers have the option to select a certain PWM system and implement system frequency. Although majority of the manufacturers recommend to operate the PWM systems at 10 Hz, there are systems which operate at 15 Hz and 30 Hz. The S1 PWM system has the option to change the system frequency to 10 Hz, 15 Hz, and 30 Hz. However, at 30 Hz frequency, the S1 PWM system provided a 10 Hz data when tested that is why it was not included in the analysis. The S2 PWM system operates at 15 Hz and 30 Hz, while the S3 PWM system has the functionality to vary the system frequency to either 10 Hz, 15 Hz, and 30 Hz. Producers should be mindful of different pressure drops and might consider these when implementing each of these systems during field application to achieve target application pressures. The varying stabilized application pressure time and flow rate when operating at higher frequencies should be carefully considered. Therefore, the frequency setting recommended by the manufacturer should be followed to minimize the application errors.

The results of the study do not implicate the impact of the resistance caused by the nozzle bodies and nozzle design. Therefore, the results only apply to the particular nozzle bodies, and nozzle types used to evaluate each PWM system and may vary if different types of nozzle bodies and nozzle types will be used.

2.5 Conclusion

The performance of the three different commercially available PWM nozzle control systems was evaluated based on the pressure drop, flow rate, and response time at various duty cycles and frequencies using two different application rates and pressures. The following conclusions were drawn;

1. Each PWM system provided a different pressure drop when applying at different application pressure and application rate. Producers need to consider these pressure drops when using a particular PWM system to apply a product at a specific application rate and pressure. Operating at a lower pressure than the recommended will impact the flow rate, droplet size, and spray pattern, significantly influencing the application efficiency due to under- application. The commercial sprayer manufacturers should consider utilizing pressure sensors on selected nozzles across the boom sections to provide the average pressure feedback to the controller and manage target nozzle pressure irrespective of nozzle type and application rate to minimize application errors caused by the pressure drop.
2. The PWM system had an inherent latency before reaching the target application pressure and continued applying the product after the solenoid closed. These latencies could impact the correct droplet size, and at the appropriate overlap during operation; while applying the product at less time than the specified duty cycle, could lead to product rate inaccuracies during each cycle. The cumulative effect of peak, stabilized application pressure and fall time could impact the overall product flow rate within a cycle, potentially resulting in off-rate errors during field operation.
3. The flow rate from each nozzle was less than the expected flow rate due to the varying pressure drop and cumulative effect of peak, stabilized pressure application and drop times.

Chapter 3 - Nozzle Pressure Uniformity and Expected Droplet Size Spectra of Pulse Width Modulation (PWM) Spray Technology

3.1 Abstract

Pulse width modulation (PWM) is currently implemented in agricultural sprayers to deliver the expected flowrate by managing the duty cycle and maintaining the target pressure and provide the desired droplet size. However, there are still issues about the application errors caused by the pressure variations when using this system as it may result in pesticide resistance and product loss. Field tests were conducted in a 30.0 hectare (ha) and 54.0 ha fields to assess the pressure uniformity and the expected droplet size of the PWM technology. These parameters were also translated to an equivalent value if a flow-based system will be used during operation.

Results showed that pressure mostly remained within the acceptable range in both fields. Pressure CV were within 10.0%, indicating the system's ability to provide acceptable pressure at varying conditions. However, nozzle pressure still varies, especially at the outer boom section where frequent duty cycle variation occurs. Pressure also deviates during acceleration and deceleration, indicating the system's latency to respond rapidly to changing conditions. In a flow-based system, the pressure varies due to varying speed as dictated by field terrain, curvilinear paths, and headland maneuvers. The droplet size also deviates from the expected droplet spectra based on the nozzle manufacturer's specification when using a PWM system. However, the PWM system can still provide the target droplet size if a nozzle selected provides the desired droplet spectra in a wide range of pressure. In a flow-based system, the droplet size was expected to vary because of the fluctuation in application pressure due to speed changes during operation.

3.2 Introduction

Pulse width modulation (PWM) is one of the variable-rate technologies that has the potential to minimize the application errors caused by varying pressure during operation as it manages the flowrate at nozzle level using an electronically actuated solenoid valve. Unlike the flow-based system, PWM system is designed to maintain the application pressure regardless of sprayer speed and swath width. The flowrate from each nozzle is managed by varying the duty cycle. It is important to have a consistent nozzle flow rate to deliver and maintain the correct application rate during operation (Needham et al., 2012). Any fluctuation in the desired nozzle flow rate may result in the inaccuracy of spray outputs (Silva et al., 2018). Han et al. (2001) reported a flow rate change of 0.5 to 2.2% caused by the inaccuracy of the pressure controller. The system should be able to deliver the product at the target application pressure to achieve the desired nozzle flowrate. In addition, the pressure also influences the spray angle and droplet size as it regulates the velocity of the liquid that exiting the nozzle. In chemical applications, it is important to follow the recommended droplet size based on the pesticide label to efficiently control pests and achieve the proper spray coverage and minimize the spray drift (Needham et al., 2012). Daggupati (2007) reported that pressure lower than 207.0 kPa may lead to a reduction in spray angle. Similarly, the reduction in pressure especially when using larger orifice size nozzles may affect the spray pattern and produce coarser droplets (Butts et al., 2019). Moreover, Butts et al., (2019) suggested operating the PWM sprayer at or above 276.0 kPa to compensate for the impact of pulsing on droplet size caused by the pressure drop across the nozzle valve. There are still issues regarding the use of the PWM technology especially in terms of operating at lower duty cycles and the ability of the controller to maintain the target pressure at varying field conditions. Lang (2013) reported variability in the volumetric median diameter in a pre-orifice nozzle and an

increase in driftable fines when the system operates at lower duty cycles. Shahemabadi et al.(2008) on the other hand, reported the inability of the control system to maintain the target pressure across the boom due to fluctuations caused by the PWM valves. Silva et al., (2018) reported a pressure drop from 345.0 kPa to 324.0 kPa when the duty cycle increased from 10.0% to 100.0% in a no-pressure-adjustment condition which may indicate that the delay in the system response may affect the application pressure. In addition, these results may also be due to the delayed response of the controller to maintain the pressure at varying field conditions. Mangus et al., (2017) observe a 20.0 milliseconds (ms) latency in each cycle before the PWM system reaches the desired system pressure. However, the pressure remains within $\pm 5.0\%$ error irrespective of section control actuation even though there is a controller latency. These studies, however, are conducted in a laboratory setting and does not consider the varying field and environmental conditions. Also, there are limited studies that exist about the pressure stability during solenoid valve actuation, during sudden speed transition wherein sprayer acceleration and deceleration may instantly vary each nozzle duty cycle and the section control actuation that may shut-off several nozzles during field operation. These conditions are difficult to simulate in the laboratory setting. In a static test, simulating the speed of the sprayer will vary the duty cycle but all nozzle across the boom will have similar duty cycle. Similarly, nozzles cannot be shut-off individually unlike in field test where individual nozzle may automatically shut-off when operating in portions of the field that had already been applied with product. Therefore, the objective of this study is to evaluate the performance of the PWM spray technology in the field setting wherein rapid and continuous speed, and section actuation occur. The study specifically aims to determine the nozzle pressure and droplet size uniformity of a PWM-equipped agricultural sprayer.

3.3 Materials and Methods

3.3.1 Machine set-up

Field tests were conducted in two different fields located at Clay Center, Kansas using a commercially available self-propelled front-mounted boom sprayer (SP370F Guardian, New Holland, PA) having a 36.6-meter (m) wet boom with 73 nozzles spaced at 0.51-m apart. (Figure 3.1).



Figure 3.1. The New Holland SP370F Agricultural Sprayer Used in the Study.

The auto-nozzle control function of the sprayer was controlled by the solenoid valves (Raven Hawkeye, Raven Industries, Inc., Sioux Falls, SD) that were mapped in the controller such that the first outer most nozzles on either side of the boom are controlled individually, the next thirty inner nozzles on the left boom and the next thirty-two inner nozzles on the right boom were controlled in pairs while the remaining inner most nozzles were controlled in groups of three (Figure 3.2). The PWM solenoid valves operate at 10 Hz system frequency.

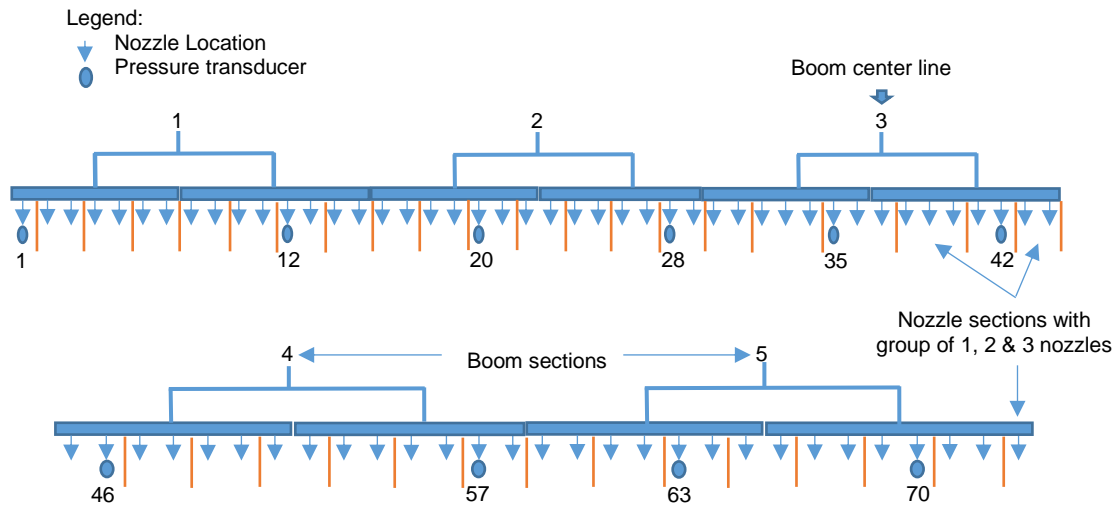


Figure 3.2. Layout of the Sprayer Boom with 73 Nozzle Sections with a Group of either 1, 2, or 3 Nozzles. The Nozzles are Numbered from Left to Right Across the Boom.

The display (IntelliView IV, Raven Industries, Inc., Sioux Falls, SD) and the sprayer control system has five control channels to actuate the boom shut-off valves. The target flow across the spray boom was regulated by utilizing feedback from an inline flow meter while controlling the hydraulic pump speed. The overall system flow rate was controlled through the hydraulic valves using pulse width modulation. The sprayer was also equipped with an auto-guidance system. Field testing was conducted on a 30.0-hectare (ha) and 54.0-ha fields referred to as field 1 and field 2 respectively, using water as the test liquid. For field 1, the sprayer was set-up to apply 140.0 liters per hectare ($L ha^{-1}$) at 324.0 kiloPascal (kPa). This application pressure was 48.0 kPa higher than the target application pressure of 276.0 kPa. The 48.0 kPa additional pressure was determined during a preliminary static test conducted on the sprayer as the pressure drop at the nozzle during operation. Hence, the 48.0 kPa was added to the target pressure to compensate for the nozzle pressure drop to maintain the target pressure of 276.0 kPa during application. The nozzle used in field 1 was an XR11008 nozzle tip (Teejet Technologies, Urbandale, IA). For field 2, the

sprayer applied at a rate of 112.0 L ha⁻¹. Similar procedure was done when setting-up the application pressure. The system was programmed to apply at an application pressure of 462.0 kPa which was also 48.0 kPa higher than the target application pressure of 414.0 kPa. The product application in field 2 was conducted using an XR11006 nozzle tip. During operation in both fields, the boom height was set at 0.50 m and maintained using the sprayer's auto-boom control.

3.3.2 Instrumentation

In all tests, high frequency (<1 ms response time) pressure transducers (1502B81EZ100PSIG, PCB Piezotronics, Depew, NY) with a measuring capacity of up to 689.5 kPa and an accuracy of 1.72 kPa were fitted in 10 randomly selected nozzles across the sprayer boom. The pressure transducers were mounted in such a way that two were located within each boom section. The solenoid valves were removed and the nozzle bodies were capped to measure the real-time boom pressure during operation (Figure 3.3). The actual nozzle pressure was calculated by subtracting 48.0 kPa from the boom pressure.



Figure 3.3. Capped Nozzle Body with the Solenoid Valve Removed to Measure Real-Time Boom Pressure.

The overall system flow rate was measured using a turbine type flow meter (FT-16, Flow Technology Inc., Tempe, AZ). The flow meter can measure a flow rate of up to 227.0 liters per minute ($L\ min^{-1}$) and has a linear response of 1.0 ms. The flow meter was installed after the existing flow meter underneath the sprayer going into the boom (Figure 3.4).



Figure 3.4. The flowmeter Used to Measure the System Flow Rate.

The duty cycle information from 36 selected nozzle control valves (NCV) was gathered by tapping into the systems controller area network (CAN) diagnostic port. The NCVs were selected such that it represents the duty cycle data from the 36 virtual sections of the sprayer. The virtual section refers to the grouping of the nozzles across the boom (Figure 3.2). The nozzles can be either controlled individually, in pairs, or in a group of three. Nozzles that were controlled in a group provided the same duty cycle during operation.

The nozzle pressure, flow rate, and duty cycle data were recorded at 40 Hz sampling frequency during the field tests. The sprayer's location and ground speed data were provided by the global navigation satellite system (GNSS) survey-grade base-rover units (GR5, Topcon, Livermore, CA) and were recorded at 10 Hz.

The nozzle pressure, flowrate, duty cycle location, and ground speed data were recorded using a data acquisition system consisting of National Instruments cRIO-9047 controller and C-series modules including NI-9221, NI-9870, and NI-9853 (Figure 3.5) and a custom LabVIEW program. The data were saved into a text file for analysis.

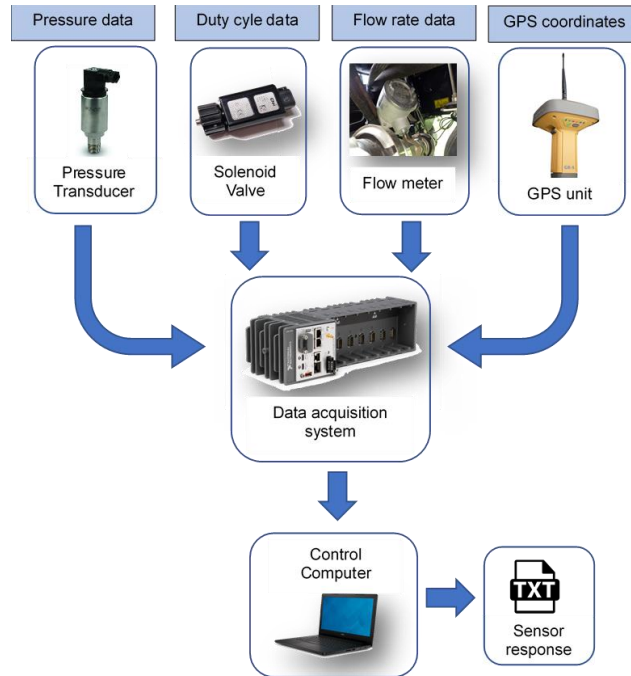


Figure 3.5. Data Acquisition System Set-Up.

3.3.3 Data collection

The sprayer speed range used during the operation was calculated based on the nozzle size, the target speed, and the desired minimum and maximum duty cycle (Fabula et al., 2019). Field operation was conducted based on the established speed ranges to employ spray application within the desired duty cycle. The speed range of 13.0 to 25.0 kph used to operate the sprayer in field 1 was calculated based on the desired duty cycle range of 50% and 75% and target operating speed of 19.0 kilometers per hour (kph). In field 2, the sprayer was operated within the speed range of

14.0 kph to 29.0 kph. The speed range used in field 2 was calculated according to the target operating speed of 24.0 kph and the desired duty cycle of 50% to 75%. In both fields, the desired maximum duty cycle of 75% was selected to provide a flexibility for the duty cycle to go beyond the 75% up to 100% duty cycle. The sprayer was operated within the established speed ranges to maintain proper spray coverage to minimize application rate errors (Mangus et al., 2017). The duty cycle data from each nozzle control valve recorded from the sprayer CAN bus was converted into the equivalent speed to determine the individual speed of each nozzle during operation

The nozzle pressure uniformity during application was evaluated by determining the instances that the nozzle application pressure was within the range wherein the application rate was at $\pm 5.0\%$ of the desired rate. The coefficient of variation (CV) was also calculated to assess the nozzle pressure uniformity across the boom. The droplet size spectra uniformity was also determined by converting the pressure data to its equivalent droplet size (coarse, medium, and fine) using the manufacturers' catalog (Teejet Catalog 51A, Spraying Systems Co., Wheaton, IL) (Table 1). The XR 11008 nozzle used in field 1 was expected to provide a coarse droplet spectra in an application pressure ranging from 103.4 kPa to 206.8 kPa, medium droplet spectra at an application pressure ranging from 276.0 kPa to 414.0 kPa. In field 2, the XR 11006 nozzle was assumed to be providing a coarse droplet spectra at an application pressure of ≤ 103.4 kPa, medium droplet spectra at 137.9 kPa to 344.7 kPa pressure range, and fine droplet spectra at an application pressure of ≥ 414.0 kPa. The uniformity of droplet size spectra was evaluated by determining the instances that the droplet remains within the expected size based on the target pressure.

Table 3.1. Expected Droplet Size Spectra at Different Application Pressures of the Nozzles Used in the Study. (www.teejet.com)

Nozzle Type	Pressure, kPa	Droplet Size Spectra
XR 11006	103.4	Coarse
	137.9	Medium
	206.8	Medium
	276.0	Medium
	344.7	Medium
	414.0	Fine
XR 11008	103.4	Coarse
	137.9	Coarse
	206.8	Coarse
	276.0	Medium
	344.7	Medium
	414.0	Medium

The equivalent nozzle pressure uniformity data was also estimated, considering a flow-based system was used during the application. The nozzle pressure was determined by calculating the nozzle flow rate based on the sprayer's speed using equation 1.

$$l/min = \frac{(l/ha)(w)(kph)}{60000} \quad (1)$$

where l/min = nozzle flow rate, liters per minute.

l/ha = application rate, liters per hectare.

w = nozzle spacing, cm.

kph = speed, kilometers per hour.

60,000 = coefficient to convert the value into liters per minute

The calculated nozzle flow rate was then used to estimate the equivalent nozzle pressure by developing a regression equation using the manufacturer data for the specific nozzle used in the application. For comparison, it was assumed that there were no boom pressure deviations, although previous study has indicated that the pressure variation can range from 6.7 to 20.0% during section actuation when using a flow-based system (Sharda et al., 2013).

The droplet size provided by each nozzle was dependent on the manufacturers' catalog. Once the average application pressure was determined, its equivalent droplet size was established using the pressure and droplet size data from the manufacturers' catalog.

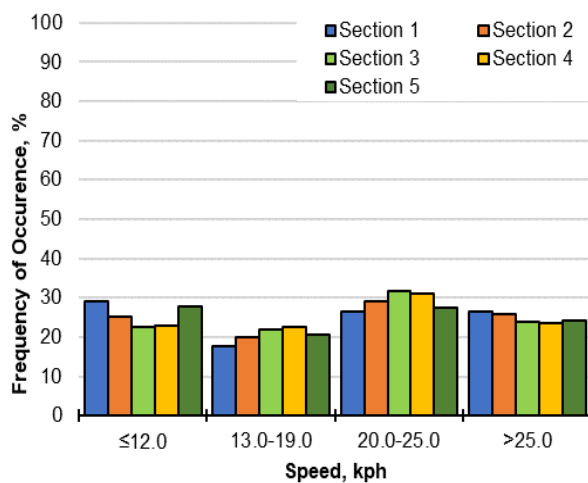
Application pressure maps were also developed using hypothetical scenarios, considering if the applications in field 1 and field 2 were conducted using flow-based control systems. Real-time application speeds, the number of On nozzle control sections, nozzle spacing, and target application rates captured using the DAQ system for field 1 and field 2 were utilized to calculate theoretical application pressures. It was assumed that the control system had no latencies, and the system always maintained the theoretically derived application pressures. The calculated application pressures were then utilized to derive equivalent size using manufacturer data for the nozzles utilized in the field application. Calculated application pressure and droplet size were mapped in ArcGIS for comparison with the PWM system. The nozzle pressure uniformity, droplet size distribution, and CV maps were generated using ArcMap 10.6 (ESRI, Redlands, CA) to illustrate the data's spatial results across the field.

3.4 Results and Discussions

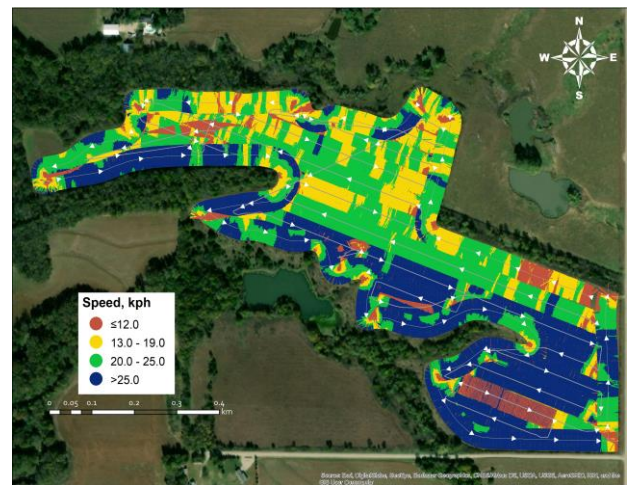
3.4.1 Speed range

In field 1, the average nozzle speed per boom section was within the target speed range of 13.0 to 25.0 kph for 50.0% of the time (Figure 3.6.a). In field 2, the sprayer was operated within the speed range of 15.0 kph to 29.0 kph for 55.0% of the time (Figure 3.7.a). Though there are no standard values regarding the acceptable duty cycle range that should be used during product application, most manufacturers suggested the 50% to 90% duty cycle. In addition, Mangus et al. (2017) and Butts et al. (2019) also reported that operating at a duty cycle lower than 50% may

impact the spray coverage and droplet size uniformity due to incomplete signal overlap between the odd and even nozzles. There were instances that the average nozzle speed per boom section was beyond the target speed range, which usually occurred when the sprayer approaches the headland, if there were changes on terrain wherein it needed to slow down or when turning on the boundary (Figure 3.6.b and 3.7.b). The nozzle speed from the outer boom sections was also faster during turns than the nozzle speed on the inner boom section (Figure 3.6.b and 3.7.b). The sprayer operation in headland, terrain change, and curvilinear passes suggests that there would invariably be instances where the operator needs to slow down or maneuver the curvilinear pass without much knowledge on the speed of boom. Further work needs to be conducted to incorporate indicators to highlight 1) good speed ranges for acceptable application and 2) speed of inside and outside of the spray boom during curvilinear passes to keep the operator informed and make adjustments in driving style in order to stay in good speed ranges. Additionally, operators may be suggested to leave and enter the headland at driving speeds, which fall in the desired speed and duty cycle.



(a)



(b)

Figure 3.6. Speed Distribution Plot (a) and Speed Range Distribution Map (b) for Field 1.

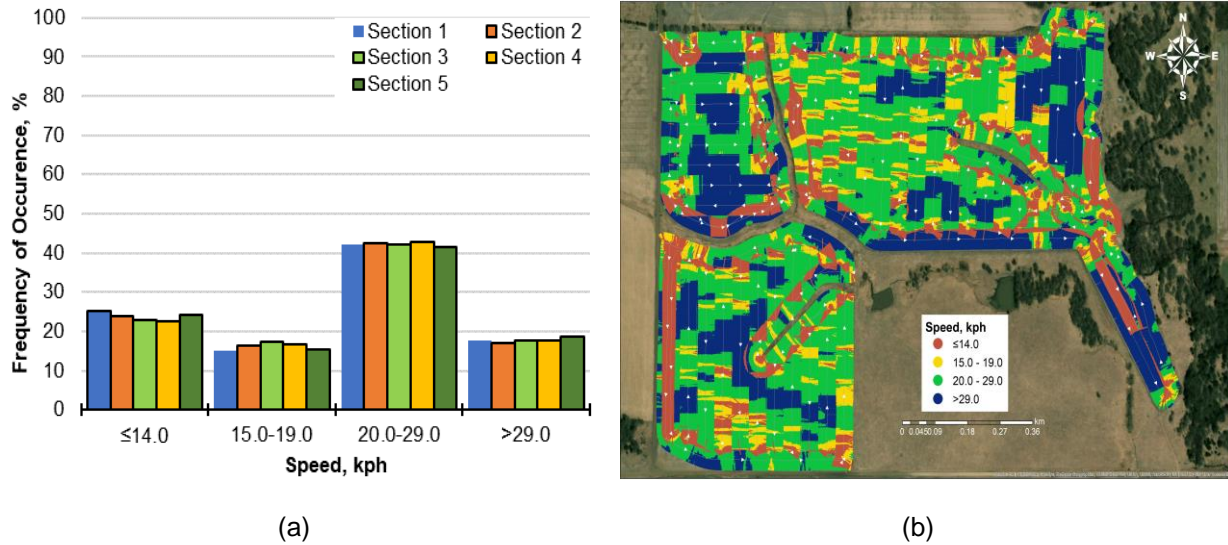


Figure 3.7. Speed Distribution Plot (a) and Speed Range Distribution Map (b) for Field 2.

The results also indicated that incidents of boom section operating beyond the target speed range were higher on field 1 than on field 2. The results were primarily due to more irregularity in field 1 requiring more frequent turns, especially on the boundary, while field 2 was mostly rectangular where the sprayer needed fewer turns. Sprayer operation at speeds greater than the speed at which the system implements a 100% duty cycle would potentially result in under-application. Currently, no warning sign or machine control is available to limit the sprayer operation beyond speeds which requires 100% duty cycles.

3.4.2 Pressure uniformity

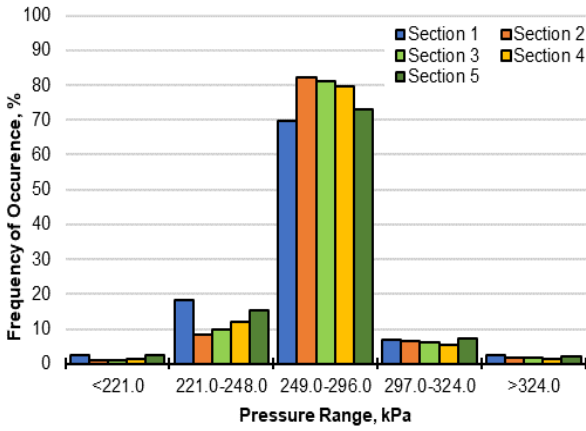
3.4.2.1 Pulse width modulation system

The results show that 77.0% of the time, the nozzle pressure was within the 249.0 kPa to 296.0 kPa target application pressure in field 1 (Figure 3.8.a), although it was an irregularly shaped field (Figure 3.8.b). However, the nozzle pressure at the outer boom sections had a lower instance of operating at the target application pressure range than the middle boom sections (71.0%) but

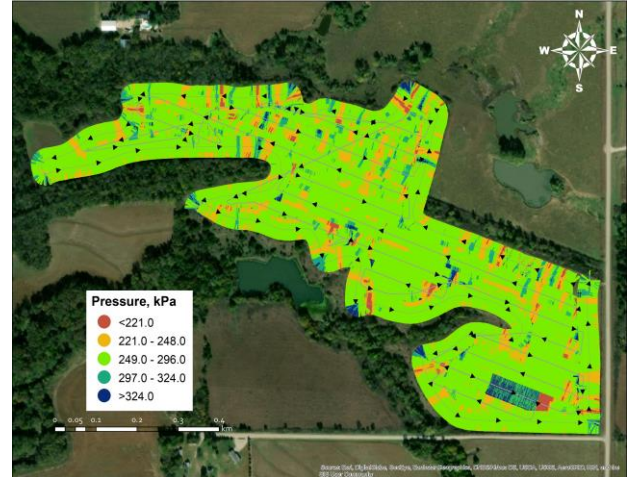
mostly remains within the preferred pressure range. There were instances that the nozzle pressure dropped below the application pressure range (14.0% of the time). There were also events that the nozzle pressure was beyond the target application pressure range (8.0% of the time) during operation.

In contrast to field 1, field 2 was more rectangular-shaped, but it has more varying terrain with terraces and grassed waterways (Figure 3.9.b). The nozzle pressure during operation in field 2 remains within the target application range of 366.0 kPa to 455.0 kPa for 89.0% of the time. The nozzle pressure on the outer boom sections also had lower occurrence of operating at the target pressure range (87.0%) though it mostly remains within the desired pressure range during application. Similar to field 1, there were events wherein the nozzle pressure during application dropped below the target application range (6.0% of the time). The nozzle pressure also went beyond the target application pressure range for 5.0% of the time (Figure 3.9.a).

The nozzle pressure in both fields mostly remains within the target application pressure range. The selected pressure range used in Figures 3.8 and 3.9 was based on the range wherein the application rate will change by $\pm 5.0\%$, $\pm 10\%$, and less than or greater than 10.0% of the target rate. The result indicated the system's ability to make the necessary adjustment to maintain the nozzle pressure within the acceptable pressure range, even at different field conditions such as varying terrains and turning at boundaries.

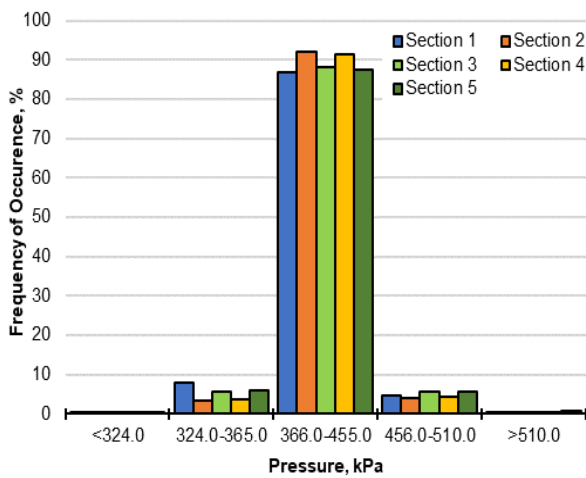


(a)



(b)

Figure 3.8. Pressure Uniformity Plot (a) and Pressure Uniformity Map (b) for Field 1 when Using a PWM System.



(a)



(b)

Figure 3.9. Pressure Uniformity Plot (a) and Pressure Uniformity Map (b) for Field 2 when Using a PWM System.

The study's result also signifies the system's capability to provide consistent nozzle pressure during section control actuation. This outcome is similar to the study conducted by Mangus et al. (2017), wherein the PWM system maintains the pressure within $\pm 5.0\%$ error irrespective of the number of active nozzles in a laboratory setting when conducting static

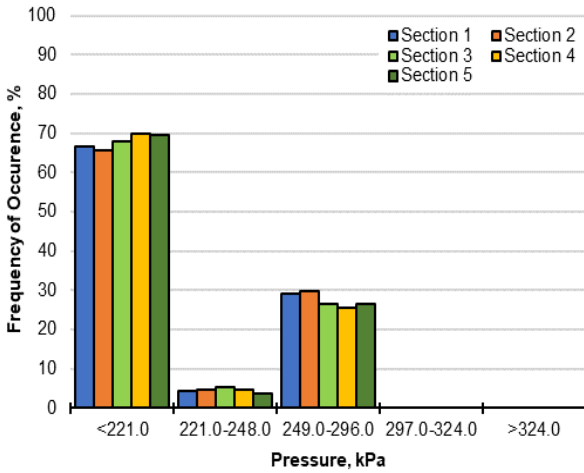
simulation tests. The result of this study is a great improvement to the spray application technology as compared to the flow-based system wherein the application pressure varies during boom section actuation, thereby impacting the application rates on sections that remained on as the system compensates to the change in flowrate (Luck et al., 2011). Though majority of the time, the nozzle pressure remains within the target application pressure, nozzle pressure on the outer section of the sprayer sometimes operates beyond the target pressure. The outer boom sections were more frequently subjected to duty cycle changes and section control actuation, especially during turning, to compensate for speed differences, which may have contributed to this error. However, these instances occurred in a much less percentage of time in a PWM system than the flow-based systems wherein the application rates variations are higher during tighter turns as the outer sections on the boom covers more area than the inner sections (Luck et al., 2011).

Sprayer deceleration when approaching obstacles such as waterways and terraces or entering the headlands and acceleration after clearing the obstacles or entering the spray zones also resulted in pressure deviations. These events required large flow rate changes from the controller managing system flow rate in the back end. The results indicated control system latencies during rapid acceleration and deceleration, resulting in the system's inability to respond rapidly in such demanding control situations. Sharda et al. (2013) and Luck et al. (2011) also reported a deviation in application rates due to variation in operating speed across the fields, which is associated with the system latencies when operating a flow-based system. However, PWM system provides pressure uniformity for a significantly higher percentage of the time. Both system latency and lower duty cycle (<40%) may result in non-uniformity of application, which may impact the efficacy of the product being applied (Mangus et al., 2017). Similarly, operating below the

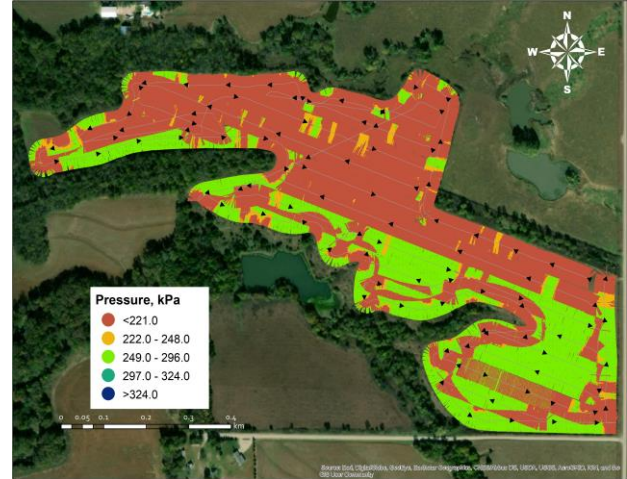
recommended pressure may also influence the nozzle's spray pattern angle, which may affect the spray coverage during operation (Daggupati, 2007).

3.4.2.2 Flow-based system

Comparing the flow-based system's behavior, assuming no pressure latencies during dynamic transient states, exhibited a different pressure distribution for field 1 and field 2 (Figure 3.10.a and 3.11.a). For field 1, nozzle pressure was less than 221.0 kPa for 68.0% of the time and less than 324.0 kPa in field 2 for 69.0% of the time. The pressure distributions would invariably happen because of changing sprayer speeds (Figures 3.6 and 3.7) due to terrain changes, operation on terraces and curvilinear paths, and headland maneuvers. Numerous studies have been conducted with flow-based systems, which indicated nozzle pressure deviation from expected pressure at real-time speed transitions and section control actuation (Sharda et al., 2010, and Sharda et al., 2013). The pressure distribution in Figure 3.10 and 3.11 is considering zero control system latencies, but nozzle pressure is bound to vary when using flow-based systems. The varying application pressures may not comply with the label specification when applying specific pesticides. The PWM control system, which can maintain target application pressure for a significantly greater percentage of the time, is more likely to conduct the application following the label specifications.

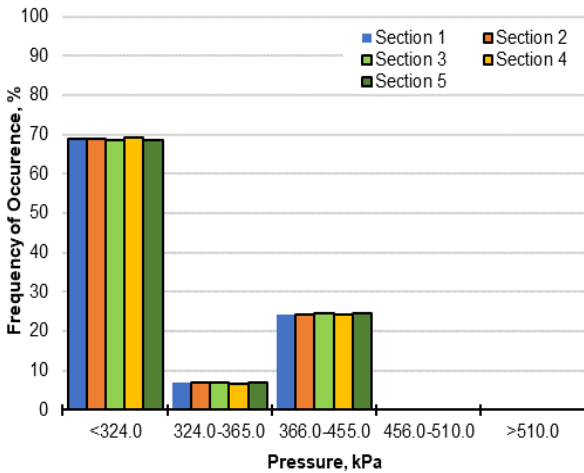


(a)

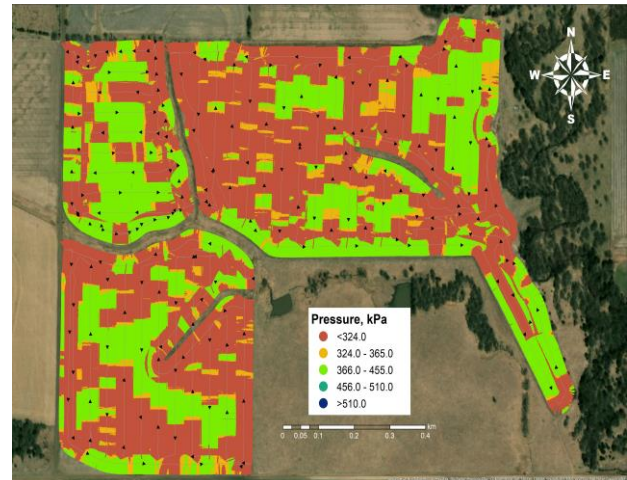


(b)

Figure 3.10. Pressure Uniformity Plot (a) and Pressure Uniformity Map (b) for Field 1 in a Flow-Based System.



(a)



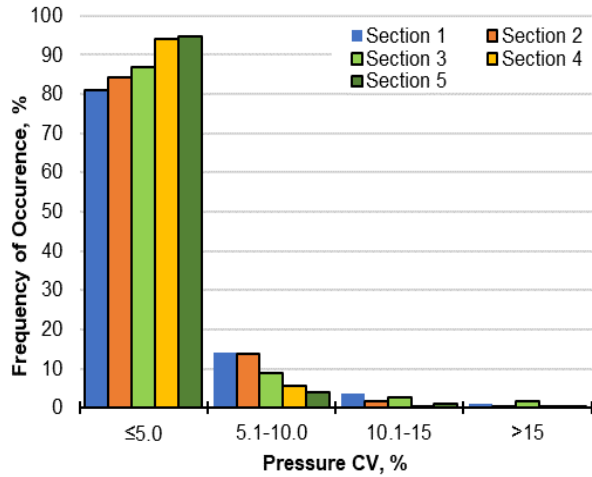
(b)

Figure 3.11. Pressure Uniformity Plot (a) and Pressure Uniformity Map (b) for Field 2 in a Flow-Based System.

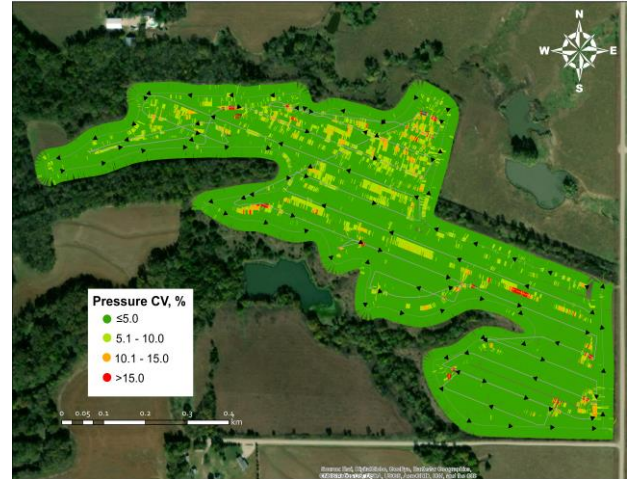
3.4.3 Coefficient of variation (CV)

The pressure CV in field 1 was less than 5.0% for 88.0% of the time and within 5.1% to 10.0% for 9.0% of the time. There were also instances that the pressure CV during operation on field 1 was beyond 10.0% but occurred for 2.0% of the time during operation (Figure 3.12.a). In

field 2, the pressure CV that was less than 5.0% happened for 78.0% of the time while 17.0% of the time the pressure CV was within the range of 5.1% to 10.0%. Also, 5.0% of the time the pressure CV was greater than 10.0% during operation (Figure 3.13.a). The pressure CV across the boom was less than 10% for most applications even though the fields varied in shape, terrain, and area, as required by the ASABE standard (ASABE Standards, 2016). The pressure CV varies during speed transitions, section actuation, and exiting or re-entering spray zones, although it mostly stays within the 10.0% CV range (Figure 3.12.b and 3.13.b). The pressure CVs were also with 10.0% for PWM systems for a much greater percentage of time (95% - 98%) compared to ones observed by Sharda et al. (2013) for a flow-based system (26%). These results indicated the ability of the PWM system to provide a uniform application pressure across the boom even at varying operating conditions. In these events, it was also expected that the system provided the desired nozzle flowrate during operation and thereby applying the correct amount of product during operation for a greater amount of time than the flow-based system. The quick acceleration of the sprayer may create a situation wherein the system may not immediately respond to the sudden change in speed and section actuation, which causes the application pressure to overshoot the target pressure.

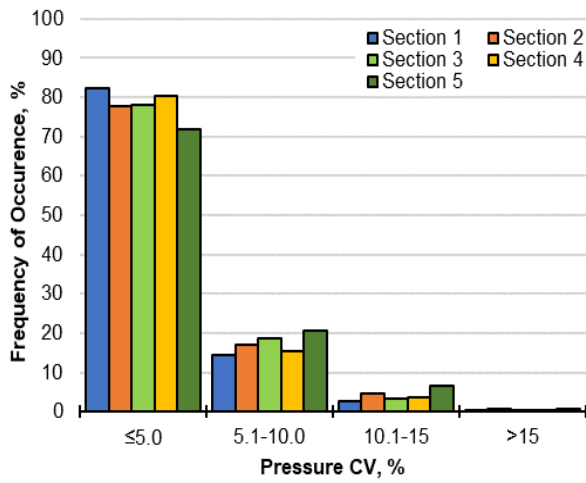


(a)



(b)

Figure 3.12. Pressure CV Plot (a) and CV Distribution Map (b) for Field 1 when Using a PWM System.



(a)



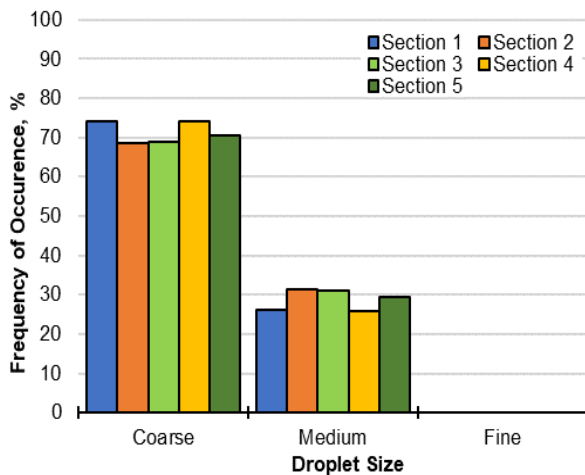
(b)

Figure 3.13. Pressure CV Plot (a) and CV Distribution Map (b) for Field 2 when Using a PWM System.

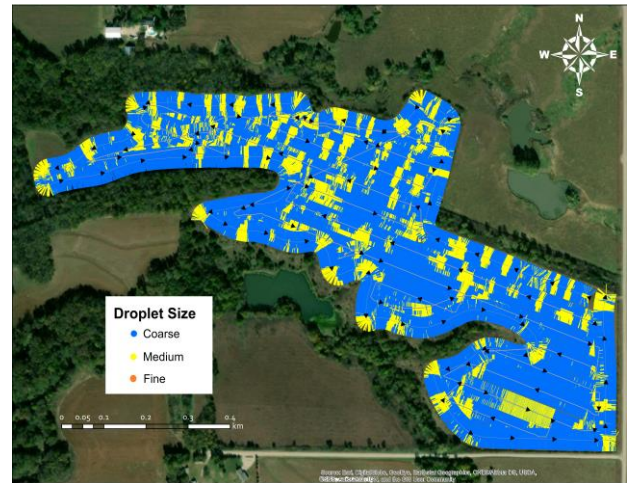
3.4.4 Expected droplet size spectra

3.4.4.1 Pulse width modulation system

The type of nozzle used during application in field 1 was an XR-11008, which was expected to provide medium droplets when operating at 276.0 kPa to 414.0 kPa application pressure. On the other hand, an XR-11006 nozzle tip used during application in field 2 was expected to provide a fine droplet size at an application pressure ≥ 414.0 kPa. Results show that the nozzle's droplet size during the operation in field 1 was mostly coarse droplets, which occurred for 71.0% of the time. The nozzle produced a medium droplet size for 29.0% of the time during operation (Figure 3.14.a and 3.14.b). Similar results were observed for field 2 with application in the fine category for 37.0% of the time (Figure 3.15.a and 3.15.b).



(a)



(b)

Figure 3.14. Droplet Size Spectra Uniformity Plot (a) and Map (b) for Field 1 when Using a PWM System.

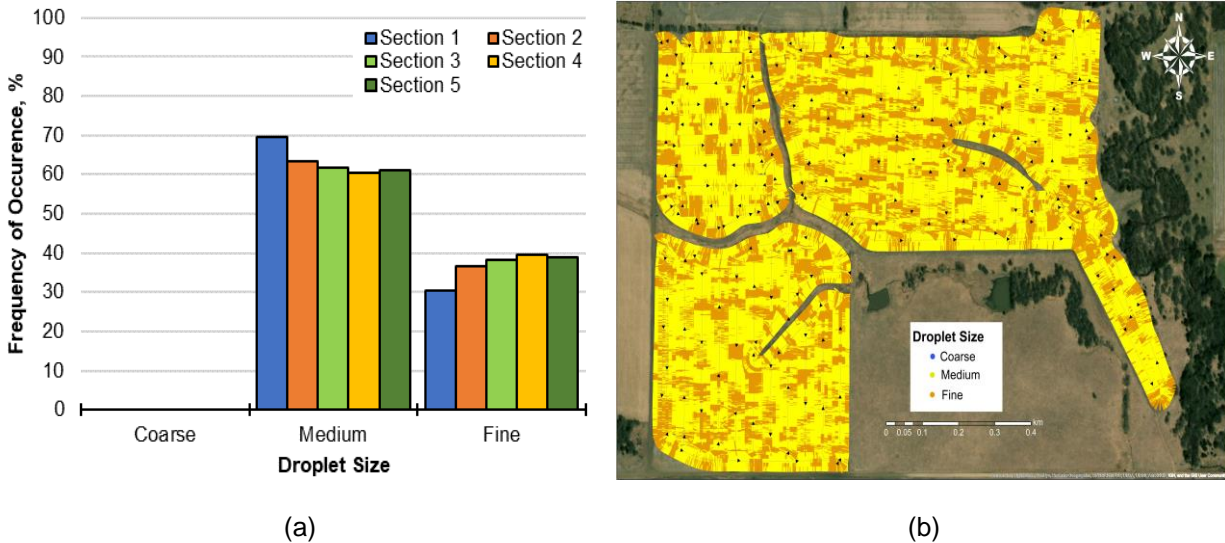


Figure 3.15. Droplet Size Spectra Uniformity Plot (a) and Map (b) for Field 2 when Using a PWM System.

These results signify a very critical aspect of correct nozzle size selection. Since the nozzles selected for field application had a boundary limit of target droplet size very close to the target pressure, even a small deviation in application pressure would change the droplet size. Creech et al. (2015) reported a change in spray droplets due to application pressure variation. The PWM system maintains the application pressure within the acceptable range for 87.0% of the time to apply the target rate within the $\pm 5.0\%$ error but the droplet size varies due to pressure variations during operation. But a correct nozzle selection should have at least provided a droplet size spectra for a similar amount of time.

The droplet size spectra uniformity results in both fields do not imply that the system could not provide the correct droplet size. It was a matter of selecting a nozzle tip that will provide the target droplet size in a wide range of application pressure. As an example, figure 3.16 shows the droplet size uniformity if an XR110-06 was used during product application in field 1 wherein the target application was 276.0 kPa. Since XR110-06 nozzle tip was expected to provide

a medium droplet size in an application pressure ranging from 138.0 kPa to 345.0 kPa therefore the system may consistently provide the target droplet size during the operation due to the wide range of pressure that delivers the target droplet size even at varying application pressure during product application. Therefore, nozzles should be carefully selected for spray application using PWM control systems (Fabula et al., 2019), and the system should be operated at higher pressure (≥ 276.0 kPa) and duty cycle ($\geq 40\%$) to reduce the impact of pulsing on droplet size (Butts et al., 2019).



Figure 3.16. Droplet Size Spectra Uniformity Map when Using a Nozzle Tip with a Wide Range of Application Pressure to Provide the Target Droplet Size.

3.4.4.2 Flow-based system

In a flow-based system, the droplet size during the application in field 1 was at the coarse category at all times (Figure 3.17.a). This could be the effect of having a pressure that was below the target during operation. Similarly, in field 2, wherein the combination of target pressure and nozzle tip was expected to provide a fine droplet size, the droplet was within the expected size category for only 16.0% of the time. During operation, the nozzle provided a medium-size droplet

for 56.0% of the time and coarse droplet size for 28.0% of the time (Figure 3.18.a). The droplet size distribution was consistent in field 1 (Figure 3.17.b) but varied in field 2 (Figure 3.18.b) if a flow-based system will be used in the application. Since pressure will increase and decrease with speed, the droplet size spectra will mostly like vary more than what was observed for the PWM control system. The speed distribution seen in the field 1 and 2, would invariably change the droplet size because of the changes expected in application pressure. Therefore, in the case of flow based-system the only option is to conduct the application in a tight speed range, which limits the productivity. On the other side, the PWM control system provides a greater speed range where both application pressure and droplet size distributions could be maintained, thus providing greater productivity opportunities. In the case of the PWM system, even though it may have the ability to maintain the application pressure within the acceptable range, the pressure fluctuation may affect the droplet size distribution (Butts et al., 2019).

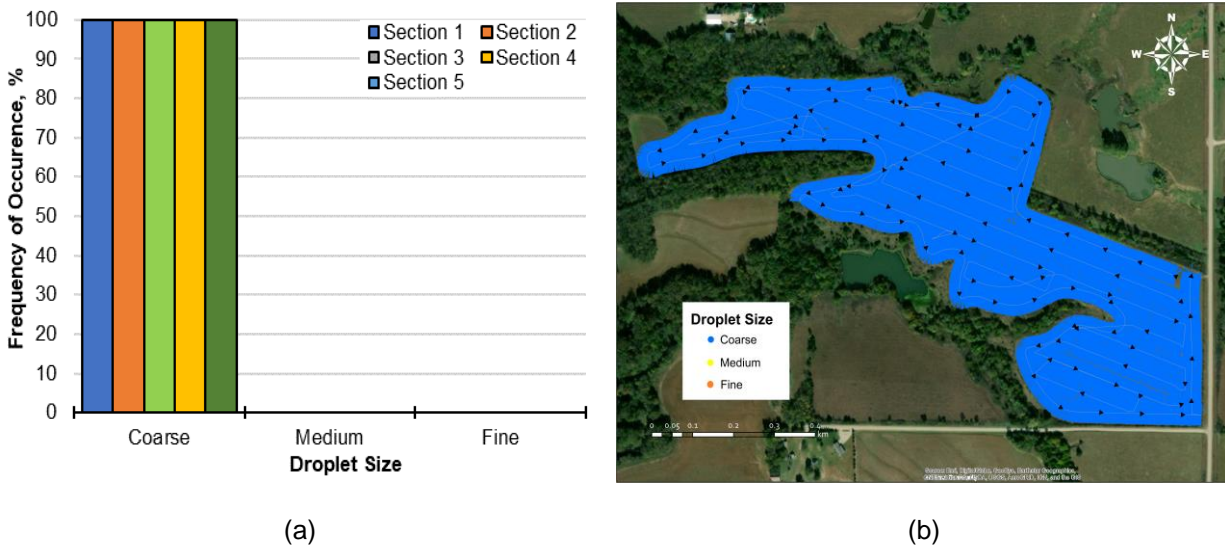
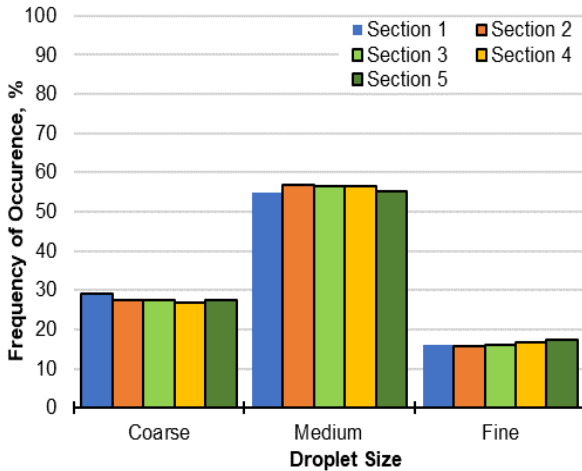
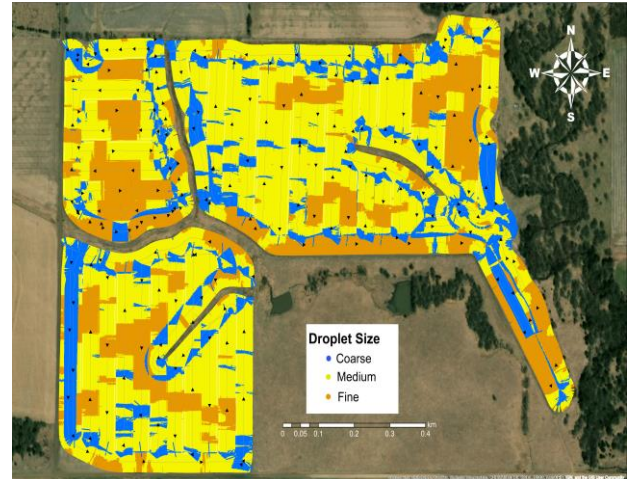


Figure 3.17. Droplet Size Spectra Uniformity Plot (a) and Map (b) for Field 1 in a Flow-Based System.



(a)



(b)

Figure 3.18. Droplet Size Spectra Uniformity Plot (a) and Map (b) for Field 2 in a Flow-Based System.

3.5 Conclusion

The field performance in terms of pressure and droplet size uniformity of an agricultural sprayer equipped with a PWM system was investigated. The sprayer was operated within the target speed range, which was determined based on the nozzle flowrate and the most desirable duty cycle selected to be used during the application. The application pressure in both fields mostly remains within the target pressure range, with the majority of pressure CV of less than 10.0%. It indicates the PWM system's capability to provide a uniform pressure even at varying field operating conditions that could aid the producers to minimize the off-rate errors. However, the operators need to understand that an abrupt change in speed may cause the pressure to fluctuate considerably, especially when clearing obstacles, re-entering, or exiting spray zones. The field's shape may have also contributed to the variation in pressure, especially on the outer booms, since these particular boom sections were subjected to frequent duty cycle changes to offset the change in speed between the boom sections during turns in the boundary. An agricultural sprayer equipped with a PWM

system performs better than a flow-based system in terms of providing a uniform pressure during operation. Although, the pressure data from a flow-based system were calculated based on the speed range and other operating conditions intended for a PWM system, several studies had already been published that show the disadvantages of a flow-based system in providing a uniform pressure during product application. Even though the PWM system may have the ability to provide uniform pressure, the droplet size distribution varies in both fields during operation. However, this result does not signify that the system cannot provide the target droplet size. Producers need to select a nozzle tip that will provide the target droplet size in a wide range of operating pressure to maintain a uniform product deposition. For future studies, it is recommended to evaluate the droplet size distribution using water-sensitive cards that may provide the actual droplet size distribution uniformity delivered by the nozzle during application.

Chapter 4 - Duty Cycle Implementation of Pulse Width Modulated (PWM) – Equipped Agricultural Sprayer

4.1 Abstract

The dependency of agriculture on chemical applications to increase crop production is increasing. Agricultural sprayers need to be properly calibrated, and the spray system should be providing the correct product volume regardless of the operator's driving style and field condition. Frequent speed changes may happen during operation, depending on the field terrain and shape. In these events, it is expected that the PWM system provides the right duty cycle that matched the speed of each nozzle across the boom to apply the product at the target rate. However, limited studies are available that investigate the PWM system's ability to provide the correct duty cycle during product application in field conditions wherein sudden speed transitions and section control actuation may happen. Hence, this study was conducted to assess the PWM system's ability to implement the correct duty cycle to provide the right amount of product during operation. A commercially available self-propelled sprayer equipped with a PWM system was used in this study. Field test was conducted in a 71.0- hectare (ha) and in a 29.0 ha field, referred to as field 1 and field 2, respectively. Product application was conducted using a Wilger MR 110-06 nozzle at a rate of 112.0 Liters per hectare ($L h^{-1}$). In both fields, the system was programmed to apply at an application pressure of 393.0 kilopascals (kPa) in field 1 and 462.0 kPa in field 2. Pressure transducers were installed in 10 selected nozzle bodies across the field to provide real-time pressure. The duty cycle data from 36 selected nozzle control valves were recorded by tapping into the controller area network (CAN) diagnostic port. It represents the duty cycle data from each sprayer's virtual section. The nozzle pressure and duty cycle data were recorded at 40 Hz sampling

frequency. The sprayer location and speed were provided by the global navigation satellite system (GNSS) survey-grade base-rover units located at the top-center of the sprayer boom section referred to as GPS 1 and an auxiliary dual-frequency GNSS receiver mounted beside nozzle 16, referred to as GPS 2. The sprayer's location and speed data were recorded at 10 Hz. The pressure, duty cycle, location, and speed data were recorded using a National Instruments data acquisition system and a LabVIEW program. The data from both GPS units were used to calculate the speed from each nozzle across the boom. The speed data were converted to its equivalent duty cycle and were compared to the actual duty cycle implemented by the PWM system. The actual application rate was also calculated using the speed, pressure, flow rate, and nozzle spacing and was also compared to the target application rate. Results show that the duty cycle and the application rate accuracy varies in both fields. These results suggest the difference between the actual duty cycle implemented by the PWM system to the expected duty cycle based on the speed of each nozzle and the actual rate that the PWM system applied to the target application rate. Both the duty cycle and application rate accuracy decrease with sudden speed transitions, which usually occurs when the sprayer accelerates when entering spray zones, decelerates when approaching headland, clearing obstacles, terrain changes, and making turns. Both the duty cycle and application rate accuracy were also low in the irregular field, which could be due to the frequent speed changes during turns in curvilinear passes, especially on nozzles located at the outer boom sections. These events may create a lot of demand for the control system, contributing to under-or over-application. The operator should maintain an acceptable speed range and adjust their driving style to minimize the duty cycle and application rate error during field operation.

4.2 Introduction

Agriculture is becoming heavily dependent on the application of agricultural chemicals to increase crop production. However, the application of chemicals to the crop is highly scrutinized because of its impact on human health and the environment. Chemical applications cause environmental concerns because of the production of volatile organic compounds (VOC). They are also resistant to degradation and, therefore, may enter waterways through surface runoff and contaminate groundwater due to deep percolation (Brady et al., 2006; Kuivila et al., 1995; Werner et al., 2004). Several pests species also developed resistance to agricultural chemicals that make them hard to control (Heap, 2020).

Agricultural sprayers became a significant part of the agricultural crop production system because of their ability to cover large fields. Hence, the spray system needs to be properly calibrated and needs to be properly working to apply the correct amount of product during operation. The improper amount of agricultural chemicals applied in the field may result in poor product efficacy, leading to reduced crop yield, additional cost to producers, and environmental contamination (Giles et al., 2008).

The development of new spray application technologies has been continuously conducted to improve the application of agricultural chemicals (Giles et al., 2008; Han et al., 2001; Lebeau et al., 2004; Miller et al., 1992; Zhang et al., 1995). These technologies have become an integral component of agricultural sprayers because of their potential to minimize the amount of chemicals that are being applied but to a level that is still effective in controlling pests and diseases and, at the same time, mitigate its impact on the environment (Loghavi et al., 2008). While the reduction of chemical emission through new technologies does not directly benefit the producers, it may

provide a potential benefit through product savings and better equipment productivity (Giles et al., 2011).

Implementing flow-based system in the past years offered an efficient way of delivering the right product volume during operation (Al-Gaadi et al., 1994; Ayers et al., 1990). A faster controller response is necessary to manage the application rates in a sprayer with wider booms operating at varying terrains. In a flow-based system, aside from the concerns regarding the application rate errors due to latency in controller response, under- and over-application, and off-target application (Porter et al., 2013; Sama et al., 2015), the system can only apply one flow rate across the sprayer boom. It increases the application error potential when applying in irregular fields due to the increase in the number of turns during operation. The system does not compensate for the difference in speed between the sprayer's inner and outer boom sections during turning. The flow-based system may implement under-application in boom section traveling faster and over-application in boom section that is traveling at slower speed.

One of the recent technologies that may have the potential to improve product application efficiency is the pulse width modulation (PWM) system. In a PWM system, agricultural chemicals are released by pulsing an electronically-actuated solenoid valve located upstream of the nozzle bodies. The solenoid valves are pulsed at a desired frequency and duty cycle varying from 0% to 100%. The system can provide a real-time change in flowrate without varying the application pressure than the other systems, such as the flow-based system wherein the pressure varies considerably during product application (Sharda et al., 2010). PWM sprayers may also provide a precise application and significant savings due to its automatic boom and individual nozzle control capability. It may also have the potential to reduce drift, increased canopy penetration, and improve product deposition. These are all possible because of its ability to provide the desired droplet size

based on the product label specification and better spray pattern overlap by maintaining a uniform application pressure during operation (Giles et al., 2008; Mangus et al., 2017). Consistent droplet spectra and uniform spray pattern overlap can be better achieved when the system is operated at higher duty cycles ($\geq 50\%$) (Butts et al., 2019; GopalaPillai et al., 1999; Mangus et al., 2017).

PWM systems are currently utilized in sprayers with wider booms and can operate faster to increase field capacity, minimize the labor cost, and apply the product in a timely manner. While larger areas can be covered, it may be susceptible to over- and under- applications due to the number of nozzles that the system needs to manage simultaneously, especially when there is a speed differential across the sprayer boom due to turning. Each nozzle should provide the correct product volume during operation. PWM signal sent to the solenoid valves controls the product's flow at the nozzle (Giles et al., 2008). Therefore, the correct implementation of the duty cycle during operation is a critical component of application rate management in a PWM system. The PWM system manages each nozzle's flow rate by changing the duty cycle representative of the nozzle speed to provide a uniform application. The PWM system's ability to provide an accurate rate of agricultural chemicals depends on the system's capability to immediately change the duty cycle based on the speed during application. The system needs to match each nozzle's speed across the boom with the correct duty cycle; otherwise, it will result in application error (Ooms et al., 2003). The PWM system's latency to actuate the solenoid according to the On/Off signal may contribute to off-rate errors, particularly of fields with varying terrains due to frequent speed transitions (Mangus et al., 2017). The boom movement may also impact the product application due to the boom's frequent back and forth action when operating in fields with varying terrain due to consistent acceleration and deceleration. In these events, the boom movement may consistently

vary each nozzle's speed, which may impact the PWM system's ability to change each nozzle's duty cycle immediately.

Limited knowledge exists regarding the PWM system's ability to match each nozzle's speed with the correct duty cycle. The system's ability to provide the correct duty cycle based on its speed is one of the key factors in achieving the target application rate, especially in a sprayer with wider booms wherein there are several nozzles that the system needs to manage simultaneously. Therefore, this study evaluates the PWM system's ability to accurately implement the correct duty cycle and apply the right product volume during a typical field operation wherein immediate speed transition and section control actuation occur.

4.3 Materials and Methods

4.3.1 Machine set-up

A commercially available self-propelled sprayer (Case Patriot 4440, CNH Industrial, Chicago, Ill.) was evaluated in two different fields at Clay Center, Kansas (Figure 4.1). The sprayer has a 36.6 meter (m) wet boom with 72 nozzles and spaced at 0.51 m.

The sprayer's auto-nozzle function was controlled by the solenoid valves (Raven Hawkeye, Raven Industries, Inc., Sioux Falls, SD). It was mapped in the controller such that some of the nozzles are controlled individually, others are coupled, and some are in group of three (Figure 4.2).



Figure 4.1. The Case Patriot 4440 Agricultural Sprayer Used in the Study.

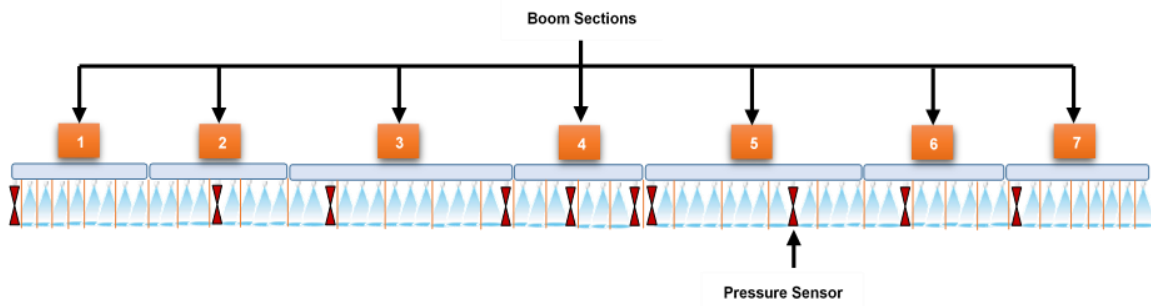


Figure 4.2. Layout of the Sprayer Boom with 72 Nozzle Sections with Groups of Either 1, 2, or 3 Nozzles. The nozzles are Numbered from Left to Right Across the Boom.

The display (Raven Viper Pro+, Raven Industries, Inc., Sioux Falls, S.D.) and the sprayer control system (Case Patriot 4440, CNH Industrial, Chicago, Ill.) has seven control channels that actuate the boom shut-off valves. The feedback from an inline flowmeter was utilized to regulate the flow across the boom while controlling the pump speed. The sprayer also has an auto-guidance system. The test was conducted in a 71.0-hectare (ha) and in 29.0 ha field referred to as field 1 and field 2, respectively. Product application was conducted using water as the test liquid. In both fields, a Wilger MR110-06 was used to apply the product at a rate of 112.0 Liters per hectare ($L h^{-1}$). In field 1, the product was applied at an application pressure of 393.0 kilopascals (kPa), while

462.0 kPa application pressure was used in field 2. Both application pressures were higher by 48.0 kPa than the target pressure to compensate for nozzle pressure drop.

4.3.2 Instrumentation

A high-frequency pressure transducers with less than one millisecond (ms) response time and an accuracy of less than 0.25% full scale were used in both fields. The pressure transducers were installed in 10 selected nozzles across the boom sections. The solenoid valve on the selected nozzle bodies was removed and capped to measure the real-time boom pressure during the operation (Figure 4.3).

The information about the duty cycle from 36 selected nozzle control valves (NCV) was recorded by connecting to the controller area network (CAN) diagnostic port. The 36 NCVs were selected to represent the duty cycle data from each sprayer's virtual section. The nozzle pressure, flowrate, and duty cycle data were recorded at 40 Hz.

The location and ground speed data of the sprayer were provided by the global navigation satellite system (GNSS) survey-grade base-rover units (GR5, Topcon, Livermore, CA) located at the top-center of the sprayer boom referred to as GPS 1 (Figure 4.4). The data were recorded at 10 Hz.

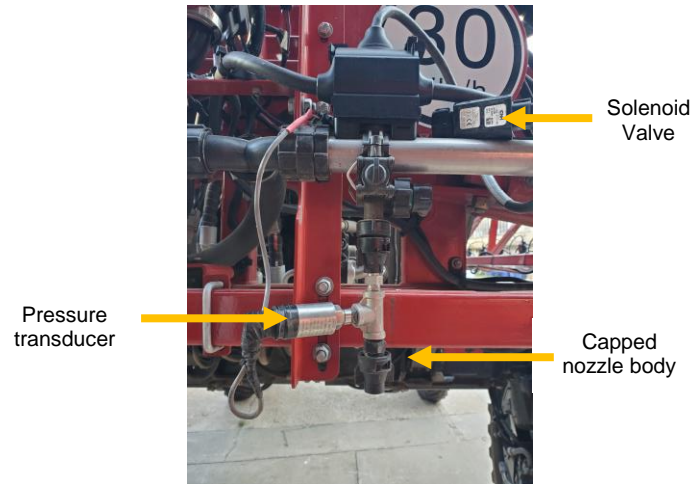


Figure 4.3. Capped Nozzle Body with the Solenoid Valve Removed to Measure Real-Time Boom Pressure.

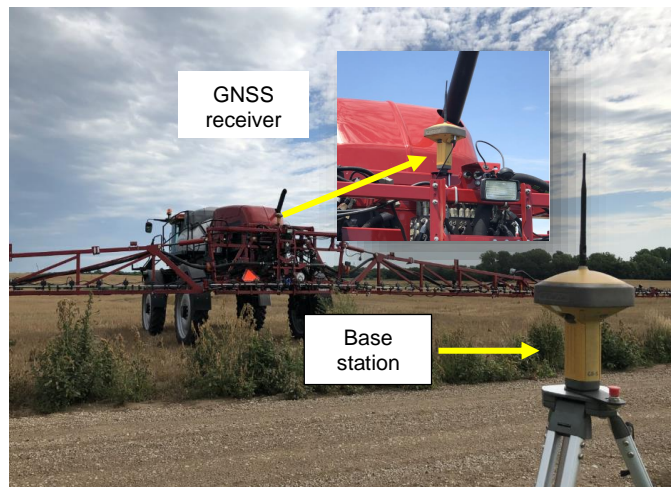


Figure 4.4. GNSS Receiver and Base Station.

An auxiliary, dual-frequency GNSS receiver (B110, Topcon, Livermore, CA) unit was mounted right next to nozzle 16, referred to as GPS 2. The GPS 2 also received RTK correction from the GR5 (Figure 4.5).



Figure 4.5. Auxiliary GNSS Receiver (B110) Located Right Next to Nozzle 16.

4.3.3 Data collection

The speed range wherein the sprayer should be applying the product was calculated according to the size of the nozzle tip, the target speed, and the desired minimum and maximum duty cycle during operation (Fabula et al., 2019). Applying the product within the target speed range may minimize the application errors caused by improper spray coverage (Mangus et al., 2017). The speed range was calculated based on the minimum 50% and maximum 75% desired duty cycle and 19 kilometers per hour (kph) target operating speed in both fields. The maximum desired duty cycle of 75% was selected to provide flexibility to operate beyond the 75% duty cycle while maintaining the application within the 100% duty cycle. The sprayer applied the product in field 1 within the speed range of 9.3 kph to 24.6 kph, while in field 2 the sprayer operated within the speed ranging from 13.7 kph to 27.5 kph.

The duty cycle accuracy was calculated by using equation 1. It was determined by computing the difference between the actual duty cycle based on the data provided by the system's CAN bus to the expected duty cycle calculated based on the speed of each nozzle. Each nozzle's speed was determined by using the speed data provided by GPS 1 and GPS 2. The speed difference

between the two GPS units was divided into the number of nozzles between them. The calculated difference was added or subtracted, depending on the sprayer turn, to each nozzle starting from the center boom section and then extrapolated to the outer nozzles within the boom sections.

$$Duty\ cycle\ accuracy, \% = \frac{Actual\ duty\ cycle - Expected\ duty\ cycle}{Expected\ duty\ cycle} \times 100 \quad (1)$$

On the other hand, the actual application rate was calculated by converting each nozzle's duty cycle data into speed value according to the calculated speed range used during the operation. The nozzle flow rate was determined by converting the pressure data provided by the pressure transducer from each nozzle by using a regression equation based on the manufacturer's catalog (Wilger, Inc., Lexington, TN). the application rate from each nozzle was then calculated using equation 2.

$$l/ha = \frac{(l/min)(w)(kph)}{60000} \quad (2)$$

where l/ha = application rate, liters per hectare.

l/min = nozzle flow rate, liters per minute.

w = nozzle spacing, cm.

kph = speed, kilometers per hour.

The application rate accuracy was determined by calculating the percent difference between the actual application rate and the target application rate, as shown in equation 3.

$$Application\ rate\ accuracy, \% = \frac{Actual\ application\ rate - Target\ application\ rate}{Target\ application\ rate} \times 100 \quad (3)$$

The nozzle pressure, flowrate, duty cycle, location, and ground speed data were recorded using a data acquisition system consisting of National Instruments controllers and modules (Figure 4.6.a) and a custom LabVIEW program (Figure 4.6.b). The data were saved into a text file for analysis.

The calculated duty cycle and application rate accuracy maps were created using ArcMap 10.6 (ESRI, Redlands, CA) to show the data's spatial results across the fields.



(a)



(b)

Figure 4.6. Data Acquisition system Set-Up (a) and LabVIEW Program Used to Record the Data.

4.4 Results and Discussions

4.4.1 Speed data

Five different straight passes were selected across field 1 during operation (Figure 4.7). This was done to determine whether there was a significant difference in each GPS unit's speed data. Table 4.1 shows the difference in speed data between the GPS1 and GPS 2 during straight runs in field 1. The speed data in both units are comparable to each other, with the GPS1 providing an average speed data of 23.0 kph while the GPS 2 had a speed of 23.1 kph on average. The standard deviation was 0.3 and an error of 2.1%.

Table 4.1. Speed Difference Between the GPS 1 and GPS 2 During Straight Passes in Field 1.

Pass	Speed, kph		Standard Deviation	Error, %
	GPS 1	GPS 2		
1	21.9	22.0	0.3	2.2
2	23.8	23.9	0.3	1.6
3	22.8	22.8	0.3	1.9
4	23.3	23.4	0.4	2.2
5	23.4	23.4	0.4	2.4
Average	23.0	23.1	0.3	2.1



Figure 4.7. Speed Accuracy map in Field 1 Considering the Difference in Speed During Straight Passes Between the GPS 1 and GPS 2.

Similarly, five straight passes were also selected in field 2 to assess the two GPS units' difference in speed data (Figure 4.8). Table 4.2 shows the speed difference between the GPS 1 and the GPS 2 units during straight passes in field 2. There was also no substantial difference between the speed data provided by the two GPS units. The GPS 1 had an average speed data of 14.8 kph while the GPS 2 had 14.9 kph during the straight passes. The standard deviation on the two GPS units' speed data was 0.4, with an error of 3.9%.

Table 4.2. Speed Difference Between the GPS 1 and GPS 2 During Straight Passes in Field 2.

Pass	Speed, kph		Standard Deviation	Error, %
	GPS 1	GPS 2		
1	16.5	16.6	0.3	3.0
2	10.8	10.8	0.4	6.0
3	15.0	15.0	0.4	3.5
4	15.2	15.3	0.3	3.1
5	16.6	16.7	0.4	3.9
Average	14.8	14.9	0.4	3.9

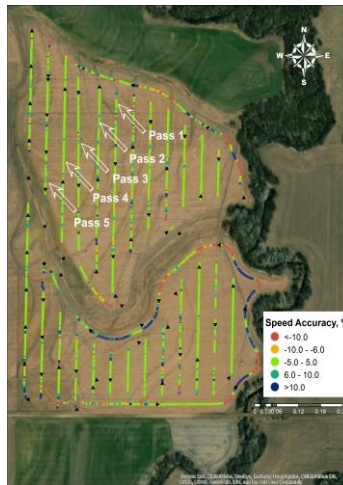
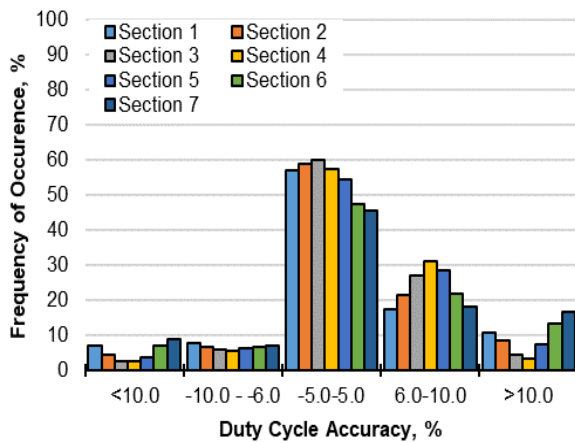


Figure 4.8. Speed Accuracy Map in Field 2 Considering the Difference in Speed During Straight Passes Between the GPS 1 and GPS 2

In both fields, the GPS 1 and GPS 2 units provided comparable speed data during straight passes. Therefore, it can be assumed that the GPS 2 also provided accurate speed data regardless of its location across the boom during turns. The result provided confidence in the accuracy of the calculated duty cycle based on the speed provided by both GPS units, hence providing an accurate calculation of duty cycle and application rate errors.

4.4.2 Duty cycle accuracy

Duty cycle accuracy in field 1 varies during product application (Figure 4.9.b). However, the majority of the duty cycle accuracy occurred within the $\pm 5.0\%$ error range (54.0%) during the operation (Figure 4.9.a). This result indicated that the difference between the actual duty cycle implemented by the PWM system and the calculated duty cycle based on the two GPS units' speed was within the acceptable range for 54.0% of the time. During these events, the system was expected to be implementing the correct duty cycle and therefore applying the right amount of product, assuming that the application pressure was consistent and there were no latencies when implementing the application pressure during product application. There were instances also that the duty cycle accuracy from each solenoid valve was beyond the range of $\pm 5.0\%$ (46.0% of the time), which usually happened when the sprayer was accelerating when entering the spray zones, decelerating when approaching headlands, clearing obstacles, or due to terrain changes, and when making turns.



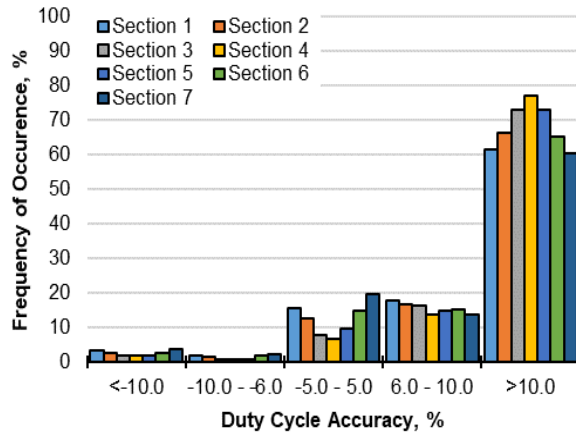
(a)



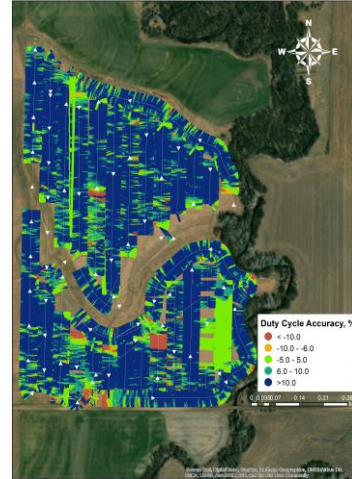
(b)

Figure 4.9. Duty Cycle Accuracy Distribution Plot (a) and Map (b) when Using a PWM System in Field 1.

The duty cycle accuracy in field 2 was mostly beyond $\pm 5.0\%$ error range, which occurred for 88.0% of the time during application while 12.0% was at the range $\pm 5.0\%$ error (Figure 4.10.a). In contrast to field 1, field 2 was irregular-shaped and with varying terrain (Figure 4.10.b). The sprayer frequently varies speed during turns in curvilinear passes and changes in terrain during operation, creating a lot of demand to the control system. The correct duty cycle may not be implemented to match the speed due to the inherent system and GPS latency (Anglund et al., 2003; Mangus et al., 2017). These events may cause under- or over application in areas where lower duty cycle accuracy occurs. Also, the duty cycle accuracy in both fields was lower in nozzles located in the outer boom. These nozzles were frequently subjected to duty cycle changes and section control actuation, which could have contributed to a lower duty cycle accuracy. Moreover, there may be instances that the duty cycle in certain nozzles should go beyond 100% duty cycle and also below 25% duty cycle to match its speed, especially when traveling in a curvilinear pass; however, the system was programmed to limit the duty cycle from 25 % up to 100% which may contribute to the inaccuracy of product application. The operator should operate within the acceptable speed range to minimize the occurrence of having an incorrect duty cycle during operation.



(a)



(b)

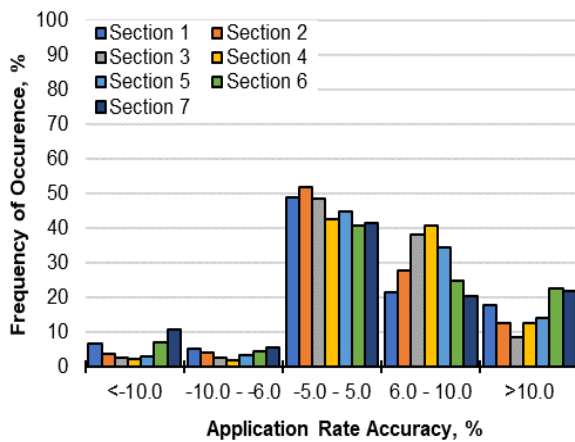
Figure 4.10. Duty Cycle Accuracy Distribution Plot (a) and Map (b) when Using a PWM System in Field 2.

4.4.3 Application rate accuracy

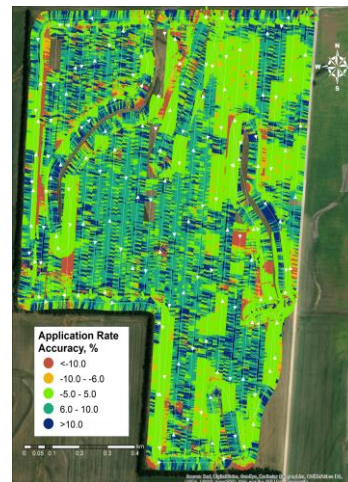
The application rate accuracy in field 1 was within the range of $\pm 5.0\%$ for 46.0% of the time, while about 54.0% of the time, the application rate accuracy was beyond the range of $\pm 5.0\%$ (Figure 4.11.a). The application rate accuracy greater than $\pm 5.0\%$ occurred for 90.0% of the time in field 2, while there were about 10.0% of the time that the application rate accuracy was within the range of $\pm 5.0\%$ (Figure 4.12.a). These results signify a substantial difference between the actual product applied and the target application rate.

The result in both field tests indicated that majority of the time, the PWM system was applying the product beyond the target rate during the operation, which could lead to application errors (Figure 4.11.b and 4.12.b). It could be due to the PWM system's inability to implement the correct duty cycle to match up each nozzle's speed during operation, which could be attributed to system latency (Han et al., 2001). Luck et al. (2011) stated that a higher application rate ($>93.5 \text{ L ha}^{-1}$) will reduce the ability of the nozzle control system to compensate for an acceleration of up to

1.34 m s⁻¹. Hence, it is recommended that the spray system should have a fast response time to quickly implement the correct duty cycle during product application to minimize application errors (Rockwell et al., 1996). Unlike in field 1, wherein it was more rectangular and had mostly flat terrain, field 2 has an irregular shape and varying terrain. These results suggest that the shape and terrain of the field may influence the PWM system's ability to implement the correct duty cycle due to frequent speed changes, which may impact the product application uniformity. A lower application rate accuracy was observed when the sprayer was applying around waterways and boundaries. The application rate accuracy was higher when operating at straight passes in field 1. However, a different case was observed in field 2 when applying in straight passes.

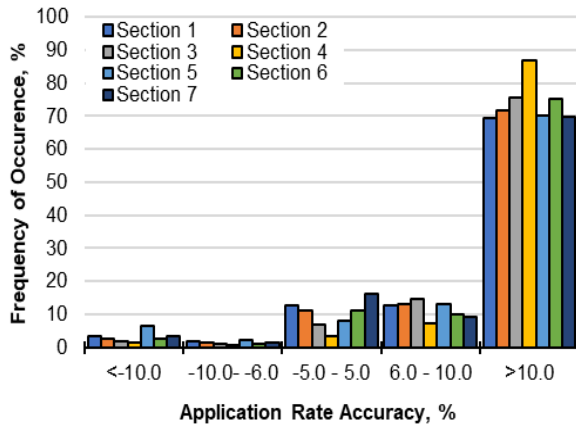


(a)

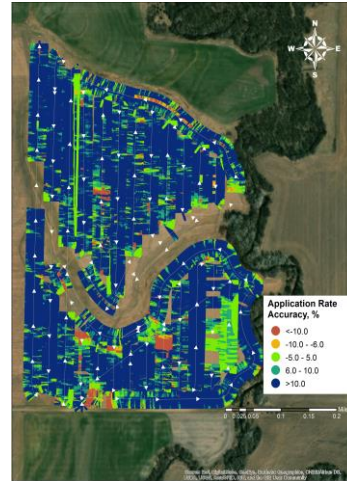


(b)

Figure 4.11. Application Rate Accuracy Distribution Plot (a) and Map (b) when Using a PWM System Field 1.



(a)



(b)

Figure 4.12. Application Rate Accuracy Distribution Plot (a) and Map (b) when Using a PWM System in Field 2.

The application rate accuracy mostly exceeded the 10.0% range that may be attributed to the field's varying terrain. Grisso et al. (2002) also reported an increase in application rate error due to field patterns. This could be attributed to the fact that the nozzle located at the sprayer's outer boom section provided the lowest application rate accuracy during turns. This could lead to areas covered by the outer boom section receiving less product than the areas covered by inner boom sections (Garcia-Ramos et al., 2011). Porter et al. (2013) also reported that the flow rate in the outer nozzles was consistently greater than the target rate, particularly during tighter turns. A study by Luck et al. (2011) stated that the speed difference between the inner and outer boom during turns in curvilinear passes could cause the system to exceed the target application in 24.0% of the field, resulting in application errors. During operation, the boom section's lateral movement may vary the nozzle speed that could cause uneven product distribution, and contribute to application rate error. Traveling in a curved path creates a challenge when operating a sprayer with a wider boom due to its impact on application errors which was not completely eliminated even

with solenoid valves (Garcia-Ramos et al., 2011). These factors may have influenced the PWM system's ability to provide the correct product volume in some instances, which could lead to off-rate error, product loss, and inefficient control of pests and diseases.

4.5 Conclusion

The PWM system's ability to provide the correct duty cycle and apply the right amount of product during the operation was investigated. The results indicate that a lower duty cycle accuracy was observed in an irregularly shaped field with varying terrain. It signifies that the PWM system could not implement the correct duty cycle due to frequent changes in speed during the operation, which could be due to the system latency. These events could impact the volume of product applied because of the system's inability to provide the right flow rate aside from the pressure drop at the nozzle. Both the duty cycle and application rate inaccuracy may result in the non-uniformity of application that may impact the product's effectiveness in controlling crop pests and diseases. Application errors will be continuously present during product application unless the manufacturers will further improve the system for precision spraying. But in the meantime, operators should be aware of the factors that can influence both the duty cycle and application error so that they can make the necessary adjustments to the sprayer settings and their driving styles. The operators can plan to apply at straight passes and operate within the established speed range as much as possible during field operation to minimize the application rate error caused by the sprayer turning movements.

Chapter 5 - Field Evaluation of Turn Compensation Feature of Pulse Width Modulation (PWM) – Equipped Agricultural Sprayer

5.1 Abstract

Agricultural sprayers were utilized in applying pesticides to control pests and diseases in crops. The increase in machine size and a better control system have been associated with increased productivity, improved efficiency, and minimized the impact of the chemical on the environment. However, the increase in boom width of agricultural sprayer makes it difficult to navigate irregular-shaped fields. A wider boom may also contribute to application error due to the difference in speed between the inner and outer boom section when applying in curvilinear passes. The introduction of the turn compensation technology has the potential to reduce errors caused by these events. However, little research has been conducted to evaluate the extent of field area typically operated on curvilinear passes and technology's performance when applying the product at different turning radius during operation. Field tests were conducted in three irregular shape fields with varying terrain using a 36.6-m self-propelled sprayer with a turn compensation technology. As-applied data was downloaded from the sprayers console monitor to utilize. GPS coordinates and heading during the operation were used to calculate the turning radius of the sprayer. The turning radius was classified as extreme turn (<20.0 m), medium turn (20.0 m to 50.0 m), and slight turn (50.0 m to 100.0 m). Straight passes were classified when the turning radius was more than 100.0 m. The results show that turning occurred near the grassed waterways, boundaries, and end of headlands. Nineteen percent of field 1 were applied with the product during turning, 17.8% in field 2, and 22.5% in field 3. These could have been the percentage of field areas that may receive more or less product if the sprayer was not equipped with turn compensation technology.

As expected, the speed difference between the inner and outer boom increases as the radius of turn decreases. The speed difference could translate to an under-application on the outer boom section where the speed is much faster and over-application on the inner boom section where the speed is slower. The application errors from such speed differential could vary from -48.2% to +1058.0 %. However, the PWM system implemented duty cycles based on turning speeds, which would potentially result in more uniform product application across the field regardless of the travel path during operation. Overall, the turn compensation advantages should be one of the producers' considerations when selecting a spray system for product application.

5.2 Introduction

Chemical application is one of the most important aspects of crop production. The application of agricultural chemicals minimizes pest damage, ensuring good crop quality, yields, and a steady supply of foods for the growing population. Agricultural sprayers are usually employed to apply agricultural chemicals, which is usually done several times during the cropping season depending on the management practices and farming system. Crop producers in the US apply 400 M kilograms and spent about \$15.2 B of pesticides annually to control pests and diseases in their fields (USDA, 2020). Increasing the machine size and improving the control system capabilities to apply the product uniformly across the field increases productivity, enhanced efficiency, and reduced the pesticides' negative impact on the environment (Sharda et al., 2010). Agricultural sprayers are now equipped with wider booms and operate faster to increase the machine's field capacity. The introduction of flow-based rate controllers in the past years provided an effective way of applying the correct product volume during operation (Al-Gaadi et al., 1994; Ayers et al., 1990). Wider sprayer boom and varying field terrain require a faster controller response to manage application rates during operation. Among many concerns, including application rate errors due to controller response, under-and over-application, and off-target application (Porter et al., 2013; Sama et al., 2015), flow-based systems can only apply one flow rate across the entire boom. Previous studies also show the impact of an irregularly shaped field on application rate errors (Luck et al., 2010a; Sharda et al., 2013). Grisso et al. (2002) also reported a lower machine efficiency when operating in asymmetrical fields, which increases the possibility of overlap and off-rate errors due to the increase in the number of turns during operation. Off-rate errors are also more prevalent when applying a product in a more complex field (Zandonadi et al., 2011).

With the increase in boom width, the inside and outside of the booms would travel at a significant speed differential, especially when traveling on curvilinear passes to cover irregular shape field boundaries and around grassed waterways. Luck et al. (2011) reported that the sprayer's outer boom sections exceeded the sprayer travel speed while a slower travel speed is observed at the inner boom sections during turning. The magnitude of speed differential on boom ends and application rate errors would depend on turning radii, boom width and travel speeds. Flow-based systems would inherently implement under-application for boom traveling faster than the sprayer travel speed and over-application for ones with lower speed. Overall, a sprayer traveling at faster speed with wider spray booms traversing smaller turning radii would have greater speed difference between inside and outside booms, which could generate significant under- and over-application.

PWM spray controllers are commonly being implemented on self-propelled agricultural sprayers. The PWM controllers manage flow at each nozzle by running solenoids at a duty cycle representative of travel speed to implement target application rates. The PWM controllers can control the nozzle flow rate both during straight and curvilinear passes. During curvilinear operation, the system increases the duty cycle of each nozzle moving at higher speed at the outer boom while decreasing the duty cycle of the nozzle traveling at slower speeds on the inner boom to manage the flow rate. The controller's ability to implement nozzle speed-based duty cycles to manage nozzle flow rates is often referred to as the curve or turn compensation feature.

The PWM system's advantage over the flow-based system is also its ability to turn the solenoid On and Off immediately, which becomes possible due to the faster response time of the valves from the nozzle bodies. The solenoid action holds the pressurized liquid close to the nozzle and provides rapid spraying when actuated to On state. The PWM system's ability to compensate for the difference in speed depends on the radius of turn and PWM duty cycle when turning.

However, there is lack of knowledge on percentage area typically farms might have which could utilize turn compensation feature and potential reduction of under-and over-application. Therefore this research was conducted to evaluate the turn compensation capability of a PWM system during operation with a specific objective to 1) quantify percent area sprayed with turn compensation feature actuated on typical agricultural fields; and 2) evaluate the application error during turning due to speed difference between the inner and outer boom sections at different turning radius without the turn compensation.

5.3 Materials and Methods

5.3.1 Sprayer set-up

A 36.6-meter (m) self-propelled front boom sprayer (SP370F Guardian, New Holland, PA) with 73 nozzles spaced at 0.51m was used in this study (Figure 5.1). The sprayer was equipped with an integrated inertial measurement unit capable of detecting the change in the direction and movement that can be used to calculate the turn compensation correction needed during product application.



Figure 5.1. The Self-Propelled Agricultural Sprayer Used in the Study.

The nozzle bodies had solenoid valves that control the auto-nozzle function (Raven Hawkeye, Raven Industries, Inc., Sioux Falls, SD) during operation. The solenoid valves were mapped in the controller so that the first outer nozzles on the left and right side of the boom were controlled individually. The following thirty inner nozzles on the left boom and the thirty-two nozzles on the right boom section were working in tandem, and the remaining nozzles were in the group of three (Figure 5.2).

The sprayer control system has five control channels that actuate the boom shut-off valves. The inline flow meter regulated the target flow across the boom. A hydraulic valve utilized a pulse width modulation system controls the overall system flow rate. The sprayer was also equipped with an auto-guidance system that minimizes the operator's control of the vehicle during straight passes. A field test was conducted in three different fields with varying shapes and terrain. Field 1 was a 57.0 hectares (ha) field, while field 2 was 53.0 ha, and field 3 was a 54.0 ha field. Field 1 was applied with the product at a rate of 93.0 L ha^{-1} at an application pressure of 462.0 kPa, while field 2 was applied with 112.0 L ha^{-1} at 324 kPa application pressure. On the other hand, field 3 was applied at 112.0 L ha^{-1} at 462.0 kPa. In all applications, an XR 110-06 nozzle tip was used.

Also, the pressure was set at 48.0 kPa higher than the target pressure to compensate for pressure drop across solenoid and nozzle body. In all fields, the operator made a single pass to cover the field boundary before applying the remainder of the fields using parallel passes.

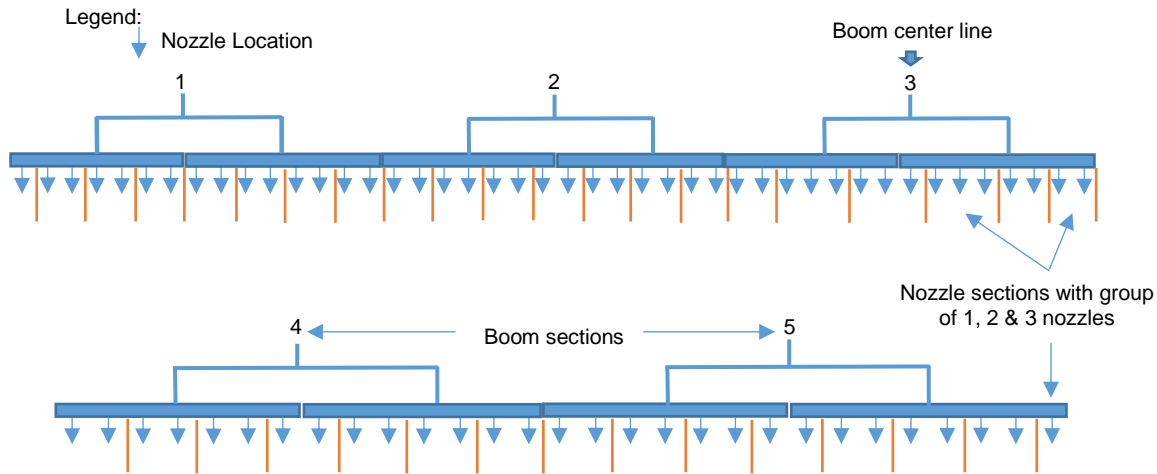


Figure 5.2. Layout of the Sprayer's Auto-Nozzle Control Function with Nozzle Valves Controlled Individually, in Tandem, or in a Group of Three.

5.3.2 Data collection and analysis

Machine as-applied data were downloaded from the sprayer console monitor after the product was applied to the three experimental fields. The data contains the GPS coordinates, speed, heading, and other operating parameters across the field. The turning radius was determined by calculating the change in the sprayer's heading between two succeeding GPS locations. The turning speed was then calculated by dividing the change in the sprayer's heading by the time it took the sprayer to travel a certain distance from the next GPS coordinate. The status of turn compensation was evaluated based on the triggering parameters set by the machine's program. In this case, the turn compensation was assumed to be active if the calculated turning speed was ≥ 0.75 deg/sec while it was assumed to be deactivated once the calculated speed was < 0.5 deg/sec. These

parameters provided the turning radius when the turn compensation was executed. Table 5.1 shows the turn classification for different ranges of turning radii.

Table 5.1. Turn Classification for Different Ranges of Turning Radii.

Turning radius, m	Turn classification	Expected Speed differential
$r < 20$	Extreme Turn	Turns with small radii resulting in over 85% speed increase from inner to outer boom of the sprayer.
$20 < r < 50$	Medium Turn	Average size turns with at least 25% speed increase from inner to outer boom of the sprayer.
$50 < r < 100$	Slight Turn	Turns just above the threshold for activating turn compensation.
$r > 100$	Straight run	Any pass with no discernible turn that would enable turn compensation.

The percentage area of the field applied with the product at different turning radii was determined using the ArcGIS. The Thiessen polygon method was used to calculate the field area where the turning occurred. It converted the calculated data into polygons corresponding to each point that contains the area surrounding the given point that is closer than any adjacent point. The Thiessen polygon provided a final output data that contains the area of each polygon.

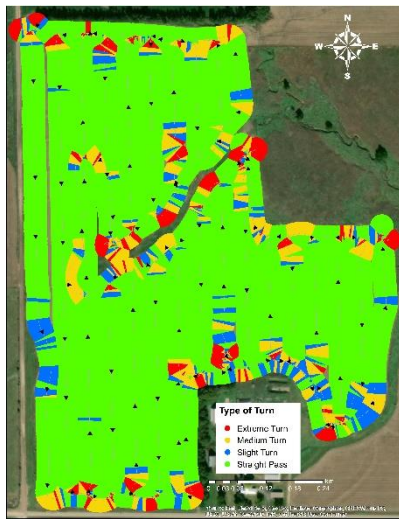
The difference in speed between the sprayer's inner and outer boom sections was calculated at each turning radius. The possible application error caused by the difference in speed of the inner and outer boom section during turning at different radius was determined to exhibit under- and over-application for systems that do not have turn compensation features.

5.4 Results and Discussions

The three experimental fields shown in figure 5.3 provide the locations that were applied with the product during extreme turning radius (red), medium turning radius (yellow), and slight turning radius (blue). The green portion on the map indicates straight passes. In fields with an

irregular shape, it is necessary to spray a significant portion of the field while turning. Nineteen percent of field 1, 17.8% of field 2, and 22.5% in field 3 were applied with the product when the sprayer was turning (Table 5.2). The maps also exhibited that curvilinear passes occurred mostly around grassed waterways, along field boundaries, and at the end of the headlands. As the field becomes more irregular due to grassed waterways and field boundary conditions had challenging terrain safe driving (like ditches, etc.), such as field 3, the number of turns that the sprayer needed to cover the whole field increased as well. During curvilinear passes, the application error may increase due to the difference in the speed between the sprayer's inner and outer boom sections, particularly when using a flow-based system (Luck et al., 2010b). Minimizing the application error when applying a product using a flow-based system may only be possible by minimizing the sprayer turns in the field and conduct the application in straight passes. However, this may not be practically feasible when operating in irregular fields. Application errors may occur at locations where the operator tends to make a turn while covering the field. Although the extent of the impact of application error to crop yield may not be established, the over-application of chemicals such as glyphosate may reduce the growth of soybeans (Reddy et al., 2000; Reddy et al., 2003). Application errors may not only cause a reduction in yield but can also increase production cost and environmental contamination. Likewise, applying the product below the target may not cause any damage to crops; however, it may result to yield loss due to weed growth when the application rate falls below the recommended rate based on product label specification (Cox et al., 2006; Shafagh-Kolvanagh et al., 2008). Over-applying chemicals may also cause environmental pollution as they may accumulate in soils and be carried by run-off that can contaminate surface and groundwater. Additionally, the field's shape may also contribute to application error due to multiple applications using a flow-based system (Luck et al., 2010b). The low efficiency of

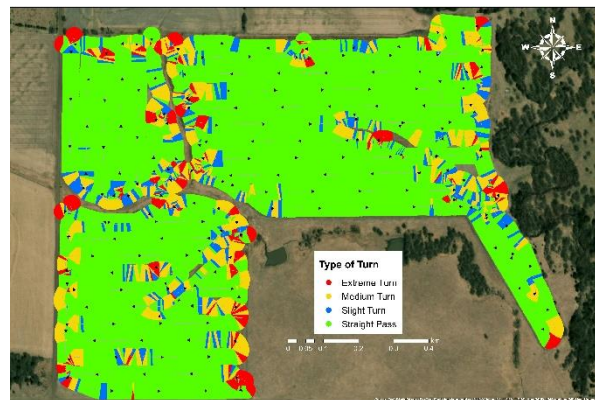
machines such as sprayers may be attributed to a higher number of turns associated with the field shapes. The increase in the number of turns may increase the chances of overlap and application error due to field patterns and the boom's reaction during turns (Grisso et al., 2002). Therefore, a higher application error potential may be expected to wider equipment such as sprayers applying on fields with greater irregular boundaries.



(a)



(b)



(c)

Figure 5.3. Maps Showing the Different Types of Turns in Field 1 (a), Field 2 (b), and Field 3 (c).

Table 5.2. Field Area Applied with Product at Different Turning Radii.

Turning Radius, m	Field area, %			Total	Average
	1	2	3		
<20.0	4.2	3.4	4.4	12.0	4.0
20.0-49.0	8.7	8.9	11.9	29.5	9.8
50.0-100.0	6.0	5.5	6.2	17.8	5.9
Total	19.0	17.8	22.5	59.3	19.7

The study was conducted on fields with varying shapes and terrain. The fields were irregular in shapes and had some non-navigable grassed waterways. A significant number of turns were necessary to navigate around the grassed waterways and field boundaries. There will be a significant difference in the inner and outer boom sections that may contribute to application error during these turns. As an example, Table 5.3 shows the speed difference between the middle boom section and the left boom section and the middle boom section and the right boom section when the sprayer was operating at 24.1 kilometers per hour (kph). It was assumed that the middle section's speed was the same as the sprayer's ground speed.

During straight passes (R0), the speed of the left boom section and the right boom section was expected to be the same as the middle boom section. However, when the sprayer was turning right and the turn radius was 20.0 m (R1), the left boom section will have a speed of 46.2 kph, which was 22.1 kph faster than the middle boom. On the other hand, the right boom section will have a speed of 2.1 kph, which was 22.1 kph slower than the middle boom section. In the case 20.0 m turn radius, there will be a speed differential of 44.1 kph between the left boom section and the right boom section. At 1000.0 m turning radius (R4), the left boom had a speed of 24.6 kph, which was only 0.4 kph faster than the middle boom, while the right boom section was only 0.4 kph slower than the middle boom section. Also, there was only a 0.9 kph speed difference between

the left boom section and the outer boom section. Overall, the speed differential between the inside and outside boom sections will be reduced with an increase in turning radius (Figure 5.4).

Table 5.3. Speed Difference Between the Boom Sections at Each Turning Radius.

Events	Travel Direction	Radius (m)	Speed, kph				
			Left Boom	Middle Boom	Right Boom	Speed Difference [1]	Speed Difference [2]
R0	Straight	0.0	24.1	24.1	24.1	0.0	0.0
R1	Right	20.0	46.2	24.1	2.1	22.1	44.1
R2	Right	50.0	33.0	24.1	15.3	8.8	17.7
R3	Right	100.0	28.6	24.1	19.7	4.4	8.8
R4	Right	1000.0	24.6	24.1	23.7	0.4	0.9

Note: [1] – Speed difference between the middle boom and left boom.
 [2] – Speed difference between the left boom and right boom.

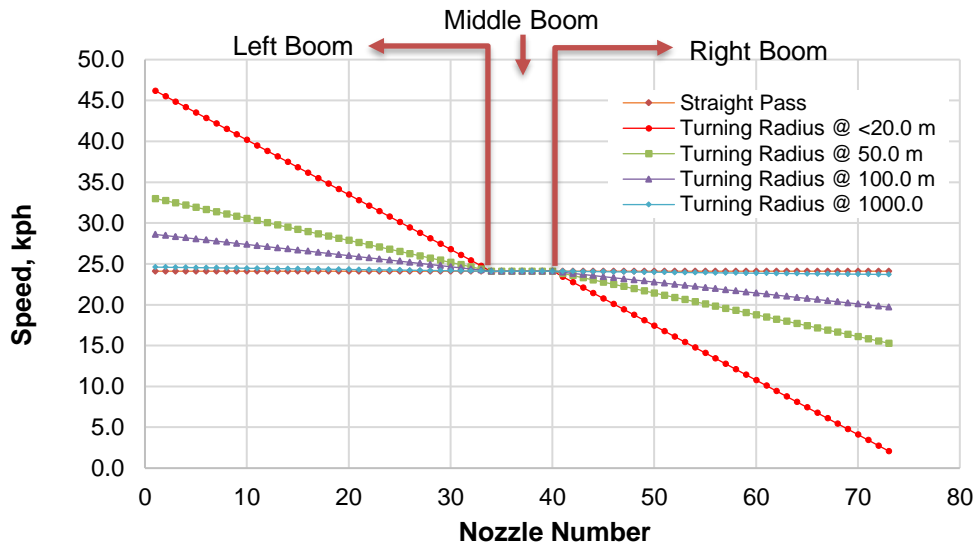


Figure 5.4. Speed of Each Nozzle During Right Turn at Different Turning Radii.

The speed difference between the boom sections may translate to the application error during operation, especially when using a system that does not have a turn compensation feature. Table 5.4 shows the application rate errors (negative values indicating under-application and positive values as over-application) between the outer boom sections during tight turns if an

application system lacks a turn compensation feature (like a flow-based rate control system). In a right turn with a 20.0 m turn radius (R1), when the middle boom section applied the target application rate of 112.0 L ha⁻¹, the left boom section was only applying 58.0 L ha⁻¹, which was 48.2% less than the target application. On the other hand, the right boom section was applying at 1,297.6 L ha⁻¹ that was about 1,058.0% higher than the target rate (Figure 5.5). This event indicates an under-application on the left boom section traveling faster and over-application on the right boom section traveling slower than the center of the sprayer. As the turning radius increases, the speed differential between inside and outside boom-sections decreased, which also reduced the application rate error. At 1000.0 m turning radius (R4), the application rate error was reduced to 2.6% on the left boom section and only 1.0% on the right boom section, indicating a fairly uniform application between the boom sections.

Table 5.4. Application Rate Error on the Left and Right Boom at Each Turning Radius.

Events	Travel Direction	Radius (m)	Application Rate, L ha ⁻¹			Application Rate Error, % [1]	Application Rate Error, % [2]
			Left Boom	Middle Boom	Right Boom		
R0	Straight	0.0	112.0	112.0	112.0	0.0	0.0
R1	Right	20.0	58.0	112.0	1297.6	-48.2	1058.0
R2	Right	50.0	81.3	112.0	175.1	-27.4	56.4
R3	Right	100.0	93.9	112.0	135.9	-16.2	21.4
R4	Right	1000.0	109.1	112.0	113.1	-2.6	1.0

Note: [1] – Application Rate Error at the left boom.

[2] – Application Rate Error at the right boom.

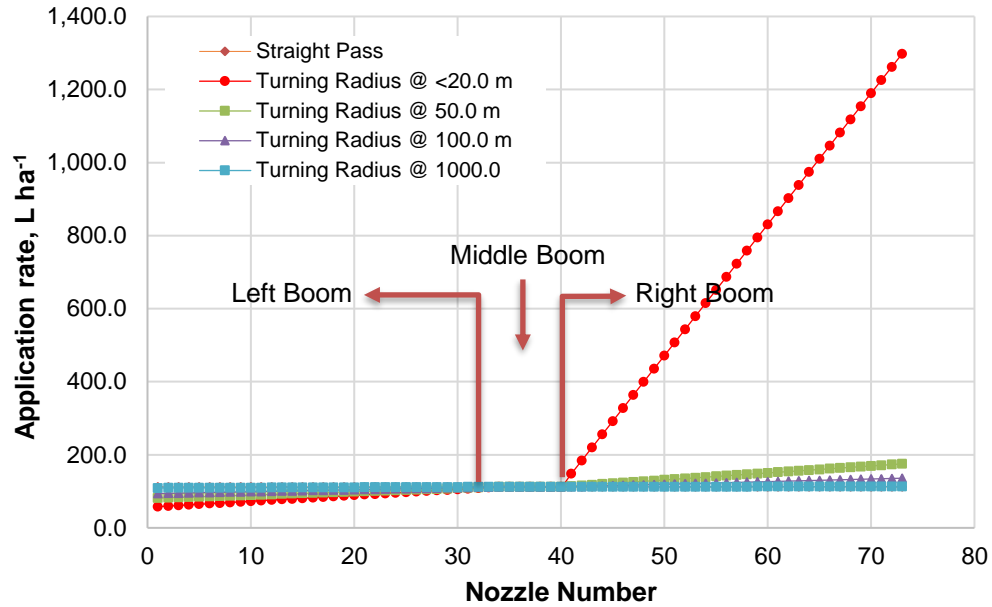


Figure 5.5. Application Rate of Each Nozzle when Turning Right at Different Turning Radii.

Table 5.4 and Figure 5.5 shows that operators should expect application rate errors on curvilinear passes when applying the product using a sprayer without the turn compensation feature. These application rate errors are generated because 1) the system did not have the intelligence to establish individual nozzle or boom control section travel speeds and; 2) lacking control ability to implement nozzle and boom control section flow rate representative of its ground speeds. Such issues can be avoided with the implementation of PWM spray application technology. PWM system can map speed of each control and can implement representative flow rate by changing duty cycles both during straight and curvilinear passes. For example, on a curvilinear pass with the sprayer turning left, the PWM can reduce the flow to 0.2 L min^{-1} for the inner boom section operating at a speed of 2.4 kph, and increase flow to 2.2 L min^{-1} for outer boom traveling at 24.0 kph, thus having the potential to implement control to manage application rates of 112.0 L ha^{-1} across the boom (Figure 5.6).

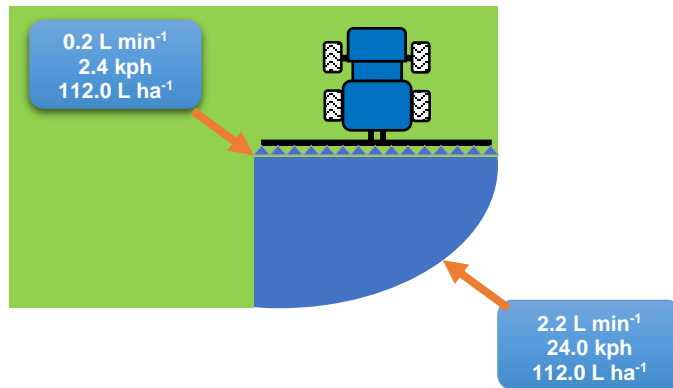


Figure 5.6. A Sprayer with Turn Compensation Feature Applying the Product Uniformly Across the Field.

5.5 Conclusion

A sprayer equipped with the turn compensation feature may have an advantage over other systems such as the flow-based system when it comes to providing a uniform application rate on curvilinear passes. The sprayer with such technology may avoid under-application on the outer boom section and over-application on the inner boom section during operation in irregular fields wherein applying in a curvilinear path is necessary to cover the entirety of the field. The 19.7% average field area covered with sprayer on a curvilinear pass constitutes a significant portion which can potentially have a significant detrimental impact from inappropriate application rates. Without the turn compensation, the areas in the field that were under – and-over-applied with the product, which usually occurs in the location where the sprayer is turning, such as grassed waterways, boundaries, and at the end of the headlands, could contribute to pesticide resistance among pest species, increase the input costs and environmental contamination. The benefits of the turn compensation feature should be considered by the producers when selecting a spray system for product application.

Chapter 6 - Conclusion, Recommendation, and Practical

Implication

6.1 General Conclusions

The following conclusions were drawn from this research:

1. The different commercially available PWM systems provided a different pressure drop when applying different application rates and pressures. The pressure drop of the PWM systems increases with the increase in the application rate and pressure. The producers need to consider the drop in pressure that a particular PWM system provides when operating at a certain rate and pressure to make the necessary adjustment during product application. This will ensure that the product was applied at the correct pressure, spray pattern, and droplet size, minimizing the application errors caused by operating at lower application pressure than the target. Each PWM system also has an inherent latency before achieving the target pressure. This latency may increase the application error, particularly in PWM systems operating at a higher frequency. Due to this latency, the evaluated PWM systems operate at less time than the specified duty cycle during each cycle time. The nozzle provided less product during operation due to the pressure drop and system latency.
2. The PWM system provided an application pressure within the acceptable range for 87.0% of the time during field operation. The result suggests the system's ability to provide an application pressure that will not vary the application rate by $\pm 10.0\%$. The majority of the pressure CV was also below 5.0%, indicating less variability in application pressure between boom sections during operation. This result was far better than a flow-based system, wherein it operates at a much lower pressure than the target for 68.0% of the time.

The variability in nozzle pressure when using a flow-based system was due to the changing sprayer speed as a result of terrain changes, operating in non-straight passes, and maneuvering in headlands. The droplet size spectra vary during the field tests. However, it does not indicate the PWM system's inability to provide the target droplet size spectra during operation but signifies the importance of selecting the correct nozzle for product application. Producers should select a nozzle that provides the target droplet size within the wide range of application pressure to ensure uniform product deposition across the field.

3. The duty cycle accuracy within the $\pm 5.0\%$ was lower in an irregularly shaped field with varying terrain (12.0%) than a rectangular field with relatively flat terrain (54.0%). The result indicates that the frequent speed transition may impact the system's ability to provide the correct duty cycle when operating in fields with varying terrain and shape due to the repeated acceleration and deceleration of the sprayer to clear the terraces, grassed waterways, and field boundaries. The application rate accuracy within the $\pm 5.0\%$ was also lower in irregularly shaped fields (10.0%) than rectangular ones (46.0%), which could be due to an incorrect duty cycle resulting in an inaccurate nozzle flow rate during product application. Lower duty cycle and application rate accuracy could result in an inconsistent application that may impact the product's efficacy to manage pests and diseases among crops.
4. The speed difference between the sprayer's inner and outer boom section increased with the decrease in the turning radius. The speed difference could impact the application rate as more products will be applied by the inner boom section than the outer boom section when making turns resulting in under- and over-application. The field area (19.7%)

covered by the sprayer with curvilinear pass constitutes a significant portion that can have a potential significant detrimental impact from inappropriate application rates. The turn compensation technology may minimize the application error caused by the difference in speed of the sprayer's inner and outer boom sections, which may usually occur in locations where the sprayer turns, such as near the grassed waterways, boundaries, and at the end of the headlands. With the turn compensation technology, the impact of pesticide resistance and environmental pollution may be minimized.

6.2 Recommendations for Future Work and Product Improvement

Agricultural sprayers continue to improve in recent years by introducing new technologies such as the PWM system. In this study, the PWM system's performance was evaluated under laboratory and field conditions wherein frequent speed transitions and section control actuation may occur. The study results suggest the system's capability to provide the target application pressure within the acceptable range. However, study should be conducted in the future to assess the system's ability to provide the desired droplet size and distribution using water-sensitive cards to evaluate the uniformity of product application under field conditions. Different nozzles that provide the desired droplet size in a narrow range of application pressure and another that delivers the desired droplet size in a wide range of pressure should be selected. This will show the significance of selecting the correct nozzle size to deliver the desired droplet size based on product label specification.

During product application, the operator needed to manually override the sprayer's auto-boom function to avoid hitting the ground, particularly in a field with terraces. This action causes the sprayer to apply the product when the boom is at a certain angle above the ground. Therefore,

the impact of the vertical boom movement on the spray distribution uniformity should be evaluated. There were also instances that the wind speed and direction drastically change as the operation continues to apply product to the entire field. Hence, the impact of the wind speed on product deposition and uniformity should also be assessed.

Operators usually perceived that the new technology was properly responding to deliver the correct product volume and droplet size at the target pressure, even at varying field conditions. The operator's understanding is usually based on the system's feedback displayed on the monitor, which serves as the only tool to indicate the sprayer's performance during product application. The operator assumes that the sprayer performs properly if the display indicates that the application rate and target pressure are maintained. However, the application pressure can vary during sprayer deceleration and acceleration when applying in irregularly shaped fields with varying terrain. Therefore, there is a need for an integration of a pressure drop mapping system for true nozzle pressure implementation. This system will be independent of nozzle selection, application pressure, and rate. The system will be intelligent enough to adjust the application pressure based on the current operating conditions. The pressure variation during operation may also vary the droplet size spectra during product application. The operator may unknowingly apply the product that does not comply with the label specification in terms of the droplet size. Integration of a nozzle pressure and nozzle type that displays the droplet size spectra is necessary. This display will give the operator confidence that the correct droplet size is applied and awareness when the droplet spectra are out of range. It may also serve as important documentation for the applicators from regulatory bodies if the product label specification was followed during the application.

The result of this study also shows that the PWM controller was not able to implement a nozzle speed-based duty cycle during operation, particularly in a field with varying terrain and

when turning. In these cases, the outer boom section may travel at a speed beyond the target speed while the inner boom section may be traveling too slow. Since the current system could not implement the correct duty cycle based on the nozzle speed, an integration of a secondary sensor on the boom is necessary for accurate nozzle speed measurement to execute a nozzle speed-based duty cycle.

Also, operators usually drive faster during operation depending on terrain and what the terraces look like to cover large areas and immediately complete the product application. However, if the sprayer operates beyond the established speed range recommended for duty cycle implementation, there is no current speed warning in the cab to inform the operator that the sprayer was operating too fast and might be implementing an under application. Integration of the speed warning on the main display is necessary to keep the operator informed that the sprayer needs to slow down to avoid applying the incorrect amount of product. Another feature that should be added to the system is the integration of the Tractor Implement Management (TIM). The TIM is one of the most advanced technologies that should be implemented in agricultural sprayers. This system will automatically control the machine to minimize application errors if the operator does not adhere to the warnings.

The recommended product improvements were all based on the learnings from this study. These product improvements were currently under research and being developed to be integrated into the current spray system.

6.3 Practical Implications

The control resolution on the agricultural sprayer is becoming smaller due to the technological advancement in sensors, computers, and actuators. The development of new

technologies in chemical applications greatly improved the efficiency of agricultural sprayers. The introduction of pulse width modulation technology in agricultural sprayers increased the control resolution due to its ability to regulate each nozzle's flow rate. The increasing demand for PWM technology in chemical applications compelled the different agricultural sprayer manufacturers to integrate the system into their agricultural sprayers. As the new technologies are introduced in the market, producers usually perceived that the technology is properly working and applying the product uniformly across the field.

As pointed out in this study, different commercially available PWM systems provided different pressure drops when applying certain application rates and pressure. The operator should consider these pressure drops when setting the target pressure to avoid application errors. The PWM system also has an inherent ON/OFF latency that may impact product application accuracy. This study will serve as a decision tool for the producers whether to select a low-frequency or high-frequency system. Producers should be well informed that higher frequency system might have a higher cumulative latency per second which could impact the product application uniformity. Therefore, it is important to understand the pressure and flow dynamics when using the PWM system in the liquid application so that producers can properly implement this technology. This research may also help the producers select a control system (flow-based system or PWM system) that can provide uniform pressure and droplet size spectra during field operation.

Frequently, agricultural sprayers are driven by the operator at a faster speed if field conditions permit to complete product application immediately. The operator's understanding is that once the sprayer is properly calibrated, the system applies the product uniformly across the field regardless of their driving style. However, the operators should recognize that operating the sprayer beyond the target speed range established for proper duty cycle implementation could

cause under-application. Hence, this study will show them the importance of staying within the target speed range to avoid application errors. This research also indicates that the PWM control system could not implement the correct duty cycle representative of the nozzle speed, particularly in an irregularly shaped field with varying terrain due to frequent speed transitions. Therefore, this study could help the operators understand that careful planning on conducting the application is necessary when operating in irregularly shaped fields with varying terrain to minimize the sudden speed changes and reduce application errors. This research may also help producers decide whether there is a need to invest in new technologies such as the turn compensation.

Manufacturers could also use the information in this study to further improve the system. Manufacturers could integrate features that may help the operators to minimize errors during operation. These features will keep the operators informed of the sprayer's real-time performance in providing the correct product rate and droplet size spectra that is critical for effective pest control.

Crop producers are adopting new technologies to improve product application efficiency. However, sprayer operators should have a better understanding of the system's performance in varying field conditions to avoid possible application errors to attain the concept of precision agriculture. Continuous research and development of spray technologies are essential to attain uniform product distribution. Producers are required to apply the product based on specifications as directed by Federal regulations. The utilization of improved precision liquid application technologies may address the problem of application error, pesticide resistance, and environmental pollution caused by chemical application.

References

- Al-Gaadi, K. A., & Ayers, P. D. (1994). Monitoring controller-based field sprayer performance. *Appl. Eng. Agric.*, *10*(2), 205–208. <https://doi.org/10.13031/2013.25843>
- Al-Gaadi, K. A., & Ayers, P. D. (1999). Integrating GIS and GPS into a spatially variable rate herbicide application system. *Appl. Eng. Agric.*, *15*(4), 255–262. <https://doi.org/10.13031/2013.5773>
- Anglund, E. A., & Ayers, P. D. (2003). Field evaluation of response times for a variable rate (pressure-based and injection) liquid chemical applicators. *Appl. Eng. Agric.*, *19*(3), 273. <https://doi.org/10.13031/2013.13659>
- ASABE Standards. (2016). S592.1: Best management practices for boom spraying. St. Joseph, MI: ASABE.
- Atwood, D. & Paisley-Jones, C. (2017). *Pesticides industry sales and usage: 2008–2012 Market Estimates*. Retrieved from https://www.epa.gov/sites/production/files/2017-01/documents/pesticides-industry-sales-usage-2016_0.pdf
- Ayers, P. D., Rogowski, S. M., & Kimble, B. L. (1990). An Investigation of Factors Affecting Sprayer Control System Performance. *Appl. Eng. Agric.*, *6*(6), 701–706. <https://doi.org/10.13031/2013.26451>
- Balsari, P., & Marucco, P. (2009). Making the most efficient use of pesticide application in vineyards – Experiences from Europe. In *Crop Protection in Vineyards Plumpton College*. Brighton, UK: The Association of Applied Biologists.
- Batte, M. T., & Ehsani, M. R. (2006). The economics of precision guidance with auto-boom control for farmer-owned agricultural sprayers. *Comput. Electron. Agric.*, *53*(1), 28–44. <https://doi.org/10.1016/j.compag.2006.03.004>
- Bennur, P. J., & Taylor, R. K. (2010). Evaluating the response time of a rate controller used with a sensor-based, variable rate application system. *Appl. Eng. Agric.*, *26*(6), 1069–1075. <https://doi.org/10.13031/2013.35903>
- Brady, J. A., Wallender, W. W., Werner, I., Fard, B. M., Zalom, F. G., Oliver, M. N., ... Upadhaya, S. (2006). Pesticide runoff from orchard floors in Davis, California, USA: A comparative analysis of diazinon and esfenvalerate. *Agric. Ecosyst. Environ.*, *115*(1–4), 56–68. <https://doi.org/10.1016/j.agee.2005.12.009>
- Butts, T. R., Butts, L. E., Luck, J. D., Fritz, B. K., Hoffmann, W. C., & Kruger, G. R. (2019). Droplet size and nozzle tip pressure from a pulse-width modulation sprayer. *Biosyst. Eng.*, *178*, 52–69. <https://doi.org/10.1016/j.biosystemseng.2018.11.004>

- Carpenter, S. R. (2005). Eutrophication of aquatic ecosystems: Bistability and soil phosphorus. *Proceedings of the National Academy of Sciences of the United States of America*, 102(29), 10002–10005. <https://doi.org/10.1073/pnas.0503959102>
- Chen, Y., Zhu, H., & Ozkan, H. E. (2012). Development of a variable-rate sprayer with laser scanning sensor to synchronize spray outputs to tree structures. *Transactions of the ASABE*, 55(3), 773–781. <https://doi.org/10.13031/2013.41509>
- Cox, W. J., Hahn, R. R., & Stachowski, P. J. (2006). Time of Weed Removal with Glyphosate Affects Corn Growth and Yield Components. *Agronomy Journal*, 98(2), 349–353. <https://doi.org/10.2134/agronj2005.0078>
- Creech, C. F., Henry, R. S., Fritz, B. K., & Kruger, G. R. (2015). Influence of herbicide active ingredient, nozzle type, orifice size, spray pressure, and carrier volume rate on spray droplet size characteristics. *Weed Technology*, 29(2), 298–310. <https://doi.org/10.1614/wt-d-14-00049.1>
- Daggupati, N. P. (2007). *Assessment of the varitarget nozzle for variable rate application of liquid crop protection products*. MS thesis. Manhattan, Kansas: Kansas State University, Department of Biological and Agricultural Engineering.
- Ebert, T. A., Taylor, R. A. J., Downer, R. A., & Hall, F. R. (1999). Deposit structure and efficacy of pesticide application. 1: Interactions between deposit size, toxicant concentration and deposit number. *Pestic. Sci.*, 55(8), 783–792. [https://doi.org/10.1002/\(SICI\)1096-9063\(199908\)55:8<783::AID-PS973>3.0.CO;2-D](https://doi.org/10.1002/(SICI)1096-9063(199908)55:8<783::AID-PS973>3.0.CO;2-D)
- Fabula, J. V., Sharda, A., & Badua, S. A. (2019). Nozzle tip selection for pulse width modulated (PWM) sprayers. Manhattan, Kansas: Kansas State University, K-State Research and Extension.
- Fabula, J. V., Sharda, A., Flippo, D., Ciampitti, I., & Kang, Q. (2020). Boom pressure and droplet size uniformity of a pulse width modulation (PWM) spray technology. *2020 ASABE Annu. Int. Virtual Meet. July 13-15, 2020*, 1-. <https://doi.org/10.13031/aim.202001041>
- Garcia-Ramos, F. J., Vidal, M., Boné, A., & Serreta, A. (2011). Methodology for the Regulation of Boom Sprayers Operating in Circular Trajectories. *Sensors*, 11, 4295–4311. <https://doi.org/10.3390/s110404295>
- Giles, D. K., Klassen, P., Niederholzer, F. J. A., & Downey, D. (2011). “Smart” sprayer technology provides environmental and economic benefits in California Orchards. *Calif. Agric.*, 65(2), 85–89. <https://doi.org/10.3733/ca.v065n02p85>
- Giles, D. K., & O’banion, J. P. (2008). *Simultaneous liquid flowrate and pressure control of sprayers*. U.S. Patent Publication No. 2008/0230624 A1.

- Giles, K. (2009). Variable rate spray application without a change in droplet size. *Australian Grain*, 38–39. Retrieved from https://www.ausgrain.com.au/BackIssues/186magrn09/38_Variable.pdf
- González, X. P., Marey, M. F., & Álvarez, C. J. (2007). Evaluation of productive rural land patterns with joint regard to the size, shape and dispersion of plots. *Agric. Syst.*, 92(1–3), 52–62. <https://doi.org/10.1016/j.agry.2006.02.008>
- Gopala Pillai, S., Tian, L., & Zheng, J. (1999). Evaluation of a flow control system for site-specific herbicide applications. *Trans. ASAE*, 42(4), 863–870. <https://doi.org/10.13031/2013.13265>
- Grisso, R. D., Jasa, P. J., & Rolofson, D. E. (2002). Analysis of traffic patterns and yield monitor data for field efficiency determination. *Appl. Eng. Agric.*, 18(2), 171–178. <https://doi.org/10.13031/2013.7782>
- Han, S., Hendrickson, L. L., Ni, B., & Zhang, Q. (2001). Modification and testing of a commercial sprayer with PWM solenoids for precision spraying. *Appl. Eng. Agric.*, 17(5), 591. <https://doi.org/10.13031/2013.6906>
- Hasan, A. R., & Prehim, J. (2013). *Ag Sprayer Boom Control Using Fuzzy Controller*. <https://doi.org/10.7763/IPEDR>
- Heap, I. 2020. The International Herbicide-Resistant Weed Database. www.weedscience.org.
- Holtz, A. J., Willoughby, R. A., Stone, M. L., Solie, J. B., & Raun, W. R. (2000). Dynamic response of valves for variable rate application of fertilizer and pesticides. *ASABE Paper No. 20003016251*. St. Joseph, MI: ASABE.
- Kuivila, K. M., & Foe, C. G. (1995). Concentrations, transport and biological effects of dormant spray pesticides in the San Francisco Estuary, California. *Environ. Toxicol. Chem.*, 14(7), 1141–1150. <https://doi.org/10.1002/etc.5620140704>
- Landers, A. (2000). Farm machinery: selection, investment and management. *Farm Mach. Sel. Invest. Manag.*
- Lang, J. P. (2013). Evaluation of pulse width modulation sprays for spray quality. *ASABE Paper No. 1131620682*. St. Joseph, MI: ASABE. <https://doi.org/10.13031/aim.20131620682>
- Larson, S. J., Capel, P. D., Goolsby, D. A., Zaugg, S. D., & Sandstrom, M. W. (1995). Relations between pesticide use and riverine flux in the Mississippi River basin. *Chemosphere*, 31(5), 3305–3321. [https://doi.org/10.1016/0045-6535\(95\)00176-9](https://doi.org/10.1016/0045-6535(95)00176-9)
- Lebeau, F., El Bahir, L., Destain, M. F., Kinnaert, M., & Hanus, R. (2004). Improvement of spray deposit homogeneity using a PWM spray controller to compensate horizontal boom speed variations. *Comput. Electron. Agric.*, 43(2), 149–161. <https://doi.org/10.1016/j.compag.2004.01.001>

- Loghavi, M., & Behzadi Mackvandi, B. (2008). Development of a target oriented weed control system. *Comput. Electron. Agric.*, 63(2), 112–118. <https://doi.org/10.1016/j.compag.2008.01.020>
- Luck, J. D., Pitla, S. K., Shearer, S. A., Mueller, T. G., Dillon, C. R., Fulton, J. P., & Higgins, S. F. (2010a). Potential for pesticide and nutrient savings via map-based automatic boom section control of spray nozzles. *Comput. Electron. Agric.*, 70(1), 19–26. <https://doi.org/10.1016/j.compag.2009.08.003>
- Luck, J. D., Zandonadi, R. S., Luck, B. D., & Shearer, S. A. (2010b). Reducing Pesticide Over-Application with Map-Based Automatic Boom Section Control on Agricultural Sprayers. *Trans. ASABE*, 53(3), 685–690. <https://doi.org/10.13031/2013.30060>
- Luck, J. D., Pitla, S. K., Zandonadi, R. S., Sama, M. P., & Shearer, S. A. (2011). Estimating off-rate pesticide application errors resulting from agricultural sprayer turning movements. *Precis. Agric.*, 12(4), 534–545. <https://doi.org/10.1007/s11119-010-9199-9>
- Luck, J. D., Shearer, S. A., Sama, M. P., & Pitla, S. K. (2015). Control system development and response analysis of an electronically actuated variable-orifice nozzle for agricultural pesticide applications. *Transactions of the ASABE*, 58(4), 997–1008. <https://doi.org/10.13031/trans.58.10945>
- Luck, J. D., Sama, M. P., Pitla, S. K., & Shearer, S. A. (2010). Pneumatic control of a variable orifice nozzle. *ASABE Paper No. 1009618. St. Joseph, MI: ASABE*. <https://doi.org/10.13031/2013.36204>
- Mangus, D. L., Sharda, A., Engelhardt, A., Flippo, D., Strasser, R., Luck, J. D., & Griffin, T. (2017). Analyzing the nozzle spray fan pattern of an agricultural sprayer using pulse width modulation technology to generate an on-ground coverage map. *Trans. ASABE*, 60(2), 315–325. <https://doi.org/10.13031/trans.11835>
- Matthews, G. A. (2008). Developments in application technology. *Environmentalist*, 28(1), 19–24. <https://doi.org/10.1007/s10669-007-9039-2>
- Miller, M. S., & Smith, D. B. (1992). A Direct Nozzle Injection Controlled Rate Spray Boom. *Trans. ASAE*, 35(3), 781–785. <https://doi.org/10.13031/2013.28662>
- Needham, D. L., Holtz, A. J., & Giles, D. K. (2012). Actuator System for Individual Nozzle Control of Flow Rate and Spray Droplet Size. *Trans. ASABE*, 55(2), 379–386. <https://doi.org/10.13031/2013.41376>
- Nicolopoulou-Stamati, P., Maipas, S., Kotampasi, C., Stamatis, P., & Hens, L. (2016). Chemical Pesticides and Human Health: The Urgent Need for a New Concept in Agriculture. *Front. Public Health* 4:148, 4, 1. <https://doi.org/10.3389/fpubh.2016.00148>

- Ooms, D., Ruter, R., Lebeau, F., & Destain, M. F. (2003). Impact of the horizontal movements of a sprayer boom on the longitudinal spray distribution in field conditions. *Crop Prot.*, 22(6), 813–820. [https://doi.org/10.1016/S0261-2194\(03\)00045-0](https://doi.org/10.1016/S0261-2194(03)00045-0)
- Panneton, B., Thériault, R., & Lacasse, B. (2001). Efficacy evaluation of a new spray–recovery sprayer for orchards. *Transactions of the ASAE*, 44(3), 473. <https://doi.org/10.13031/2013.6102>
- Pimentel, D., & Burgess, M. (2014). Environmental and economic costs of the application of pesticides primarily in the United States. In *Integrated Pest Management* (Vol. 3, pp. 47–71). https://doi.org/10.1007/978-94-007-7796-5_2
- Popp, J., Pető, K., & Nagy, J. (2013). Pesticide productivity and food security. A review. *Agronomy for Sustainable Development*, Vol. 33, pp. 243–255. <https://doi.org/10.1007/s13593-012-0105-x>
- Porter, W. M., Rascon, J. A., Shi, Y., Taylor, R. K., & Weckler, P. A. (2013). Laboratory Evaluation of a Turn Compensation Control System for a Ground Sprayer. *Appl. Eng. Agric.*, 29(5), 655–662. <https://doi.org/10.13031/aea.29.10075>
- Ramon, H., & De Baerdemaeker, J. (1997). Spray boom motions and spray distribution: Part 1, derivation of a mathematical relation. *J. Agric. Eng. Res.*, 66(1), 23–29. <https://doi.org/10.1006/jaer.1996.0114>
- Reddy, K. N., & Zablotowicz, R. M. (2003). Glyphosate-resistant soybean response to various salts of glyphosate and glyphosate accumulation in soybean nodules. *Weed Science*, 51(4), 496–502. [https://doi.org/10.1614/0043-1745\(2003\)051\[0496:gsrtvs\]2.0.co;2](https://doi.org/10.1614/0043-1745(2003)051[0496:gsrtvs]2.0.co;2)
- Reddy, K. N., Hoagland, R. E., & Zablotowicz, R. M. (2000). Effect of glyphosate on growth, chlorophyll, and nodulation in glyphosate-resistant and susceptible soybean (*Glycine max*) varieties. *Journal of New Seeds*, 2(3), 37–52. https://doi.org/10.1300/J153v02n03_03
- Rockwell, A. D., & Ayers, P. D. (1996). A variable rate, direct nozzle injection field sprayer. *Appl. Eng. Agric.*, 12(5), 531–538. <https://doi.org/10.13031/2013.25680>
- Sama, M. P., Evans, J. T., Turner, A. P., & Dasika, S. S. (2016). As-applied estimation of volumetric flow rate from a single sprayer nozzle series using water-sensitive spray cards. *Transactions of the ASABE*, 59(3), 861–869. <https://doi.org/10.13031/trans.59.11538>
- Sama, M. P., Luck, J. D., & Stombaugh, T. S. (2015). Scalable Control Architecture for Variable-Rate Turn Compensation. *Appl. Eng. Agric.*, 31(3), 425–435. <https://doi.org/10.13031/aea.31.10848>
- Shafagh-Kolvanagh, J., Zehtab-Salmasi, S., Javanshir, A., Moghaddam, M., Dabbagh, A., Nasab, M., & Rastilantie, M.-. (2008). Effects of nitrogen and duration of weed interference on grain yield and SPAD (chlorophyll) value of soybean (*Glycine max* (L.) Merrill.) WFL Publisher Science and Technology. In *Journal of Food, Agriculture & Environment* (Vol. 6). Retrieved from www.world-food.net

- Shahemabadi, A. R., & Moayed, M. J. (2008). An algorithm for pulsed activation of solenoid valves for variable rate application of agricultural chemicals. *Proceedings - International Symposium on Information Technology 2008*, 3. <https://doi.org/10.1109/ITSIM.2008.4631863>
- Sharda, A., Franzen, A., Clay, D. E., & Luck, J. D. (2018). Precision Variable Equipment. In *Precision Agriculture Basics* (pp. 155–168). <https://doi.org/10.2134/precisionagbasics.2016.0094>
- Sharda, A., Fulton, J. P., McDonald, T. P., Zech, W. C., Darr, M. J., & Brodbeck, C. J. (2010). Real-Time Pressure and Flow Dynamics Due to Boom Section and Individual Nozzle Control on Agricultural Sprayers. *Trans. ASABE*, 53(5), 1363–1371. <https://doi.org/10.13031/2013.34891>
- Sharda, A., Fulton, J. P., & Taylor, R. K. (2016). Performance of variable-orifice nozzles for liquid fertilizer applications. *Applied Engineering in Agriculture*, 32(3), 347–352. <https://doi.org/10.13031/aea.32.11428>
- Sharda, A., Fulton, J. P., McDonald, T. P., & Brodbeck, C. J. (2011). Real-time nozzle flow uniformity when using automatic section control on agricultural sprayers. *Computers and Electronics in Agriculture*, 79(2), 169–179. <https://doi.org/10.1016/j.compag.2011.09.006>
- Sharda, A., Luck, J. D., Fulton, J. P., McDonald, T. P., & Shearer, S. A. (2013). Field application uniformity and accuracy of two rate control systems with automatic section capabilities on agricultural sprayers. *Precis. Agric.*, 14(3), 307–322. <https://doi.org/10.1007/s11119-012-9296-z>
- Shearer, C. A., Luck, J. D., Evans, J. T., Fulton, J. P., & Sharda, A. (2020). Pesticide application coverage training (PACT) tool: development and evaluation of a sprayer performance diagnostic tool. *Precis. Agric.*, 1–21. <https://doi.org/10.1007/s11119-020-09761-z>
- Shen, Y., Zhu, H., Liu, H., Chen, Y., & Ozkan, E. (2017). Development of a Laser-Guided, Embedded-Computer-Controlled, Air-Assisted Precision Sprayer. *Trans. ASABE*, 60(6), 1827–1838. <https://doi.org/10.13031/trans.12455>
- Silva, J. E., Zhu, H., & Cunha, J. P. A. R. da. (2018). Spray outputs from a variable-rate sprayer manipulated with pwm solenoid valves. *Applied Engineering in Agriculture*, 34(3), 527–534. <https://doi.org/10.13031/aea.12556>
- Tian, L., & Zheng, J. (2000). Dynamic deposition pattern simulation of modulated spraying. *Trans. ASAE*, 43(1), 5–11. <https://doi.org/10.13031/2013.2687>
- Townson, H. (1992). Public health impact of pesticides used in agriculture. *Transactions of the Royal Society of Tropical Medicine and Hygiene*, 86(3), 350. [https://doi.org/10.1016/0035-9203\(92\)90345-D](https://doi.org/10.1016/0035-9203(92)90345-D)
- United Nations. (2019). World population prospects 2019: Highlights. Retrieved January 21, 2021, from

https://www.un.org/en/development/desa/population/publications/pdf/popfacts/PopFacts_2019-6.pdf

- USDA. (2020). ERS's Farm Income and Wealth Statistics. Retrieved November 25, 2020, from https://data.ers.usda.gov/reports.aspx?ID=17834#Pb947376daa9a4b6b91294605f2262a48_2_150iT0R0x0
- Van Der Werf, H. M. G. (1996). Assessing the impact of pesticides on the environment. *Agriculture, Ecosystems and Environment*, 60(2–3), 81–96. [https://doi.org/10.1016/S0167-8809\(96\)01096-1](https://doi.org/10.1016/S0167-8809(96)01096-1)
- Werner, I., Zalom, F. G., Oliver, M. N., Deanovic, L. A., Kimball, T. S., Henderson, J. D., ... Wallender, W. W. (2004). Toxicity of storm-water runoff after dormant spray application in a french prune orchard, Glenn County, California, USA: Temporal patterns and the effect of ground covers. *Environ. Toxicol. Chem.*, 23(11), 2719. <https://doi.org/10.1897/03-572>
- World Health Organization & United Nations Environment Programme. (1990). Public health impact of pesticides used in agriculture. *World Health Organization*.
- Yang, C. (2001). A variable rate applicator for controlling rates of two liquid fertilizers. *Appl. Eng. Agric.*, 17(3), 409–417. <https://doi.org/10.13031/2013.6203>
- Zandonadi, R. S., Luck, J. D., Stombaugh, T. S., Sama, M. P., & Shearer, S. A. (2011). A Computational Tool for Estimating Off-Target Application Areas in Agricultural Fields. *Trans. ASABE*, 54(1), 41–49. <https://doi.org/10.13031/2013.36251>
- Zhang, N., & Chaisattapagon, C. (1995). Effective Criteria for Weed Identification in Wheat Fields Using Machine Vision. *Trans. ASAE*, 38(3), 965–974. <https://doi.org/10.13031/2013.27914>

Appendix A - Equipment Specifications

A.1 New Holland SP370F Sprayer



Engine:	FPT Cursor 9 / 8.7 L / Tier 4B
Rated Power:	328 (244)
Power Bulge:	369 (275)
Fuel Tank Capacity:	150 (568)
DEF Tank Capacity:	24 (91)
Transmission:	Hydrostatic drive with electronic controlled Danfoss H1 series heavy-duty twin 130 cc pumps
Speed Range:	4 User set speed ranges: 0 – 32 (0 – 51)
Crop Clearance:	74 (187.96) or 76 (193.04)
Tank Material:	Stainless Steel
Tank Capacity:	1200 (4542) / 1400 (5300) / 1600 (6056)
Rinse System:	Standard electric controls or optional Auto Rinse 150 gal. (568 L) poly tank with 2 in. (5.08 cm) fill connection
Mono Boom Width (ft):	90/60, 100/60, 120/70
Truss Boom Width (ft):	120/73, 132/73, 135/73
Spray-Air Boom Width (ft):	–
Nozzle Bodies:	3 way, 5 way, 3+1, IntelliSpray
Shipping Height (cm):	154 (391)
Shipping Width (Mono):	145 (368)

A.2 Case Patriot 4440 Sprayer



Model:	Patriot 4440
Rated power:	335 hp (250kW)
Peak power:	374 hp (279 kW)
Peak torque:	1,143 ft-lb (1550 Nm)
Number of cylinders:	6
Displacement:	531 cu. in (8.7 L)
Engine make:	Case IH FPT
Engine model:	Cursor 8.7
Tank size:	1,200 gal (4542 L)
Solution tank:	Stainless Steel
Solution pump:	Centrifugal-hydraulic motor driven
Boom location:	Rear
Boom width:	120 ft (30.5 m)
Boom sections:	7
Ground height:	24 to 84 in (61 to 213 cm)
Nozzle spacing:	20 in (50.8 cm)

A.3 PCB Piezotronics Thin Film Membrane Pressure Transducer



Manufacturer:	PCB Piezotronics
Part number:	1502B81EZ100psiG
Measurement range, kPa (psi g):	0-690 (0-100)
Output, (Vdc):	0-10
Accuracy:	≤ 0.25% FS
Drift:	≤ 0.2 % FS/Year
Sensitivity, mV/kPa (mV/psi):	14.5 (100)
Resolution:	≤ 0.01 % FS
Response time, ms:	≤ 1
Environment:	
Proof pressure:	2X FS
Burst Pressure:	> 35X FS
Fatigue life:	108 FS cycles
Electrical:	
Supply voltage, VDC:	11.5 to 30
Current consumption, mA:	6
Physical:	
Pressure port:	1/4-18 NPT
Thread:	External

A.4 Flow Technology Inc. Flow Meter



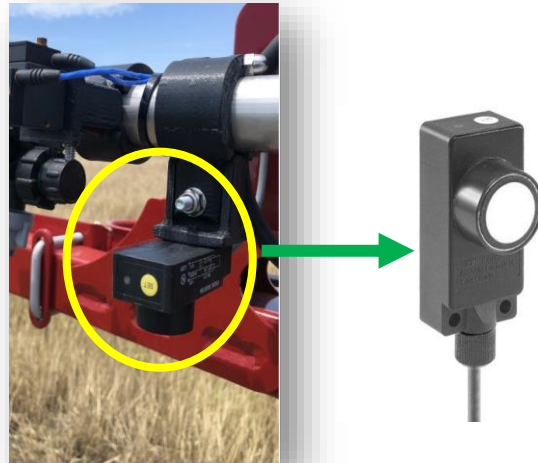
Manufacturer:	Flow Technology Inc.
Part Number:	FT-16
Calibration accuracy:	$\pm 0.05\%$ of reading, traceable to NIST
Repeatability:	$\pm 0.05\%$ of reading
Linearity:	$\pm 0.10\%$ with linearizing electronics
Response time:	3-4mS typical
Housing material:	316 stainless steel, standard
Rotor material:	430F stainless steel, standard
Temperature range:	-450 to 750°F, dependent on bearing and pick-off
Operating pressure:	Up to 30,000PSIG, dependent on fitting
Ball bearing material:	440C stainless steel or equivalent, Ceramic
Journal bearing material:	Ceramic, tungsten carbide, graphite
Pick-off's:	Modulated carrier and magnetic
Straight Run:	10D upstream and 5D downstream minimum
Recommended filtration:	Ball bearings: 10 to 100 microns (less filtration with larger sizes) Journal bearings: 75 to 100 microns

A.5 High Sensitivity DC Accelerometer



Manufacturer:	PCB Piezotronics
Part Number:	3741E1210G
Sensitivity:	($\pm 3\%$) 400 mV/g (40.8 mV/(m/s ²))
Measurement Range:	± 10 g pk (± 98.1 m/s ² pk)
Broadband Resolution:	0.4 mg rms (0.004 m/s ² rms)
Temperature Range:	-65 to 250 °F (-54 to 121 °C)
Frequency Range:	(± 3 dB) 0 to 500 Hz
Electrical Connector:	Integral Cable

A.6 Baumer Ultrasonic Sensor



Primary brand:	Baumer
Main function:	Sensor (Distance)
Product series / family name:	Distance sensors (ultrasonic measuring)
Sub-range name:	UNDK series
Supply voltage (DC):	15-30Vdc (24Vdc nom.)
Sensing distance:	200mm - 2000mm (scanning range Sd)
Shape:	Rectangular body
Connection type:	Pre-wired with 2m cable terminated with bare end flying leads
Analog outputs:	1 x analog output (0-10Vdc / 10-0Vdc)
Measurement accuracy:	<0.5mm (resolution) <1mm (repeatability)
Degree of protection:	IP67
Dimensions:	W30mm x H65mm x D31mm
Material:	polyester / die-cast zinc (housing)
Ambient air temperature for operation:	-10...+60 °C
Functions:	Long-range ultrasonic distance measurement sensor. Teach-in alignment aid with flashing target indication
Protection functions:	Short-circuit protection reverse polarity protection
Visual position indicator:	yellow LED / red LED
Current consumption:	35mA / 0.035 A
Emission frequency:	200kHz

A.7 Topcon GR5 Receiver



Tracking

Number of Channels:	216 Universal Channels Signals Tracked G3 Technology = GPS, GLONASS and GALILEO*
WAAS / EGNOS / MSAS:	Yes

Accuracy

RTK:	H: 10 mm + 1 ppm / V: 15 mm + 1 ppm
Static:	H: 3mm + 0.5ppm
Fast Static:	V: 5mm + 0.5ppm

Communications

Optional Radio Type:	Integrated UHF Transmit (TX) and Receive (RX), or 915MHz Spread Spectrum
Base Radio Output:	0.01 - 1.0 Watt, user selectable
Cellular Communications:	Integrated GSM/GPRS or CDMA
Wireless Communications:	Integrated Bluetooth® 2.0 compliant

Data & Memory

Memory Internal:	Removable SD/SDHC Memory Card
Data Update/Output Rate:	1Hz to 100Hz Selectable
Real Time Data Output Format:	TPS, RTCM SC104, CMR, CMR+
ASCII Output:	NMEA 0183 version 2.x and 3.0

Environmental

Enclosure:	Magnesium I-Beam Housing
Operating Temperature:	-40°C to +70°C** (-40°F to 158°F)
Dust and Water Protection:	International Protection Rating 66 (IP66)
Shock Rating:	2 meter pole drop to concrete, IEC 60068-2-29, IEC 60068-2-27
Vibration Rating:	SAE J1211, Section 4.7, MIL-STD 202G, Method 214A

A.8 Raven Viper 4+ Monitor



Dimension	Height:	9.626 in.
	Width:	12.015 in.
	Depth:	1.786 in.
	Diagonal:	12.1 in
Power	Weight:	4.7 lbs (approx.)
	Operating Voltage:	9 to 16 V DC Nominal
Input/Output	USB:	2 (USB 2.0)
	Ethernet:	Category 5 Connectivity with Adapter Cable
	Audio:	3.5 mm Stereo Minijack
	Video:	Camera/Video Input – PAL/NTSC Formats Display Output – DVI Port
	GPS:	TNC Antenna Port – NMEA Messages
	CAN:	4 CAN Communication Ports (Raven Proprietary CANbus, ISOBUS, J1939, Open)
Mounting	Switch:	2 Digital Switch Inputs
	Plate Arm:	RAM Mounting Plate and Socket Arm
	Hardware:	Screws – 10-32 x 1/2" and 1/4-20 x 3/8" (Black) Washers – Flat and Split Lock
Environmental	Operating Conditions:	32° to 158° F
	Storage Conditions:	-40° to 185° F
	Relative Humidity:	Non-condensing

A.9 Capstan Solenoid Valve



Input Voltage:	12 V
Power:	7 w
Current:	0.58 A
Resistance:	21 -23.5 Ω
Duty Cycle:	10-100%
Frequency:	3-31 Hz

A.10 Raven Hawkeye Nozzle Control Valve



Dimension	Height:	3.8 in.
	Width:	1.39 in.
	Depth:	1.35 in.
	Weight:	7.1 oz (approx.)
	Operating Voltage:	13.6 V DC nominal (10 V drop-out to 16 V spike tolerant)
Power		
Input/Output	CAN:	CANBUS 2.0 Compliant
Environmental Conditions	Switched (In/Out):	3 V
	Operating Conditions:	-22 to 140 F
	Storage Conditions:	-40 to 158 F
	Relative Humidity:	10 to 95% relative

A.11 John Deere ExactApply Solenoid Valve



No Available Data

A.12 FT205EV Digital Wind Sensor



Wind speed

Range	0-75m/s 0-270km/h 0-145.8 knots
Resolution	0.1m/s 0.1km/h 0.1knots
Accuracy	±0.3m/s (0-16m/s) ±2% (16-40m/s) ±4% (40-75m/s)

Wind direction

Range	0 to 360°
Resolution	1°
Accuracy	4° RMS
Compass accuracy	5° RMS

Acoustic temperature

Resolution	0.1°C
Accuracy	±2°C
Under the following conditions:	
Speed Range	5m/s - 60m/s
Operating Range	-20°C to +60°C
Difference between air and sensor temperature	<10°C

Sensor performance

Measurement principle	Acoustic Resonance
Units of measure	Meters per second, kilometers per hour or knots

Data update rate	Up to 10Hz
Altitude	0-4000m operating range
Temperature range	-20° to +70°C (operational), -40° to +85°C (storage)
Humidity	0-100%
Power requirements	
Supply voltage	6V to 30V DC operating range
Supply current	30mA
Physical	
Sensor height	55.1mm
Sensor diameter	56.4mm
I/O connector	Molex CLIK-Mate
I/O cable	Molex CLIK-Mate
Sensor weight	100g
Sensor material	3D printed graphite and nylon composite
Mounting method	Surface-Mount with compressed gasket and 3x screw fit. An adaptor is provided for pole-mounting (the pole is not supplied)
Digital Sensor	
Interface	RS422 (full-duplex). RS485 (half-duplex), UART (full-duplex, 3V & 5V)
Format encoding	ASCII

A.13 WatchDog Sprayer Station 3349SSH



Wind resolution

Speed:	0.1 mph (0.2 km/h)
Direction:	1°
Wind Speed Range:	0 to 90 mph (0 to 145 km/h)
Wind Speed Accuracy:	<12 mph (19 km/h): ± 1.1 mph (1.7 km/h) + 10%; >12 mph (19 km/h): ± 2.3 mph (3.7 km/h) or ± 5%
Wind Direction Accuracy:	4 to 11 mph (6 to 18 km/h): ±5°; >12 mph (19 km/h): ±2°
Wind Accuracy Temperature Range:	32° to 131°F (0° to 55°C)
Operating Temperature:	-13° to 131°F (-25° to 55°C)
Temperature Accuracy:	±1.8°F (±1°C) with wind above 4.6 mph (7.4 km/h)
Relative Humidity Range:	10 to 95%
Relative Humidity Accuracy:	±4% with wind above 4.6 mph (7.4 km/h)
Barometric Pressure Range:	24 to 33 in-Hg (800 to 1100 hPa)
Barometric Pressure Accuracy:	± 0.029 in-Hg (± 1 hPa)
Power Supply Voltage:	9 to 40 VDC; Current: <70 mA

A.14 Topcon B110 GNSS Receiver



Tracking

Channels: 226 Universal Tracking Channels
 Signals Tracked: GPS: L1, L2, L2C; GLONASS: L1, L2, L2C; SBAS-QZSS: L1, L2C

WAAS/EGNOS/MSAS

Yes

Accuracy

Standalone: H: 1.2 m; V: 1.8 m
 DGPS: H: 0.3 m; V: 0.5 m
 SBAS: H: 0.8 m; V: 1.2 m
 Static: H: 3 mm +0.5 ppm x baseline; V: 4 mm + 1.0 ppm x baseline
 RTK: H: 10 mm +0.5 ppm x baseline; V: 15 mm + 1.0 ppm x baseline
 RTK Initialization: <10 seconds
 RTK Initialization Reliability: > 99%
 Velocity: 0.02 m/seconds
 Time: 30 nsec

Acquisition Time

Hot/Warm/Cold Start: <10 sec/< 35 sec < 60 sec
 Reacquisition: <1 sec
 Communication Interfaces
 RS232: 2x ports up to 460.8 kbps
 LVTTL UART: 4x ports up to 460.8 kbps
 USB 2.0 (client): 1 x port up to 480 mbps (High Speed)
 CAN: 1x port (without transceivers), LVTTL, NMEA2000 compliant

I ² C interface:	Communicates with external I ² C enabled devices
PPS:	1x port with 5 ns resolution, < 30ns precision, LVTTTL, configurable polarity and period
EVENT:	5 ns resolution, LVTTTL, programmable active edge

Data and Memory

SD/MMC card support:	Physical interface, 20 Hz writing rate, up to 2GB capacity
Data update/Output Rate:	1Hz – 100 Hz Selectable
Real time Data Output:	TPS, RTCM SC104.2.x and 3.x, CMR, CMR+
ASCII Output:	NMEA 0183 version 2.x and 3.0
Geoid/Magnetic Variation:	Yes
Grid Coordinates Output:	Yes

Environmental

Temperature:	Operating: -40°C to 85 °C; Storage: -40°C to 85 °C
Vibration:	4g Sine Vibe (SAEJ1211); 7.7g Random Vibe (MIL-STD 810F)
Humidity:	95%, non-condensing
Shock:	30g (IEC 68-2-27)
Acceleration:	20 g

Power

Voltage/Power Consumption:	3.4 VDC to 4.5 VDC / 1.0 W typical
LNA Power:	3.3 V (internal), 5.0 V (external) at 0-100 mA
Physical	
Dimensions/ Weight:	40 x 55 x 10 mm / <20 g
Main Connector:	60 pin Molex
Antenna Inputs:	2 (to connect internal or external antenna) ESD protected
Antenna Connectors:=	Hirose H.FL

Appendix B - Data Acquisition System Specifications

B.1 CompactRIO (cRIO) Controller



Model:	cRIO-9047
Processor	
CPU:	Intel Atom E3940
Number of cores:	4
CPU frequency:	1.6 GHz (base), 1.8 GHz (burst)
On-die L2 cache:	2 MB
Software	
Supported operating system:	NI Linux Real-Time (64-bit)
Supported C Series module programming modes:	Real-Time (NI-DAQmx) Real-Time Scan (I/O Variables) LabVIEW FPGA
Application software LabVIEW	LabVIEW 2017 or later, LabVIEW Real-Time Module 2017 or later, LabVIEW FPGA Module 2017 or later,
C/C++ Development Tools for NI Linux Real-Time Driver software	Eclipse Edition 2014 or later NI CompactRIO Device Drivers December 2017 or later
Network/Ethernet Port	
Number of ports:	2
Network interface:	10Base-T, 100Base-TX, and 1000Base-T Ethernet
Compatibility:	IEEE 802.3

Communication rates:	10 Mb/s, 100 Mb/s, 1000 Mb/s auto-negotiated
Maximum cabling distance:	100 m/segment

Network Timing and Synchronization

Protocol:	IEEE 802.1AS-2011 IEEE 1588-2008 (default end-to-end profile)
Supported ethernet ports:	Port 0, port 1
Network synchronization accuracy:	<1 μ s

RS-232 Serial Port

Maximum baud rate:	115,200 b/s
Data bits:	5, 6, 7, 8
Stop bits:	1, 2
Parity:	Odd, even, mark, space
Flow control:	RTS/CTS, XON/XOFF, DTR/DSR
RI wake maximum low level:	0.8 V
RI wake minimum high level:	2.4 V
RI overvoltage tolerance:	\pm 24 V

RS-485 Serial Port

Maximum baud rate:	230,400 b/s
Data bits:	5, 6, 7, 8
Stop bits:	1, 2
Parity:	Odd, even, mark, space
Flow control:	XON/XOFF
Wire mode:	4-wire, 2-wire, 2-wire auto
Isolation voltage:	60 V DC continuous, port to earth ground
Cable requirement:	Unshielded, 30 m maximum length (limited by EMC/surge)

USB Ports

Port 1

Type:	USB Type-A, host port
USB interface:	USB 2.0, Hi-Speed
Maximum data rate:	480 Mb/s
Maximum current:	900 mA

Port 2

Type:	USB Type-C, host port
USB interface:	USB 3.1 Gen1, SuperSpeed
Maximum data rate:	5 Gb/s
Maximum current:	900 mA
Alternate modes:	DisplayPort

Port 3

Type:	USB Type-C, dual role port (device or host)
USB interface:	USB 3.1 Gen1, SuperSpeed
Maximum data rate:	5 Gb/s
Maximum current:	900 mA

DisplayPort over USB Type-C	
Maximum resolution:	3840 × 2160 at 60 Hz
Supported standard:	DisplayPort 1.2
Supported USB ports:	Port 2
Maximum resolution:	3840 × 2160 at 60 Hz
SD Card Slot	
SD card support:	SD and SDHC standards
Supported interface speeds:	UHS-I SDR50 and DDR50
Memory	
Nonvolatile memory (SSD):	4 GB
Nonvolatile memory (SSD) type:	Planar SLC NAND
Volatile memory (DRAM):	
Density:	4 GB
Type:	DDR3L
Maximum theoretical data rate:	12.8 GB/s
Reconfigurable FPGA	
FPGA type:	Xilinx Kintex-7 7K70T
Number of flip-flops:	82,000
Number of 6-input LUTs:	41,000
Number of DSP slices (18 × 25 multipliers):	240
Available block RAM:	4,860 kbits
Number of DMA channels:	16
Number of logical interrupts:	32
Internal Real-Time Clock	
Accuracy:	200 ppm; 40 ppm at 25 °C
Controller PFI 0	
Maximum input or output frequency:	1 MHz
Cable length:	3 m (10 ft)
Cable impedance:	50 Ω
PFI 0 connector:	SMB
Power-on state:	High impedance
I/O standard compatibility:	5 V TTL
I/O voltage protection:	±30 V
Maximum operating conditions:	
I _{OL} output low current:	8 mA maximum
I _{OH} output high current:	-8 mA maximum
Real-Time Streaming Performance	
Data throughput from system memory to target	
SD card:	40 MB/s
USB Type-C:	100 MB/s
Real-Time (NI-DAQmx) Mode	
Analog Input	
Input FIFO size:	253 samples per slot

Maximum sample rate:	Determined by the C Series module or modules
Timing accuracy:	50 ppm of sample rate
Timing resolution:	12.5 ns
Number of channels supported:	Determined by the C Series module or modules
Number of hardware-timed tasks:	8
Analog Output	
Hardware-timed tasks	
Number of hardware-timed tasks:	8
Number of channels supported	
Onboard regeneration:	16
Non-regeneration:	Determined by the C Series module or modules
Non-hardware-timed tasks	
Number of non-hardware-timed tasks:	Determined by the C Series module or modules
Number of channels supported:	Determined by the C Series module or modules
Maximum update rate:	1.6 MS/s
Timing accuracy:	50 ppm of sample rate
Timing resolution:	12.5 ns
Waveform onboard regeneration FIFO:	8,191 samples shared among channels used
Waveform streaming FIFO:	253 samples per slot
General-Purpose Counters/Timers	
Number of counters/timers:	4
Resolution:	32 bits
Counter measurements:	Edge counting, pulse, semi-period, period, two-edge separation, pulse width
Position measurements:	X1, X2, X4 quadrature encoding with Channel Z reloading; two-pulse encoding
Output applications:	Pulse, pulse train with dynamic updates, frequency division, equivalent time sampling
Internal base clocks:	80 MHz, 20 MHz, 13.1072 MHz, 12.8 MHz, 10 MHz, 100 kHz
External base clock frequency:	0 MHz to 20 MHz
Base clock accuracy:	50 ppm
Output frequency:	0 MHz to 20 MHz
Inputs:	Gate, Source, HW_Arm, Aux, A, B, Z, Up_Down
Routing options for inputs:	Any module PFI, controller PFI, analog trigger, many internal signals

FIFO:	Dedicated 127-sample FIFO
Frequency Generator	
Number of channels:	1
Base clocks:	20 MHz, 10 MHz, 100 kHz
Divisors:	1 to 16 (integers)
Base clock accuracy:	50 ppm
Output:	Any controller PFI or module PFI terminal
Module PFI	
Functionality:	Static digital input, static digital output, timing input, and timing output
Timing output sources:	Many analog input, analog output, counter, digital input, and digital output timing signals
Timing input frequency:	0 MHz to 20 MHz
Timing output frequency:	0 MHz to 20 MHz
Digital Triggers	
Source:	Any controller PFI or module PFI terminal
Polarity:	Software-selectable for most signals
Analog input function:	Start Trigger, Reference Trigger, Pause Trigger, Sample Clock, Sample Clock Timebase
Analog output function:	Start Trigger, Pause Trigger, Sample Clock, Sample Clock Timebase
Counter/timer function:	Gate, Source, HW_Arm, Aux, A, B, Z, Up_Down
Power Requirements	
Voltage input range (measured at the cRIO-9047 power connector)	
V1:	9 V to 30 V
V2:	9 V to 30 V
Maximum power consumption:	60 W
Typical standby power consumption:	3.4 W at 24 V DC input
Recommended power supply:	100 W, 24 V DC
Power input connector:	4-position, 3.5 mm pitch, pluggable screw terminal with screw locks, Sauro CTF04BV8-AN000A
Physical Characteristics	
Weight (unloaded):	2,250 g (4 lbs, 15 oz)
Dimensions (unloaded):	328.8 mm × 88.1 mm × 121.2 mm (12.94 in. × 3.47 in. × 4.77 in.)
Power connector wiring	
Gauge:	0.5 mm ² to 2.1 mm ² (20 AWG to 14 AWG) copper conductor wire
Wire strip length:	6 mm (0.24 in.) of insulation stripped from the end

Temperature rating:	85 °C
Torque for screw terminals:	0.20 N · m to 0.25 N · m (1.8 lb · in. to 2.2 lb · in.)
Wires per screw terminal:	One wire per screw terminal
Connector securement	
Securement type:	Screw flanges provided
Torque for screw flanges:	0.20 N · m to 0.25 N · m (1.8 lb · in. to 2.2 lb · in.)
Insulation rating:	300 V, maximum

Environmental

Temperature (Tested in accordance with IEC 60068-2-1 and IEC 60068-2-2)	
Operating:	-40 °C to 70 °C
Storage:	-40 °C to 85 °C
Ingress protection:	IP20
Operating humidity (Tested in accordance with IEC 60068-2-30):	10% RH to 90% RH, noncondensing
Storage humidity (Tested in accordance with IEC 60068-2-30):	5% RH to 95% RH, noncondensing
Pollution Degree:	2
Maximum altitude:	5,000 m

Shock and Vibration

Operating vibration	
Random (IEC 60068-2-64):	5 grms, 10 Hz to 500 Hz
Sinusoidal (IEC 60068-2-6):	5 g, 10 Hz to 500 Hz
Operating shock (IEC 60068-2-27):	30 g, 11 ms half sine; 50 g, 3 ms half sine; 18 shocks at 6 orientations

B.2 National Instruments 9221 C Series Voltage Input Module



Input Characteristics

Number of channels	8
ADC resolution	12 bits
Type of ADC	Successive approximation register (SAR)
Maximum Sample Rate (Aggregate)	
R Series Expansion Chassis	475 kS/s
All Other Chassis	800 kS/s
Input range	± 60 V
Measurement voltage, channel-to-COM (V)	
Minimum	± 61.4
Typical	± 62.50
Maximum	± 63.8
Overvoltage protection, channel-to-COM	± 100 V
Stability	
Gain drift	± 34 ppm/ $^{\circ}$ C
Offset drift	± 580 μ V/ $^{\circ}$ C
Input bandwidth (-3 dB)	950 kHz min
Input impedance	
Resistance	1 M Ω
Capacitance	5 pF
Input noise, code-centered	
RMS	0.7 LSB _{rms}
Peak-to-peak	5 LSB
No missing codes	12 bits
DNL	-0.9 to 1.5 LSB
INL	± 1.5 LSB
Crosstalk, at 10 kHz	-75 dB

Settling time, to 1 LSB	1.25 μ s
MTBF	1,092,512 hours at 25 °C; Bellcore Issue 2, Method 1, Case 3, Limited Part Stress Method

Power Requirements

Power consumption from chassis	
Active mode	1 W maximum
1 W maximum S	1 mW maximum
Thermal dissipation (at 70 °C)	
Active mode	1 W maximum
Sleep mode	32 mW maximum

Physical Characteristics

Screw-terminal wiring	
Gauge	0.2 mm ² to 2.5 mm ² (26 AWG to 14 AWG) copper conductor wire
Wire strip length	13 mm (0.51 in.) of insulation stripped from the end
Temperature rating	90 °C minimum
Torque for screw terminals	0.5 N · m to 0.6 N · m (4.4 lb · in. to 5.3 lb · in.)
Wires per screw terminal	One wire per screw terminal; two wires per screw terminal using a 2-wire ferrule
Ferrules	0.25 mm ² to 2.5 mm ²
Weight	
NI 9221 with screw termina	165 g (5.8 oz)

B.3 National Instruments 9870 C Series Serial Interface Module



Maximum baud rate:	921.6 kbps
Maximum cable length:	250 pF equivalent
Maximum RS232 Receive signal (RXD, CTS, DSR, DCD, RI) Continuous	± 8 V
Voltage:	
Data line ESD protection (human body model):	± 15 kV
MTBF:	448,008 hours at 25 °C; Bellcore Issue 6, Method 1, Case 3, Limited Part Stress Method

Power Requirements

Power consumption from chassis	
Active mode:	0.5 W max
Sleep mode :	50 μ W max
Thermal dissipation (at 70 °C)	
Active mode:	1.5 W max
NI 9870 Sleep mode:	0.5 W max
Required external supply voltage range (V _{sup}):	+8 to +28 VDC
Power supply consumption from external supply V _{sup}	
Typical:	0.5 W
Maximum:	2 W

Physical Characteristics

Weight:	Approx. 154 g (5.4 oz)
---------	------------------------

Safety

RS232 Receive Signal-to-COM (RXD, CTS, DSR, DCD, RI):	± 25 V max, Measurement Category I
---	--

RS232 Transmit Signal-to-COM (TX, RTS, DTR):	±13.2 V max, Measurement Category I
Vsup -to-COM:	±28 V max, Measurement Category I

Isolation Voltages

Port-to-earth ground	
Withstand:	1000 V , verified by a dielectric withstand test, 5 s
Continuous:	60 VDC, Measurement Category I

Shock and Vibration

Operating vibration, random (IEC 60068-2-64):	5 grms , 10 to 500 Hz
Operating shock (IEC 60068-2-27):	30 g, 11 ms half sine, 50 g, 3 ms half sine, 18 shocks at 6 orientations
Operating vibration, sinusoidal (IEC 60068-2-6):	5 g, 10 to 500 Hz

Environmental

Operating temperature:	−40 to 70 °C
Storage temperature:	−40 to 85 °C
Ingress protection:	IP 30
Operating humidity:	10 to 90% RH, noncondensing
Storage humidity:	5 to 95% RH, noncondensing
Maximum altitude:	2,000 m
Pollution Degree (IEC 60664):	2

B.4 National Instruments 9853 2-Port, High Speed Serial Interface Module



High-Speed CAN Characteristics

Transceiver:	Philips TJA1041
Max baud rate:	1 Mbps
CAN_H, CAN_L bus lines voltage:	-27 to +40 VDC
Supply voltage range (VSUP)	
CAN0:	N/A
CAN1:	+8 to +25 VDC
MTBF:	1,816,913 hours at 25 °C; Bellcore Issue 6, Method 1, Case 3, Limited Part Stress Method

Power Requirements

Power consumption from chassis	
Active mode:	625 mW max
Transmitting:	400 mW max
Sleep mode:	25 μ W max
Thermal dissipation (at 70 °C)	
Active mode:	1 W max
Sleep mode:	250 mW max

Physical Characteristics

Weight:	Approx. 144 g (5.0 oz)
---------	------------------------

Safety

Maximum Voltage	
Port-to-COM:	-27 to +40 VDC max, Measurement Category I

Isolation Voltages	
Port-to-port	

Continuous:	60 VDC, Measurement Category I up to 5,000 m altitude
Withstand:	500 Vrms, verified by a 5 s dielectric withstand test
Port-to-earth ground	
Continuous:	60 VDC, Measurement Category I up to 5,000 m altitude
Withstand:	500 Vrms, verified by a 5 s dielectric withstand test

Environmental

Operating temperature:	-40 to 70 °C
Storage temperature:	-40 to 85 °C
Ingress protection:	IP 40
Operating humidity:	10 to 90% RH, noncondensing
Storage humidity:	5 to 95% RH, noncondensing
Pollution Degree (IEC 60664):	2
Maximum altitude:	5,000 m

Shock and Vibration

Operating vibration, random (IEC 60068-2-64):	5 grms, 10 to 500 Hz
Operating shock (IEC 60068-2-27):	30 g, 11 ms half sine, 50 g, 3 ms half sine, 18 shocks at 6 orientations
Operating vibration, sinusoidal (IEC 60068-2-6):	5 g, 10 to 500 Hz

B.5 National Instruments 9205 C Series Voltage Input Module



Analog Input Characteristics

Number of channels:	16 differential/32 single-ended channels
ADC resolution:	16 bits
DNL:	No missing codes guaranteed
Conversion time (maximum sampling rate)	
CompactRIO & CompactDAQ chassis:	4.00 μ s (250 kS/s)
R Series Expansion chassis:	4.50 μ s (222 kS/s)
Input coupling:	DC
Nominal input ranges:	± 10 V, ± 5 V, ± 1 V, ± 0.2 V
Minimum overrange, ± 10 V range:	4%
Maximum working voltage for analog inputs (signal + common mode):	Each channel must remain within ± 10.4 V of COM
Input impedance (AI-to-COM)	
Powered on:	>10 G Ω in parallel with 100 pF
Powered off/overload:	4.7 k Ω minimum
Input bias current:	± 100 pA
Crosstalk, at 100 kHz	
Adjacent channels:	-65 dB
Non-adjacent channels:	-70 dB
Analog bandwidth:	370 kHz
Overvoltage protection	
AI channel, 0 to 31	± 30 V, one channel only
AISENSE:	± 30 V
Settling time for multichannel measurements, accuracy, all ranges	
± 120 ppm of full-scale step, ± 8 LSB:	4 μ s convert interval
± 30 ppm of full-scale step, ± 2 LSB:	8 μ s convert interval
Analog triggers	
Number of triggers:	1

Resolution:	10 bits, 1 in 1,024
Bandwidth, -3 dB:	370 kHz
Accuracy:	±1% of full scale
Scaling coefficients	
±10 V range:	328 μV/LSB
±5 V range:	164.2 μV/LSB
±1 V range:	32.8 μV/LSB
±0.2 V range:	6.57 μV/LSB
CMRR, DC to 60 Hz:	100 dB

Analog Input Absolute Accuracy

Residual gain error	
±10 V range:	115 ppm of reading
±5 V range:	135 ppm of reading
±1 V range:	155 ppm of reading
±0.2 V range:	215 ppm of reading
Gain tempco:	11 ppm/°C
Reference tempco:	5
Residual offset error	
±10 V range:	20 ppm of range
±5 V range:	20 ppm of range
±1 V range:	25 ppm of range
±0.2 V range:	40 ppm of range
Offset tempco	
±10 V range:	44 ppm of range/°C
±5 V range:	47 ppm of range/°C
±1 V range:	66 ppm of range/°C
±0.2 V range:	162 ppm of range/°C
INL error	76 ppm of range

Digital Characteristics

Number of channels:	1 digital input channel, 1 digital output channel
Overvoltage protection:	±30 V
Digital logic levels	
Input high, V _{IH}	
Minimum:	2.0 V
Maximum:	3.3 V
Input low, V _{IL}	
Minimum:	0 V
Maximum:	0.34 V
Output high, V _{OH} , sourcing 75 μA	
Minimum:	2.1 V
Maximum:	3.3 V
Output low, V _{OL} , sinking 250 μA	
Minimum:	0 V
Maximum:	0.4 V
External digital triggers	

Source:	PFI0
Delay:	100 ns maximum
Power Requirements	
Power consumption from chassis	
Active mode:	625 mW maximum
Sleep mode:	15 mW
Thermal dissipation (at 70 °C)	
Active mode:	625 mW maximum
Sleep mode:	15 mW
Physical Characteristics	
Spring terminal wiring	
Gauge:	0.13 mm ² to 1.5 mm ² (26 AWG to 16 AWG) copper conductor wire
Wire strip length:	10 mm (0.394 in.) of insulation stripped from the end
Temperature rating:	90 °C, minimum
Wires per spring terminal:	One wire per spring terminal; two wires per spring terminal using a 2-wire ferrule
Ferrules:	0.14 mm ² to 1.5 mm ²
Connector securement	
Securement type:	Screw flanges provided
Torque for screw flanges:	0.2 N · m (1.80 lb · in.)
Weight	
NI 9205 with DSUB:	148 g (5.3 oz)
Safety Voltages	
Maximum voltage	
Channel-to-COM:	±30 V DC
NI 9205 with DSUB Isolation Voltages	
Channel-to-channel:	None
Channel-to-earth ground	
Continuous:	60 V DC, Measurement Category I
Withstand	
up to 2,000 m:	1,000 V RMS, verified by a 5 s dielectric withstand test
up to 5,000 m:	500 V RMS
Shock and Vibration	
Operating vibration	
Random (IEC 60068-2-64):	5 grms, 10 Hz to 500 Hz
Sinusoidal (IEC 60068-2-6):	5 g, 10 Hz to 500 Hz
Operating shock (IEC 60068-2-27):	30 g, 11 ms half sine; 50 g, 3 ms half sine; 18 shocks at 6 orientations
Environmental	
Operating temperature (IEC 60068-2-1, IEC60068-2-2):	-40 °C to 70 °C

Storage temperature (IEC 60068-2-1, IEC 60068-2-2):	-40 °C to 85 °C
Ingress protection:	IP40
Operating humidity (IEC 60068-2-78):	10% RH to 90% RH, noncondensing
Storage humidity (IEC 60068-2-78):	5% RH to 95% RH, noncondensing
Pollution Degree:	2
Maximum altitude:	5,000 m

B.6 Dell Latitude 14 3470



Brand:	Dell
Bluetooth:	Bluetooth 4.0+LE
CPU:	2.5-GHz Intel Core i7-6500 CPU
Card Slots:	SD memory reader
Company Website:	dell.com
Display Size:	14
Graphics Card:	Nvidia GeForce 920M
Hard Drive Size:	128GB SSD
Native Resolution:	1920x1080
Ports (excluding USB):	Security lock slot, USB 2.0, USB 3.0, Ethernet, VGA, HDMI, Headphone/Mic, SD card slot
RAM:	8GB
Size:	13.45 x 9.57 x 0.91/1.7 with extended battery
Touchpad Size:	4.1 x 2.5 inches
USB Ports:	3
Video Memory:	2048MB
Weight:	4.4 pounds
Wi-Fi:	802.11a/b/g/n
Wi-Fi Model:	Dell Wireless 1802 802.11a b g n adapter

B.7 Keysight U8030 Triple-Output DC Power Supply



www.grainger.com

Electrical Specifications

Total power output (W):	0 – 375 W
Voltage output (V)	0 to 30 V
Output Channel 1 & 2 (@ 0 to 40 °C):	
Current output (A)	0 to 6 A
Output Channel 1 & 2 (@ 0 to 40 °C):	
Number of outputs:	Three isolated outputs
	– Two variable: CV and CC operation
	– One fixed: CV operation only
5 V fixed output	– Voltage/Current output: 5 V, 3A
Output Channel 3:	– Output accuracy: $\leq 5\%$ or $(5\text{ V} \pm 0.25\text{ V})$
	– Vrms: $< 2\text{ mVrms}$, or Vpp: $< 50\text{ mVpp}$ –
	– Load and line regulation: $\leq 5\text{ mV}$
	– Overload condition: 3 A + 20% (typical)
Line & load regulation (for variable output):	CV: $< 0.01\% + 2\text{ mV}$ CC: $< 0.02\% + 2\text{ mA}$
Ripple & noise :	CV: $\leq 1\text{ mVrms}$, 0.5 mVrms (typical) or $\leq 10\text{ mVpp}$, 5 mVpp (typical) CC: $\leq 1\text{ mArms}$
Load transient response time :	$< 50\text{ us}$
Stability (output drift) :	Voltage: $< 0.02\%$
	Current: $< 0.1\%$
Programming accuracy (23 °C \pm 5 °C):	CV: $\leq 0.25\% + 15\text{ mV}$ CC: $\leq 0.30\% + 15\text{ mA}$
Meter readback accuracy (23 °C \pm 5 °C):	CV: $\leq 0.25\% + 10\text{ mV}$ CC: $\leq 0.25\% + 10\text{ mA}$
Programming/meter resolution:	Voltage: 10 mV (4 digits) Current: 10 mA (3 digits)

Maximum output float voltage: ± 240 Vdc

Physical characteristics

Display: LCD with amber backlight

Rotary knob for reading adjustment: Yes

Size: 4U, half rack

Dimensions (H x W x D): 179.0 x 212.3 x 379.0 mm

Weight: 8.2 kg

AC power input specifications

Input power option (selectable): 100 Vac $\pm 10\%$, 47 to 63 Hz 115 Vac $\pm 10\%$, 47 to 63 Hz 230 Vac $\pm 10\%$, 47 to 63 Hz

Maximum input power: 600 VA

Fuse: External, located at the rear panel

Environmental specifications

Operating temperature: 0 to 40 °C

Storage temperature: -40 to 70 °C Humidity 15% RH (relative

Humidity: 15% RH (relative humidity) to 85% RH at 40 °C (non-condensing)

Altitude: Up to 2000 m

Fan acoustic noise: 60 dB sound power

Environment of use:
– Installation category II
– Pollution Degree 2

Connection specifications

Output connections: +Out, –Out, and chassis ground on the front panel.

Binding posts: Output binding post located horizontally and side by side

I/O connections: N/A

AC input: 3 pins standard IEC AC power connector with fuse and line selection at the rear

Appendix C - LabVIEW Program

C.1 The LabVIEW Program User Interface

Valve Index Path: C:\Users\...\support files\Case_Patriot_36_VS.csv

Log File Path: C:\Users\jonathanfabula\celerometer\data\Cott Farm 2020h.csv

PGN: EFF9

Valve Index

Channel Names	Slopes	Offsets	Analogs
Pressure 1	9.98004	0	51.3621
Pressure 2	10	0	46.2891
Pressure 3	10	0	55.1172
Pressure 4	10	0	46.25
Pressure 5	10	0	47.168
Pressure 6	10	0	45.6445
Pressure 7	10	0	46.5625
Pressure 8	10	0	52.0898
Pressure 9	10.0107	0	54.824
Pressure 10	10	0	50.1562
Flow	6	0	22.5937
Left_Boom_Ht	0.1809	0.1917	1.55198
Center_Boom_	0.1808	0.1898	1.54403
Right_Boom_H	0.1814	0.1937	1.55278
Pressure 14	0	0	0
Pressure 15	0	0	0
Accel_1_1306	2.50689	-0.00777	-0.62959
Accel_2_1307	2.46305	0.00493	0.880467
Accel_3_1332	2.51193	0.00226	0.841205
Accel_4_1308	2.49439	-0.00748	0.508937
Accel_5_1311	2.48942	0.02564	1.24118
Accel_6_1313	2.49688	0.01473	1.60454
Left_Ht	1	0	0
Center_Ht	1	0	0
Right_Ht	1	0	0

Any ID: 18EFF903

Matched: Frames lost?

Duty Cycles

Byte Timeout (ms): 80

Port 1: GNVTG,179.979,T,,M,8.2060,N,15.1975,K,D*2C **Timed OUT 1**

GPS Values

GPS Time	Latitude	Northing	Longitude	RTK Fix	Velocity	Elevation
2240260	39.39308	N	97.22736	4	15.3065	384.028

Port 2: **Timed OUT 2**

Spectrum Sensor

AirTemp	RH	WindDir(T)	WindSpd
27.6	42.6	153.0	6.9

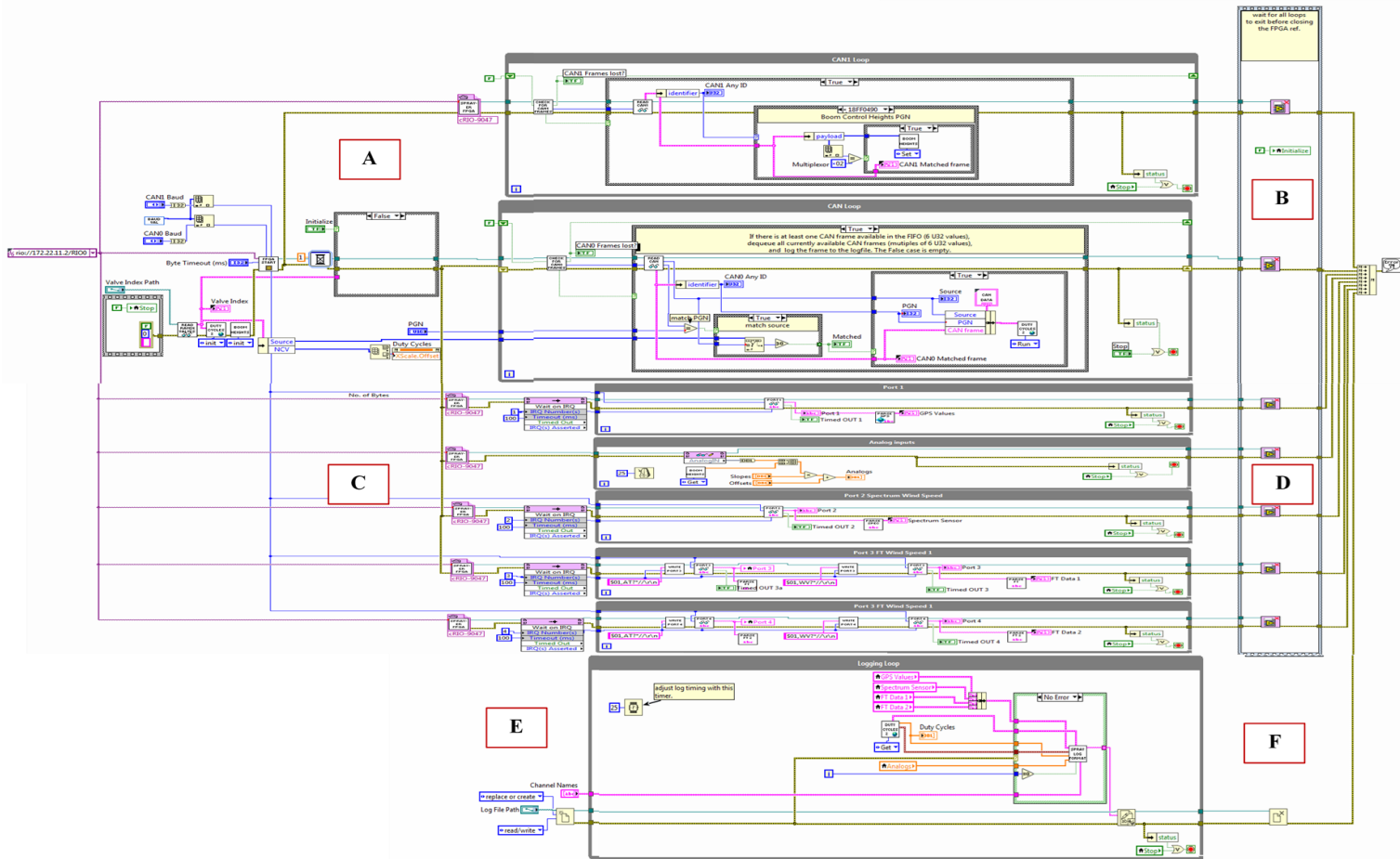
Port 3: \$WIMWV,353,R,013.0,M,A*39\r\n **Timed OUT 3**

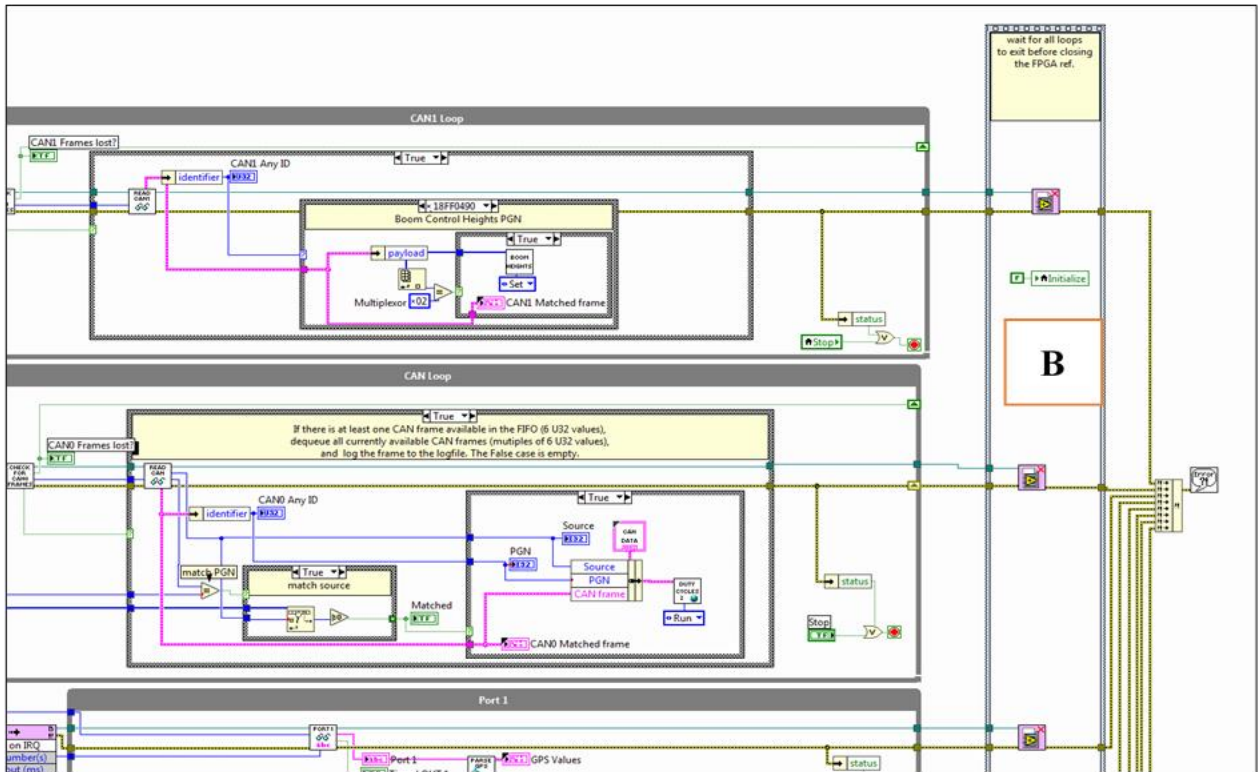
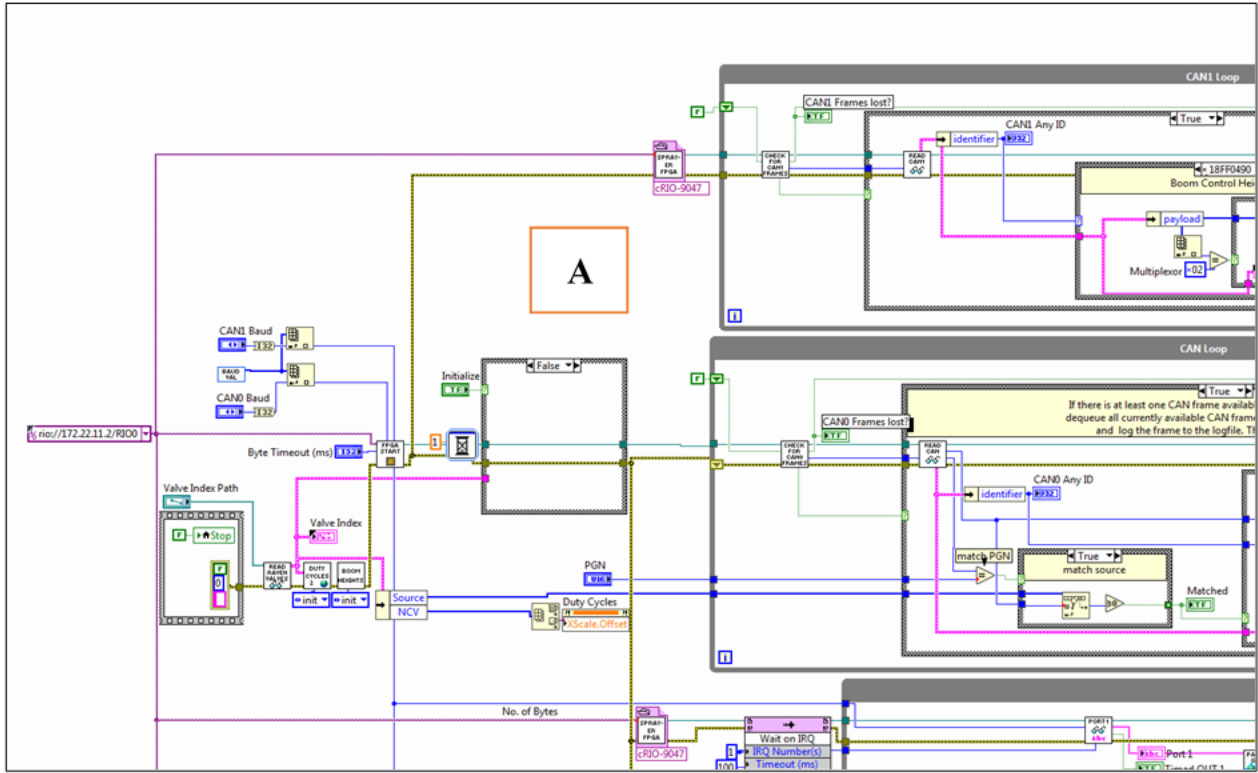
FT Data 1: WindSpd 13.0, WindAngle 352, AirTemp 30.8 **Timed OUT 3a**

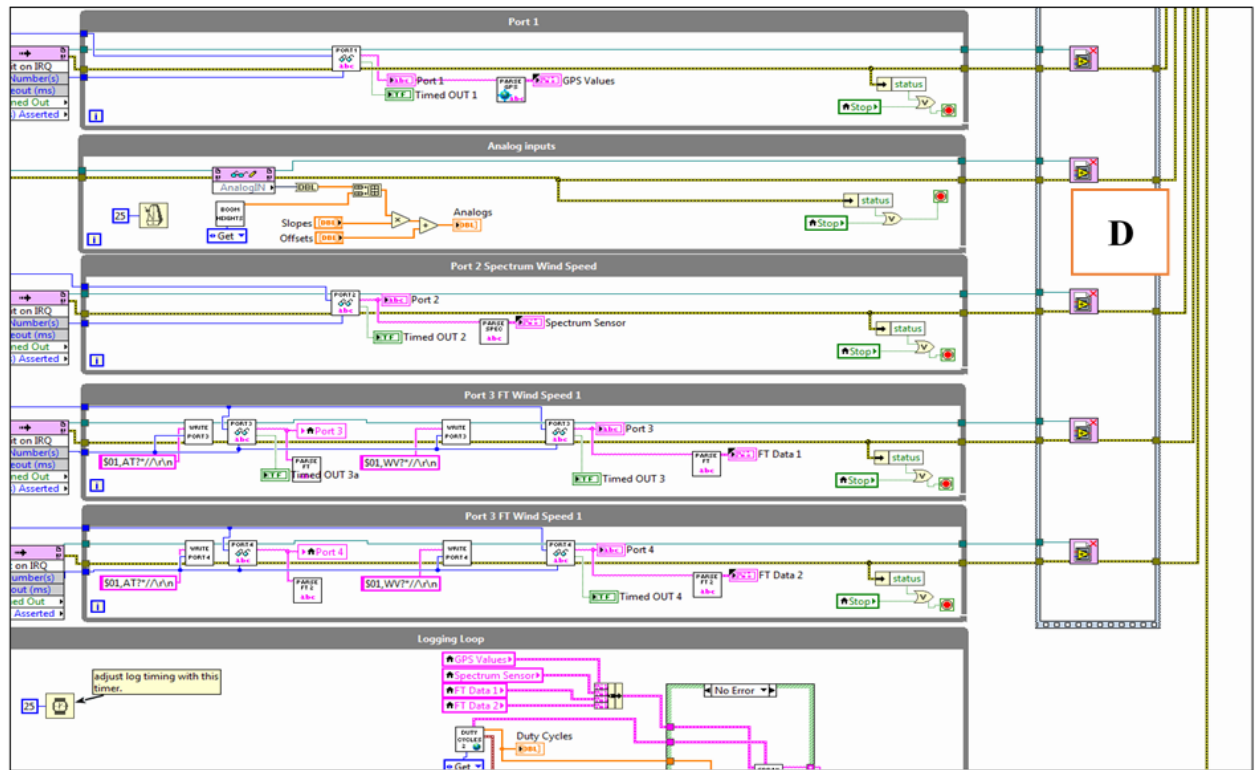
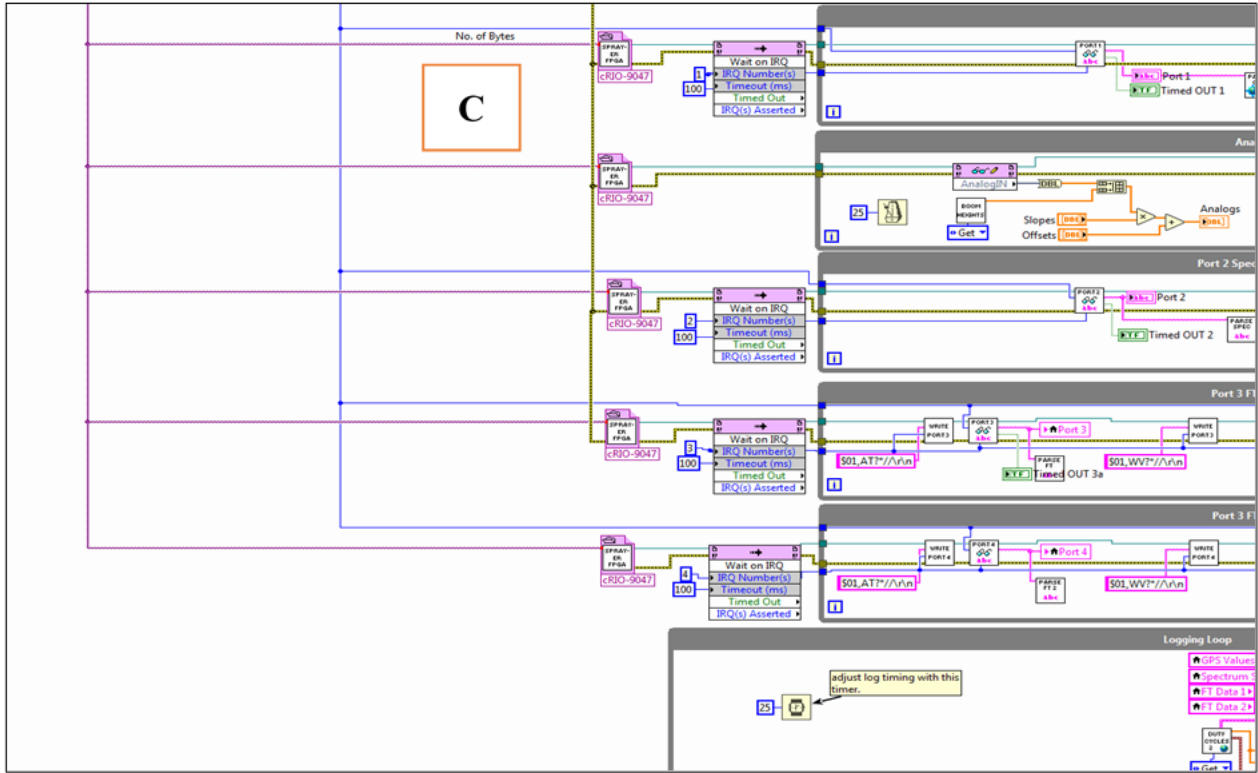
Port 4: 0,C,A*1D **Timed OUT 4**

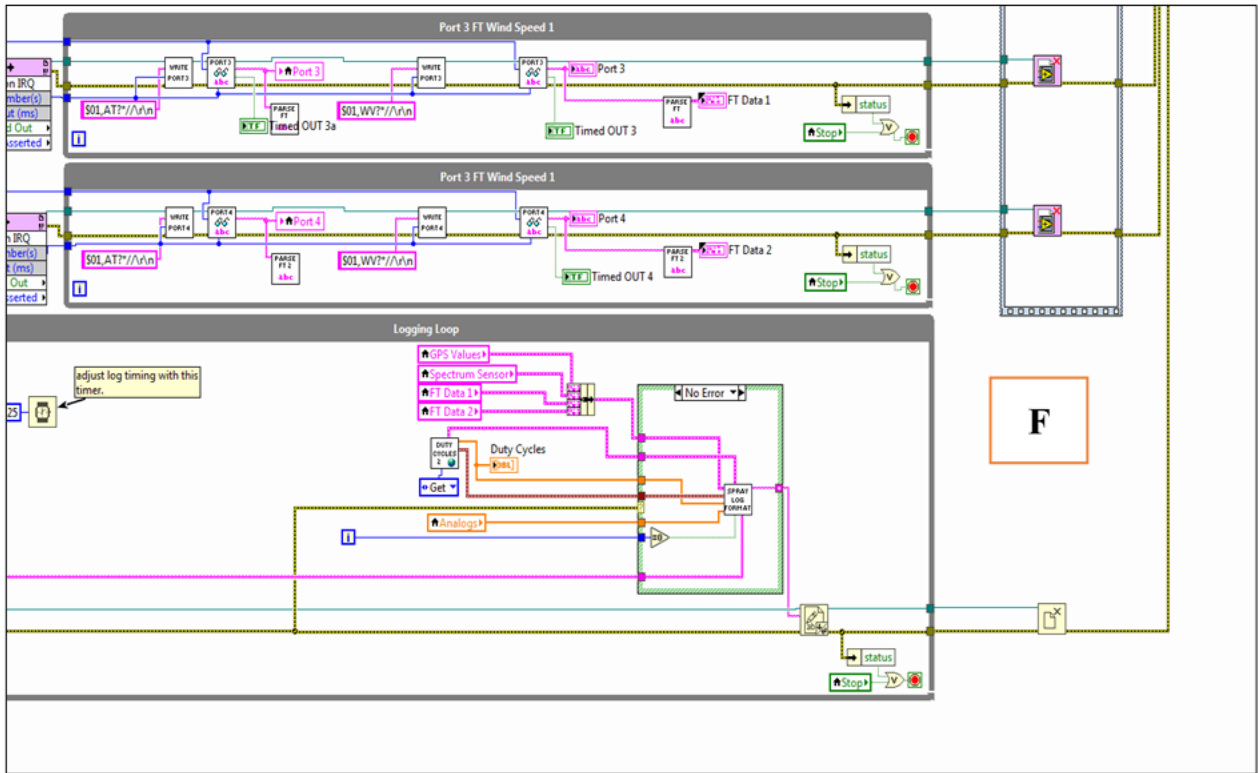
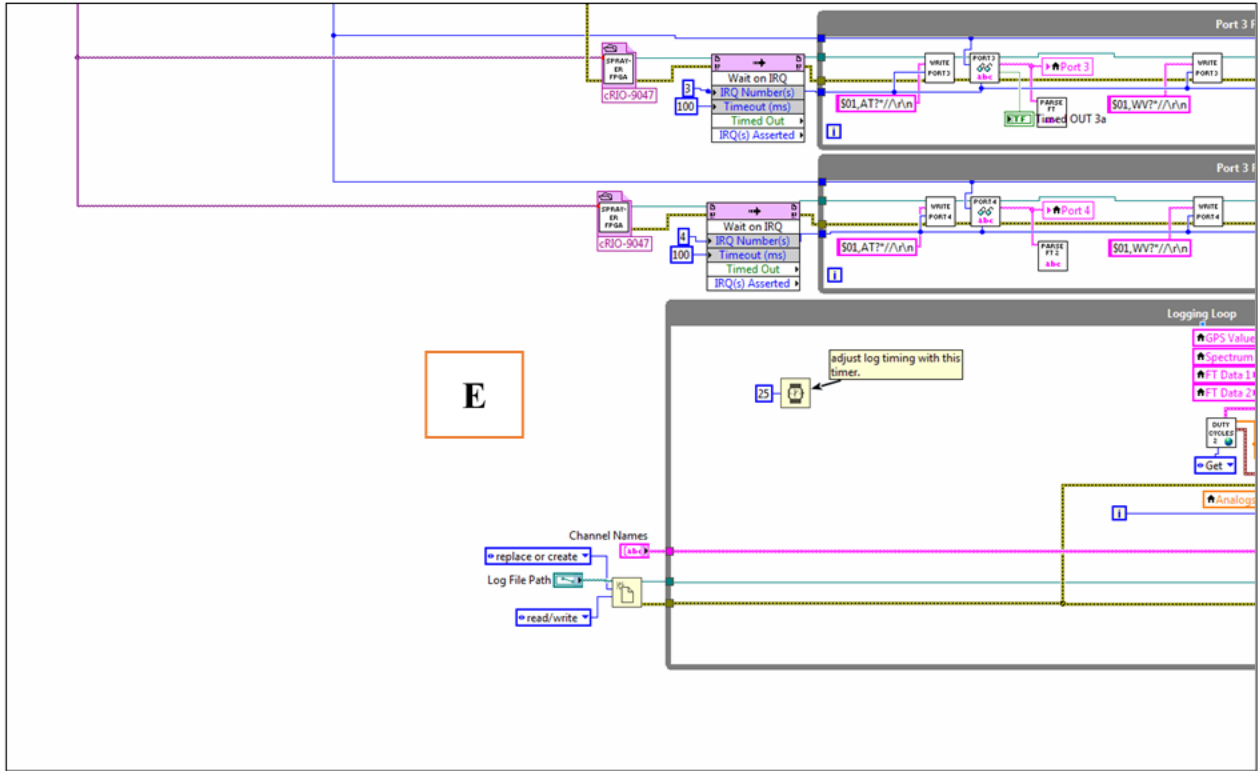
FT Data 2: WindSpd 0.0, WindAngle 002, AirTemp -17.0

C.2 The LabVIEW Program, Block Diagram









Appendix D - SAS Code Used in Data Analysis

D.1 Pressure Drop

```
/*PD_12_40_10 */
PROC IMPORT DATAFILE="/folders/myfolders/Pressure_Drop.xlsx"
  OUT=PD_12_40_10
  DBMS=XLSX
  REPLACE;
  Sheet="12.40.10";
RUN;

PROC PRINT DATA=PD_12_40_10;
RUN;

proc anova data=PD_12_40_10;
  class Sys DC;
  model PD = Sys|DC;
run;

proc mixed data=PD_12_40_10 method=type3;
class Sys DC;
model PD = Sys|DC;
store out2way;
run;

ods graphics on;
ods html path="/folders/myfolders" style=statistical sge=on;
proc plm restore=out2way;
lsmeans Sys|DC / adjust=tukey plot=meanplot cl lines;
ods exclude diffs diffplot;
run; title; run;

/*PD_12_65_10 */
PROC IMPORT DATAFILE="/folders/myfolders/Pressure_Drop.xlsx"
  OUT=PD_12_65_10
  DBMS=XLSX
  REPLACE;
  Sheet="12.65.10";
RUN;

PROC PRINT DATA=PD_12_65_10;
RUN;
```

```
proc anova data=PD_12_65_10;
  class Sys DC;
  model PD = Sys|DC;
run;
```

```
proc mixed data=PD_12_65_10 method=type3;
class Sys DC;
model PD = Sys|DC;
store out2way;
run;
```

```
ods graphics on;
ods html path='/folders/myfolders' style=statistical sge=on;
proc plm restore=out2way;
lsmeans Sys|DC / adjust=tukey plot=meanplot cl lines;
ods exclude diffs diffplot;
run; title; run;
```

```
/*PD_20_40_10 */
PROC IMPORT DATAFILE="'/folders/myfolders/Pressure_Drop.xlsx'"
  OUT=PD_20_40_10
  DBMS=XLSX
  REPLACE;
  Sheet="20.40.10";
RUN;
```

```
PROC PRINT DATA=PD_20_40_10;
RUN;
```

```
proc anova data=PD_20_40_10 ;
  class Sys DC;
  model PD = Sys|DC;
run;
```

```
proc mixed data=PD_20_40_10 method=type3;
class Sys DC;
model PD = Sys|DC;
store out2way;
run;
```

```
ods graphics on;
ods html path='/folders/myfolders' style=statistical sge=on;
proc plm restore=out2way;
lsmeans Sys|DC / adjust=tukey plot=meanplot cl lines;
ods exclude diffs diffplot;
```

```
run; title; run;
```

```
/*PD_20_65_10 */  
PROC IMPORT DATAFILE="/folders/myfolders/Pressure_Drop.xlsx"  
    OUT=PD_20_65_10  
    DBMS=XLSX  
    REPLACE;  
    Sheet="20.65.10";  
RUN;
```

```
PROC PRINT DATA=PD_20_65_10;  
RUN;
```

```
proc anova data=PD_20_65_10 ;  
    class Sys DC;  
    model PD = Sys|DC;  
run;
```

```
proc mixed data=PD_20_65_10 method=type3;  
class Sys DC;  
model PD = Sys|DC;  
store out2way;  
run;
```

```
ods graphics on;  
ods html path='/folders/myfolders' style=statistical sge=on;  
proc plm restore=out2way;  
lsmeans Sys|DC / adjust=tukey plot=meanplot cl lines;  
ods exclude diffs diffplot;  
run; title; run;
```

```
/*PD_12_40_15 */  
PROC IMPORT DATAFILE="/folders/myfolders/Pressure_Drop.xlsx"  
    OUT=PD_12_40_15  
    DBMS=XLSX  
    REPLACE;  
    Sheet="12.40.15";  
RUN;
```

```
PROC PRINT DATA=PD_12_40_15;  
RUN;
```

```
proc anova data=PD_12_40_15;  
    class Sys DC;
```

```

    model PD = Sys|DC;
run;

proc mixed data=PD_12_40_15 method=type3;
class Sys DC;
model PD = Sys|DC;
store out2way;
run;

ods graphics on;
ods html path='/folders/myfolders' style=statistical sge=on;
proc plm restore=out2way;
lsmeans Sys|DC / adjust=tukey plot=meanplot cl lines;
ods exclude diffs diffplot;
run; title; run;

/*PD_12_40_30 */
PROC IMPORT DATAFILE="'/folders/myfolders/Pressure_Drop.xlsx'"
    OUT=PD_12_40_30
    DBMS=XLSX
    REPLACE;
    Sheet="12.40.30";
RUN;

PROC PRINT DATA=PD_12_40_30;
RUN;

proc anova data=PD_12_40_30;
    class Sys DC;
    model PD = Sys|DC;
run;

proc mixed data=PD_12_40_30 method=type3;
class Sys DC;
model PD = Sys|DC;
store out2way;
run;

ods graphics on;
ods html path='/folders/myfolders' style=statistical sge=on;
proc plm restore=out2way;
lsmeans Sys|DC / adjust=tukey plot=meanplot cl lines;
ods exclude diffs diffplot;
run; title; run;

```

```

/*PD_12_65_15 */
PROC IMPORT DATAFILE="/folders/myfolders/Pressure_Drop.xlsx"
    OUT=PD_12_65_15
    DBMS=XLSX
    REPLACE;
    Sheet="12.65.15";
RUN;

PROC PRINT DATA=PD_12_65_15;
RUN;

proc anova data=PD_12_65_15;
    class Sys DC;
    model PD = Sys|DC;
run;

proc mixed data=PD_12_65_15 method=type3;
class Sys DC;
model PD = Sys|DC;
store out2way;
run;

ods graphics on;
ods html path='/folders/myfolders' style=statistical sge=on;
proc plm restore=out2way;
lsmeans Sys|DC / adjust=tukey plot=meanplot cl lines;
ods exclude diffs diffplot;
run; title; run;

/*PD_12_65_30 */
PROC IMPORT DATAFILE="/folders/myfolders/Pressure_Drop.xlsx"
    OUT=PD_12_65_30
    DBMS=XLSX
    REPLACE;
    Sheet="12.65.30";
RUN;

PROC PRINT DATA=PD_12_65_30 ;
RUN;

proc anova data=PD_12_65_30 ;
    class Sys DC;
    model PD = Sys|DC;
run;

```

```

proc mixed data=PD_12_65_30 method=type3;
class Sys DC;
model PD = Sys|DC;
store out2way;
run;

ods graphics on;
ods html path='/folders/myfolders' style=statistical sge=on;
proc plm restore=out2way;
lsmeans Sys|DC / adjust=tukey plot=meanplot cl lines;
ods exclude diffs diffplot;
run; title; run;

/*PD_20_40_15 */
PROC IMPORT DATAFILE=""/folders/myfolders/Pressure_Drop.xlsx""
OUT=PD_20_40_15
DBMS=XLSX
REPLACE;
Sheet="20.40.15";
RUN;

PROC PRINT DATA=PD_20_40_15 ;
RUN;

proc anova data=PD_20_40_15 ;
class Sys DC;
model PD = Sys|DC;
run;

proc mixed data=PD_20_40_15 method=type3;
class Sys DC;
model PD = Sys|DC;
store out2way;
run;

ods graphics on;
ods html path='/folders/myfolders' style=statistical sge=on;
proc plm restore=out2way;
lsmeans Sys|DC / adjust=tukey plot=meanplot cl lines;
ods exclude diffs diffplot;
run; title; run;

/*PD_20_40_30 */
PROC IMPORT DATAFILE=""/folders/myfolders/Pressure_Drop.xlsx""

```

```

        OUT=PD_20_40_30
        DBMS=XLSX
        REPLACE;
        Sheet="20.40.30";
RUN;

PROC PRINT DATA=PD_20_40_30 ;
RUN;

proc anova data=PD_20_40_30 ;
    class Sys DC;
    model PD = Sys|DC;
run;

proc mixed data=PD_20_40_30  method=type3;
class Sys DC;
model PD = Sys|DC;
store out2way;
run;

ods graphics on;
ods html path='/folders/myfolders' style=statistical sge=on;
proc plm restore=out2way;
lsmeans Sys|DC / adjust=tukey plot=meanplot cl lines;
ods exclude diffs diffplot;
run; title; run;

/*PD_20_65_15 */
PROC IMPORT DATAFILE=""/folders/myfolders/Pressure_Drop.xlsx""
    OUT=PD_20_65_15
    DBMS=XLSX
    REPLACE;
    Sheet="20.65.15";
RUN;

PROC PRINT DATA=PD_20_65_15 ;
RUN;

proc anova data=PD_20_65_15 ;
    class Sys DC;
    model PD = Sys|DC;
run;

proc mixed data=PD_20_65_15  method=type3;
class Sys DC;

```

```
model PD = Sys|DC;
store out2way;
run;
```

```
ods graphics on;
ods html path='/folders/myfolders' style=statistical sge=on;
proc plm restore=out2way;
lsmeans Sys|DC / adjust=tukey plot=meanplot cl lines;
ods exclude diffs diffplot;
run; title; run;
```

```
/*PD_20_65_30 */
PROC IMPORT DATAFILE="'/folders/myfolders/Pressure_Drop.xlsx'"
    OUT=PD_20_65_30
    DBMS=XLSX
    REPLACE;
    Sheet="20.65.30";
RUN;
```

```
PROC PRINT DATA=PD_20_65_30 ;
RUN;
```

```
proc anova data=PD_20_65_30 ;
    class Sys DC;
    model PD = Sys|DC;
run;
```

```
proc mixed data=PD_20_65_30    method=type3;
class Sys DC;
model PD = Sys|DC;
store out2way;
run;
```

```
ods graphics on;
ods html path='/folders/myfolders' style=statistical sge=on;
proc plm restore=out2way;
lsmeans Sys|DC / adjust=tukey plot=meanplot cl lines;
ods exclude diffs diffplot;
run; title; run;
```

D.2 Stabilized Pressure Application Time Change

```
/*ST_12_40_10 */
PROC IMPORT DATAFILE=""/folders/myfolders/Stab_Time.xlsx"
    OUT=ST_12_40_10
    DBMS=XLSX
    REPLACE;
    Sheet="12.40.10";
RUN;

PROC PRINT DATA=ST_12_40_10;
RUN;

proc anova data=ST_12_40_10;
    class Sys DC;
    model ST = Sys|DC;
run;

proc mixed data=ST_12_40_10 method=type3;
class Sys DC;
model ST = Sys|DC;
store out2way;
run;

ods graphics on;
ods html path='/folders/myfolders' style=statistical sge=on;
proc plm restore=out2way;
lsmeans Sys|DC / adjust=tukey plot=meanplot cl lines;
ods exclude diffs diffplot;
run; title; run;

/*ST_12_65_10 */
PROC IMPORT DATAFILE=""/folders/myfolders/Stab_Time.xlsx"
    OUT=ST_12_65_10
    DBMS=XLSX
    REPLACE;
    Sheet="12.65.10";
RUN;

PROC PRINT DATA=ST_12_65_10;
RUN;

proc anova data=ST_12_65_10;
    class Sys DC;
    model ST = Sys|DC;
```

```

run;

proc mixed data=ST_12_65_10 method=type3;
class Sys DC;
model ST = Sys|DC;
store out2way;
run;

ods graphics on;
ods html path='/folders/myfolders' style=statistical sge=on;
proc plm restore=out2way;
lsmeans Sys|DC / adjust=tukey plot=meanplot cl lines;
ods exclude diffs diffplot;
run; title; run;

/*ST_20_40_10 */
PROC IMPORT DATAFILE="/folders/myfolders/Stab_Time.xlsx"
  OUT=ST_20_40_10
  DBMS=XLSX
  REPLACE;
  Sheet="20.40.10";
RUN;

PROC PRINT DATA=ST_20_40_10;
RUN;

proc anova data=ST_20_40_10 ;
  class Sys DC;
  model ST = Sys|DC;
run;

proc mixed data=ST_20_40_10 method=type3;
class Sys DC;
model ST = Sys|DC;
store out2way;
run;

ods graphics on;
ods html path='/folders/myfolders' style=statistical sge=on;
proc plm restore=out2way;
lsmeans Sys|DC / adjust=tukey plot=meanplot cl lines;
ods exclude diffs diffplot;
run; title; run;

```

```

/*ST_20_65_10 */
PROC IMPORT DATAFILE="/folders/myfolders/Stab_Time.xlsx"
    OUT=ST_20_65_10
    DBMS=XLSX
    REPLACE;
    Sheet="20.65.10";
RUN;

PROC PRINT DATA=ST_20_65_10;
RUN;

proc anova data=ST_20_65_10 ;
    class Sys DC;
    model ST= Sys|DC;
run;

proc mixed data=ST_20_65_10 method=type3;
class Sys DC;
model ST = Sys|DC;
store out2way;
run;

ods graphics on;
ods html path='/folders/myfolders' style=statistical sge=on;
proc plm restore=out2way;
lsmeans Sys|DC / adjust=tukey plot=meanplot cl lines;
ods exclude diffs diffplot;
run; title; run;

/*ST_12_40_15 */
PROC IMPORT DATAFILE="/folders/myfolders/Stab_Time.xlsx"
    OUT=ST_12_40_15
    DBMS=XLSX
    REPLACE;
    Sheet="12.40.15";
RUN;

PROC PRINT DATA=ST_12_40_15;
RUN;

proc anova data=ST_12_40_15;
    class Sys DC;
    model ST= Sys|DC;
run;

```

```

proc mixed data=ST_12_40_15 method=type3;
class Sys DC;
model ST= Sys|DC;
store out2way;
run;

ods graphics on;
ods html path='/folders/myfolders' style=statistical sge=on;
proc plm restore=out2way;
lsmeans Sys|DC / adjust=tukey plot=meanplot cl lines;
ods exclude diffs diffplot;
run; title; run;

/*ST_12_40_30 */
PROC IMPORT DATAFILE=""/folders/myfolders/Stab_Time.xlsx"
      OUT=ST_12_40_30
      DBMS=XLSX
      REPLACE;
      Sheet="12.40.30";
RUN;

PROC PRINT DATA=ST_12_40_30;
RUN;

proc anova data=ST_12_40_30;
  class Sys DC;
  model ST = Sys|DC;
run;

proc mixed data=ST_12_40_30 method=type3;
class Sys DC;
model ST = Sys|DC;
store out2way;
run;

ods graphics on;
ods html path='/folders/myfolders' style=statistical sge=on;
proc plm restore=out2way;
lsmeans Sys|DC / adjust=tukey plot=meanplot cl lines;
ods exclude diffs diffplot;
run; title; run;

/*ST_12_65_15 */
PROC IMPORT DATAFILE=""/folders/myfolders/Stab_Time.xlsx"

```

```

        OUT=ST_12_65_15
        DBMS=XLSX
        REPLACE;
        Sheet="12.65.15";
RUN;

PROC PRINT DATA=ST_12_65_15;
RUN;

proc anova data=ST_12_65_15;
    class Sys DC;
    model ST = Sys|DC;
run;

proc mixed data=ST_12_65_15 method=type3;
class Sys DC;
model ST = Sys|DC;
store out2way;
run;

ods graphics on;
ods html path='/folders/myfolders' style=statistical sge=on;
proc plm restore=out2way;
lsmeans Sys|DC / adjust=tukey plot=meanplot cl lines;
ods exclude diffs diffplot;
run; title; run;

/*ST_12_65_30 */
PROC IMPORT DATAFILE=""/folders/myfolders/Stab_Time.xlsx""
    OUT=ST_12_65_30
    DBMS=XLSX
    REPLACE;
    Sheet="12.65.30";
RUN;

PROC PRINT DATA=ST_12_65_30 ;
RUN;

proc anova data=PD_12_65_30 ;
    class Sys DC;
    model PD = Sys|DC;
run;

proc mixed data=ST_12_65_30 method=type3;
class Sys DC;

```

```
model ST = Sys|DC;
store out2way;
run;
```

```
ods graphics on;
ods html path='/folders/myfolders' style=statistical sge=on;
proc plm restore=out2way;
lsmeans Sys|DC / adjust=tukey plot=meanplot cl lines;
ods exclude diffs diffplot;
run; title; run;
```

```
/*ST_20_40_15 */
PROC IMPORT DATAFILE="'/folders/myfolders/Stab_Time.xlsx'"
    OUT=ST_20_40_15
    DBMS=XLSX
    REPLACE;
    Sheet="20.40.15";
RUN;
```

```
PROC PRINT DATA=ST_20_40_15 ;
RUN;
```

```
proc anova data=ST_20_40_15 ;
    class Sys DC;
    model ST= Sys|DC;
run;
```

```
proc mixed data=ST_20_40_15 method=type3;
class Sys DC;
model ST = Sys|DC;
store out2way;
run;
```

```
ods graphics on;
ods html path='/folders/myfolders' style=statistical sge=on;
proc plm restore=out2way;
lsmeans Sys|DC / adjust=tukey plot=meanplot cl lines;
ods exclude diffs diffplot;
run; title; run;
```

```
/*ST_20_40_30 */
PROC IMPORT DATAFILE="'/folders/myfolders/Stab_Time.xlsx'"
    OUT=ST_20_40_30
    DBMS=XLSX
```

```

        REPLACE;
        Sheet="20.40.30";
RUN;

PROC PRINT DATA=ST_20_40_30 ;
RUN;

proc anova data=ST_20_40_30 ;
    class Sys DC;
    model ST = Sys|DC;
run;

proc mixed data=ST_20_40_30    method=type3;
class Sys DC;
model ST = Sys|DC;
store out2way;
run;

ods graphics on;
ods html path='/folders/myfolders' style=statistical sge=on;
proc plm restore=out2way;
lsmeans Sys|DC / adjust=tukey plot=meanplot cl lines;
ods exclude diffs diffplot;
run; title; run;

/*ST_20_65_15 */
PROC IMPORT DATAFILE="'/folders/myfolders/Stab_Time.xlsx'"
    OUT=ST_20_65_15
    DBMS=XLSX
    REPLACE;
    Sheet="20.65.15";
RUN;

PROC PRINT DATA=ST_20_65_15 ;
RUN;

proc anova data=ST_20_65_15 ;
    class Sys DC;
    model ST = Sys|DC;
run;

proc mixed data=ST_20_65_15    method=type3;
class Sys DC;
model ST = Sys|DC;
store out2way;

```

```

run;

ods graphics on;
ods html path='/folders/myfolders' style=statistical sge=on;
proc plm restore=out2way;
lsmeans Sys|DC / adjust=tukey plot=meanplot cl lines;
ods exclude diffs diffplot;
run; title; run;

/*ST_20_65_30 */
PROC IMPORT DATAFILE="'/folders/myfolders/Stab_Time.xlsx'"
      OUT=ST_20_65_30
      DBMS=XLSX
      REPLACE;
      Sheet="20.65.30";
RUN;

PROC PRINT DATA=ST_20_65_30 ;
RUN;

proc anova data=ST_20_65_30 ;
      class Sys DC;
      model ST = Sys|DC;
run;

proc mixed data=ST_20_65_30    method=type3;
class Sys DC;
model ST = Sys|DC;
store out2way;
run;

ods graphics on;
ods html path='/folders/myfolders' style=statistical sge=on;
proc plm restore=out2way;
lsmeans Sys|DC / adjust=tukey plot=meanplot cl lines;
ods exclude diffs diffplot;
run; title; run;

```

D.3 Flow Rate Change

```
/*FR_12_40_10 */
PROC IMPORT DATAFILE=""/folders/myfolders/FR_Stat.xlsx"
    OUT=FR_12_40_10
    DBMS=XLSX
    REPLACE;
    Sheet="12.40.10";
RUN;

PROC PRINT DATA=FR_12_40_10;
RUN;

proc anova data=FR_12_40_10;
    class Sys DC;
    model FR = Sys|DC;
run;

proc mixed data=FR_12_40_10 method=type3;
class Sys DC;
model FR = Sys|DC;
store out2way;
run;

ods graphics on;
ods html path='/folders/myfolders' style=statistical sge=on;
proc plm restore=out2way;
lsmeans Sys|DC / adjust=tukey plot=meanplot cl lines;
ods exclude diffs diffplot;
run; title; run;

/*FR_12_65_10 */
PROC IMPORT DATAFILE=""/folders/myfolders/FR_Stat.xlsx"
    OUT=FR_12_65_10
    DBMS=XLSX
    REPLACE;
    Sheet="12.65.10";
RUN;

PROC PRINT DATA=FR_12_65_10;
RUN;

proc anova data=FR_12_65_10;
    class Sys DC;
    model FR= Sys|DC;
```

```

run;

proc mixed data=FR_12_65_10 method=type3;
class Sys DC;
model FR= Sys|DC;
store out2way;
run;

ods graphics on;
ods html path='/folders/myfolders' style=statistical sge=on;
proc plm restore=out2way;
lsmeans Sys|DC / adjust=tukey plot=meanplot cl lines;
ods exclude diffs diffplot;
run; title; run;

/*FR_20_40_10 */
PROC IMPORT DATAFILE="/folders/myfolders/FR_Stat.xlsx"
  OUT=FR_20_40_10
  DBMS=XLSX
  REPLACE;
  Sheet="20.40.10";
RUN;

PROC PRINT DATA=FR_20_40_10;
RUN;

proc anova data=FR_20_40_10 ;
  class Sys DC;
  model FR = Sys|DC;
run;

proc mixed data=FR_20_40_10 method=type3;
class Sys DC;
model FR= Sys|DC;
store out2way;
run;

ods graphics on;
ods html path='/folders/myfolders' style=statistical sge=on;
proc plm restore=out2way;
lsmeans Sys|DC / adjust=tukey plot=meanplot cl lines;
ods exclude diffs diffplot;
run; title; run;

```

```

/*FR_20_65_10 */
PROC IMPORT DATAFILE= "/folders/myfolders/FR_Stat.xlsx"
    OUT=FR_20_65_10
    DBMS=XLSX
    REPLACE;
    Sheet="20.65.10";
RUN;

PROC PRINT DATA=FR_20_65_10;
RUN;

proc anova data=FR_20_65_10 ;
    class Sys DC;
    model FR= Sys|DC;
run;

proc mixed data=FR_20_65_10 method=type3;
class Sys DC;
model FR = Sys|DC;
store out2way;
run;

ods graphics on;
ods html path='/folders/myfolders' style=statistical sge=on;
proc plm restore=out2way;
lsmeans Sys|DC / adjust=tukey plot=meanplot cl lines;
ods exclude diffs diffplot;
run; title; run;

/*FR_12_40_15 */
PROC IMPORT DATAFILE= "/folders/myfolders/FR_Stat.xlsx"
    OUT=FR_12_40_15
    DBMS=XLSX
    REPLACE;
    Sheet="12.40.15";
RUN;

PROC PRINT DATA=FR_12_40_15;
RUN;

proc anova data=FR_12_40_15;
    class Sys DC;
    model FR= Sys|DC;
run;

```

```

proc mixed data=FR_12_40_15 method=type3;
class Sys DC;
model FR= Sys|DC;
store out2way;
run;

ods graphics on;
ods html path='/folders/myfolders' style=statistical sge=on;
proc plm restore=out2way;
lsmeans Sys|DC / adjust=tukey plot=meanplot cl lines;
ods exclude diffs diffplot;
run; title; run;

/*FR_12_40_30 */
PROC IMPORT DATAFILE=""/folders/myfolders/FR_Stat.xlsx"
      OUT=FR_12_40_30
      DBMS=XLSX
      REPLACE;
      Sheet="12.40.30";
RUN;

PROC PRINT DATA=FR_12_40_30;
RUN;

proc anova data=FR_12_40_30;
  class Sys DC;
  model FR = Sys|DC;
run;

proc mixed data=FR_12_40_30 method=type3;
class Sys DC;
model FR = Sys|DC;
store out2way;
run;

ods graphics on;
ods html path='/folders/myfolders' style=statistical sge=on;
proc plm restore=out2way;
lsmeans Sys|DC / adjust=tukey plot=meanplot cl lines;
ods exclude diffs diffplot;
run; title; run;

/*FR_12_65_15 */
PROC IMPORT DATAFILE=""/folders/myfolders/FR_Stat.xlsx"

```

```

        OUT=FR_12_65_15
        DBMS=XLSX
        REPLACE;
        Sheet="12.65.15";
RUN;

PROC PRINT DATA=FR_12_65_15;
RUN;

proc anova data=FR_12_65_15;
    class Sys DC;
    model FR = Sys|DC;
run;

proc mixed data=FR_12_65_15 method=type3;
class Sys DC;
model FR = Sys|DC;
store out2way;
run;

ods graphics on;
ods html path='/folders/myfolders' style=statistical sge=on;
proc plm restore=out2way;
lsmeans Sys|DC / adjust=tukey plot=meanplot cl lines;
ods exclude diffs diffplot;
run; title; run;

/*FR_12_65_30 */
PROC IMPORT DATAFILE=""/folders/myfolders/FR_Stat.xlsx"
    OUT=FR_12_65_30
    DBMS=XLSX
    REPLACE;
    Sheet="12.65.30";
RUN;

PROC PRINT DATA=FR_12_65_30 ;
RUN;

proc anova data=FR_12_65_30 ;
    class Sys DC;
    model FR = Sys|DC;
run;

proc mixed data=FR_12_65_30 method=type3;
class Sys DC;

```

```
model FR = Sys|DC;
store out2way;
run;
```

```
ods graphics on;
ods html path='/folders/myfolders' style=statistical sge=on;
proc plm restore=out2way;
lsmeans Sys|DC / adjust=tukey plot=meanplot cl lines;
ods exclude diffs diffplot;
run; title; run;
```

```
/*FR_20_40_15 */
PROC IMPORT DATAFILE='"/folders/myfolders/FR_Stat.xlsx"'
    OUT=FR_20_40_15
    DBMS=XLSX
    REPLACE;
    Sheet="20.40.15";
RUN;
```

```
PROC PRINT DATA=FR_20_40_15 ;
RUN;
```

```
proc anova data=FR_20_40_15 ;
    class Sys DC;
    model FR= Sys|DC;
run;
```

```
proc mixed data=FR_20_40_15    method=type3;
class Sys DC;
model FR = Sys|DC;
store out2way;
run;
```

```
ods graphics on;
ods html path='/folders/myfolders' style=statistical sge=on;
proc plm restore=out2way;
lsmeans Sys|DC / adjust=tukey plot=meanplot cl lines;
ods exclude diffs diffplot;
run; title; run;
```

```
/*FR_20_40_30 */
PROC IMPORT DATAFILE='"/folders/myfolders/FR_Stat.xlsx"'
    OUT=FR_20_40_30
    DBMS=XLSX
```

```

        REPLACE;
        Sheet="20.40.30";
RUN;

PROC PRINT DATA=FR_20_40_30 ;
RUN;

proc anova data=FR_20_40_30 ;
    class Sys DC;
    model FR = Sys|DC;
run;

proc mixed data=FR_20_40_30    method=type3;
class Sys DC;
model FR = Sys|DC;
store out2way;
run;

ods graphics on;
ods html path='/folders/myfolders' style=statistical sge=on;
proc plm restore=out2way;
lsmeans Sys|DC / adjust=tukey plot=meanplot cl lines;
ods exclude diffs diffplot;
run; title; run;

/*FR_20_65_15 */
PROC IMPORT DATAFILE="'/folders/myfolders/FR_Stat.xlsx'"
    OUT=FR_20_65_15
    DBMS=XLSX
    REPLACE;
    Sheet="20.65.15";
RUN;

PROC PRINT DATA=FR_20_65_15 ;
RUN;

proc anova data=FR_20_65_15 ;
    class Sys DC;
    model FR = Sys|DC;
run;

proc mixed data=FR_20_65_15    method=type3;
class Sys DC;
model FR = Sys|DC;
store out2way;

```

```

run;

ods graphics on;
ods html path='/folders/myfolders' style=statistical sge=on;
proc plm restore=out2way;
lsmeans Sys|DC / adjust=tukey plot=meanplot cl lines;
ods exclude diffs diffplot;
run; title; run;

/*FR_20_65_30 */
PROC IMPORT DATAFILE="'/folders/myfolders/FR_Stat.xlsx'"
  OUT=FR_20_65_30
  DBMS=XLSX
  REPLACE;
  Sheet="20.65.30";
RUN;

PROC PRINT DATA=FR_20_65_30 ;
RUN;

proc anova data=FR_20_65_30 ;
  class Sys DC;
  model FR = Sys|DC;
run;

proc mixed data=FR_20_65_30 method=type3;
class Sys DC;
model FR = Sys|DC;
store out2way;
run;

ods graphics on;
ods html path='/folders/myfolders' style=statistical sge=on;
proc plm restore=out2way;
lsmeans Sys|DC / adjust=tukey plot=meanplot cl lines;
ods exclude diffs diffplot;
run; title; run;

```